ELECTRON SPIN RESONANCE STUDIES OF TRANSIENT RADICAL - ANIONS PRODUCED IN LIQUID AMMONIA AT 200 K

by

IAN HAMILTON ELSON

A dissertation submitted in part fulfilment
of the requirements for the degree of
Doctor of Philosophy at the University of Warwick

September 1972

ACKNOWLEDGEMENTS

I would like to thank Dr. T. J. Kemp for not only providing the opportunity to carry out this work but also for his encouragement throughout its course. Thanks are also due to Professor V. M. Clark for providing the facilities of the Department of Molecular Sciences and to the many other members of the academic and technical staff for their assistance. The services of the glass-blowing workshop, under the direction of Mr. K. Holden, and the help of Drs. D. Greatorex and D. Benton in operating the flow system is gratefully acknowledged. I would also like to thank Miss Rosemary Went for typing this thesis. I am indebted to I.C.I. Ltd. (Mond Division) who co-operated with this work and provided financial assistance through a C.A.P.S. studentship and to the S.R.C. for the maintenance award.

CONTENTS

ABSTRACT

ABSTRACT

In this work is described the application of esr spectroscopy to the study of novel transient radical-anions formed by the addition of the ammoniated electron to both anions and neutral molecules at 200 K.

The apparatus used employs the multicapillary mixing chamber described by earlier workers in this field[48] with the addition of a low temperature modification to the main flow system. Prior to mixing, solutions of sodium and the substrate in liquid ammonia are cooled to temperatures in the range ≈ 200 to 240 K by passing them through a cryostat comprising ca. 2m of 6mm i.d. glass tubing immersed in a methanol/CO_2 bath set slightly below the required temperature. The heat capacity of the bath is sufficient to prevent any appreciable heating (< 1° K) while the esr spectrum is recorded. The temperature of the solutions is maintained during transference to the multicapillary mixer by means of vacuum jacketed tubing. Chapter 5 describes the application of this technique to a series of ring- and N-substituted benzamides and thiobenzamides. In general, ring-substituted benzamides exist in their mono-ionised form in liquid ammonia and electron attachment to these results in the formation of the radical-dianions $ArCONH^{2-}$. These radical-dianions show restricted rotation about the bond from the ring to the amide group and give rise to esr spectra of low symmetry. N-methyl- and 2-fluoro- benzamides showed anomalous behaviour in that their esr spectra afford couplings from from a full complement of magnetic nuclei, i.e. electron attachment takes place to the unionised molecules. The

N,N-dimethyl- substituted benzamides, having no acidic amide protons, give rise to their corresponding radical-anions $ArCONH(Me)_2^-$ and these, unlike the ring-substituted compounds, afford highly symmetric spectra. MO calculations are employed to facilitate the assignment of coupling constants to particular nuclei; the assymetry of the spin density distribution being simulated by application of the so-called β effect. A value of $Q_{CH}^{H} = -2{\cdot}75 \pm 0{\cdot}24$ mT is derived for the σ-Π-interaction parameter for the benzamide ring. Benzamide radical-anions in general have half-lives of the order of ms. N,N-dimethylbenzamide is unique in that it is stable for up to an hour at 200 K and can be observed by a conventional static reduction technique.

Ethylene itself proves resistant to reduction by solutions of alkali metals in liquid ammonia but substitution in this molecule by groups such as carboxy-, acetyl-, or vinyl- have an activating effect. Chapters 6 and 7 describe the preparation and characterisation by esr spectroscopy of a series of partially reduced α,β-unsaturated carbonyl compounds. Chapter 6 is devoted to the ketyls of acyclic and cyclic α,β-unsaturated ketones, and Chapter 7 to the radical-anions of α,β-unsaturated acids, esters and nitriles.

The open-chain ketyls are found to exist, like the neutral molecules, as s-cis and s-trans conformers. A value of -2·45 mT has been derived for the σ-Π-interaction parameter for the vinyl protons. Vaules of "experimental" spin densities are compared with those derived from simple MO theory, to facilitate the assignemnt of coupling constants. The simple MO theory is modified to distinguish between s-cis and s-trans conformations. Assignment of coupling

constants in the series of cyclic ketyls derived from 2-cyclohexenone is straightforward. The couplings show that in most cases the ketyls exist in conformations with lifetimes generally greater than 10^{-6}s and that the methylene protons are either in almost pure axial or equatorial positions. The ketyl of 2-cyclopentenone is planar. The esr spectrum of the 2-cyclohexenone ketyl shows modulation of certain hyperfine couplings due to ring inversion occuring during the time of the esr experiment with an activation energy of 23·59 kJ mol^{-1}.

Inclusion of a proton source in the reduction medium of 3,5,5-trimethyl-2-cyclohexenone enables the neutral radical to be observed. Static reduction tends to lead to the formation of semidiones arising through oxidation of the radical-anions. Ionisation of the α,β-unsaturated acids in liquid ammonia results in the s-cis and s-trans isomers becoming equivalent and single species corresponding to $[R_1R_2C = CR_3CO_2]^{2\cdot-}$ are observed in the flow system. These radical-anions are short lived and give rise to esr spectra of low intensity. The radical-anion of fumaric acid was observed by reduction of acetylenedicarboxylic acid. Partial reduction of α,β-unsaturated esters yields somewhat more stable radical-anions which show s-cis and s-trans conformations. Radical-anions of maleic and fumaric esters are found to isomerise and give rise to several isomeric and conformeric species. Reduction of ethyl propiolate gives rise not only to its own radical-anion but also to that of ethyl acrylate as a secondary species. The high-field spectral lines of the former compound are of enhanced intensity, probably through the agency of Chemically Induced Dynamic Electron Polarisation (CIDEP).

ABBREVIATIONS AND CONSTANTS

esr	electron spin resonance
nmr	nuclear magnetic resonance
pr	pulse radiolysis
fp	flash photolysis
uv	ultra violet
ir	infra red
mT	millitesla
ms	millisecond
nm	nanometer
THF	tetrahydrofuran
HMPA	hexamethylphosphoramide
DME	dimethylsulphoxide
MVK	methyl vinyl ketone
MO	molecular orbital
VB	valence bond
h	Planck's constant
$\hbar$	$h/2\pi$
γ_e	magnetogyric ratio for the electron
β_e	Bohr magneton for the electron
β_N	Bohr magneton for the nucleus
g_e	g-factor for the electron
g_N	g-factor for the nucleus

PART A

INTRODUCTORY SECTION

CHAPTER 1

LIQUID AMMONIA

1 LIQUID AMMONIA

Chemistry in liquid ammonia solution has been studied extensively and many comprehensive review articles have been published[1].

1.1 Liquid Ammonia as a Solvent

Liquid ammonia, because of its almost unique combination of properties, possesses solvent characteristics many of which are intermediate between those of water and aliphatic alcohols of low molecular weight. It has a comparatively high dielectric constant (≈27 at 213 K, ≈23 at 240 K) and dipole moment (1·3 Debye), and its high boiling point (239·78 K) is a reflection of its ability to form hydrogen bonds. Being one of the most basic solvents, acids for which pK <~12 in aqueous solution are strong acids in liquid ammonia. The solution power of water depends mainly on its dipole moment, whereas that for ammonia is almost equally dependent on its polarisability. When solute molecules not only have high dipole moments but are also highly polarisable, the polarisation effects may outweigh those of the dipole orientation. Hence ammonia tends to be a poorer solvent than water for ionic salts and highly polarisable molecules, but is better for non-polar species. Salts of poly-negative anions are practically insoluble in liquid ammonia, the solvation energy being insufficient to compensate for their high lattice energies. Substances capable of hydrogen-bond formation exhibit high solubilities.

1.2 Metal-Ammonia Solutions

Probably one of the most important properties of liquid ammonia, from the synthetic chemist's point of view, is its

ability to dissolve, inter alia, alkali metals to form powerfully reducing solutions. The reason for this is attributed to the equilibrium

$$M_{amm} \rightleftharpoons M^{+}_{amm} + e^{-}_{amm} \qquad 1.1$$

but such a model is a gross oversimplification (section 1.2.1), and the abundance of literature[1,2,3(a)] available on their exact nature is indicative of the dilemma which exists about them. The properties and nature of concentrated solutions (>1M) are not discussed here, but an account is given by Lepoutre and Lelieur[3(b)].

1.2.1 Models for Metal-Ammonia Solutions

Since they were first studied by Weyl[4] in 1864 many models for metal-ammonia systems have been proposed. Dye[3(c)] has categorised these under one or more of three general categories: (a) metal based species, (b) double occupancy of cavities, (c) electrostatic aggregates.

(a) Metal Based Species

Kraus[5] has described the situation in terms of a simple dissociation model, equation 1.1, a description significant only for very dilute solutions. In order to explain molar susceptibility measurements Huster[6] proposed that molecular dimers were formed.

$$M_{2\,amm} \rightleftharpoons 2M^{+}_{amm} + 2e^{-}_{amm}$$

Bingel[7] introduced the idea of a species of stoichiometry M^{-}, arising from the capture of an electron pair at a cation site.

$$M_{amm} + 2e^{+}_{amm} \rightleftharpoons M^{-}_{amm}$$

Deigen[8] proposed the presence of species of stoichiometry M, M_2 and M^{-} by analogy with colour centres in crystals. Golden and co-workers[9] and Arnold and Patterson[10] also

invoked species of this stoichiometry, the former workers describing M and M_2 as ion-pairs and M^- as a solvated anion. A model involving the dimerisation and polymerisation of monomers formed from electron capture by solvated cations has also been put forward[11]. All such treatments as these fail to account for the fact that partial molar volumes and optical spectra of the solutions are almost concentration independent which implies that these properties for M_2 and M^- should be the same as for two separate electrons.

(b) Double Occupancy Models

The basis of this model, originally proposed by Ogg[12] and employed by Kaplan[13] and Symons[14], considers the location of an electron pair in the same polarisation centre. Such models must include the existence of the ion-paired species $M^+ \cdot e_2^{2-}$ (giving the stoichiometry M^-). In liquid ammonia this species would give rise to very low concentrations of e_2^{2-} and at low concentrations, when ion-pair dissociation is significant, spin unpairing would be complete. Again those properties largely independent of concentration present the biggest objection to such a model.

(c) Electrostatic Aggregates

Probably the most acceptable description is that proposed by Jolly et al.[15] in which it is postulated that ionic aggregates of M^+ and e^- are formed without the destruction of their individual character. The great advantage of this theory is its ability to deal with the volume and spectral properties and clusters of the principal species M^+ and e^- are used to account for species of stoichiometry M, M_2 and M^-.

In contrast to metal-ammonia systems, metal-amine and

metal-ether solutions show new optical bands[16] and esr[17] absorptions which are characteristic of metal-containing species. Esr shows unequivocally that at least one species with stoichiometry M is present, and in more recent work by Dye et al[18], the 650 nm absorption in sodium-ethylenediamine has been shown to originate from species of stoichiometry M^-. Clearly the absence of any definite changes with concentration in the optical properties of metal-ammonia solutions must indicate that metal-containing and spin-paired species can only be formed by weak interactions among solvated electrons and alkali metal cations.

1.2.2 Reduction by Metal-Ammonia Solutions

The ammoniated electron, from the kinetic point of view has an advantage over the aquated electron in that (a) it can be prepared homogeneously and stored over a wide range of concentrations, (b) many reactions of the electron that are too slow to follow in water by the pr method[19] can be studied in ammonia, and (c) many of the intermediates produced by electron capture are kinetically more stable in liquid ammonia than in water.

1.2.3 Theories of Reduction by Metal-Ammonia Systems

One of the earliest theories of reduction by alkali metals in protic solvents was proposed by von Baeyer[20] to explain the reduction of alkenes by sodium amalgam. The theory, which was fairly widely accepted, involved the production of hydrogen atoms by the interaction of the metal with the solvent. The reactive "nascent" hydrogen then added to the substrate. This theory was superceded by two others which, with appropriate modifications, are still in current use. Willstätter, Seitz and Bumm[21], also by studying

the reactions of sodium amalgam with unsaturated compounds, found it impossible to correlate the high yields of reduction with hydrogen atom production, and proposed instead that the initial step was the addition of sodium to the unsaturated centre, followed by solvolysis:

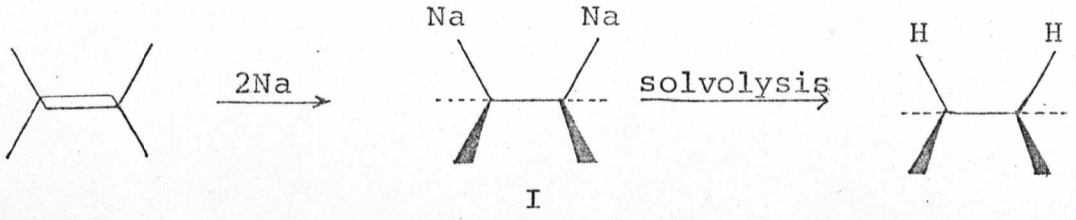

I

However, the theory does not imply any direct rôle of the solvent in the primary reaction. The formation of salt-like adducts of alkali-metals and polycyclic aromatic hydrocarbons lent support to this theory.

Burton and Ingold[22] put forward the view that the primary reaction involved polarisation by the surface of the dissolving metal of the multiple bond undergoing reduction, and thereby allowing protonation to take place. Subsequent addition of two electrons produced a carbanion which then became protonated to form the neutral species:

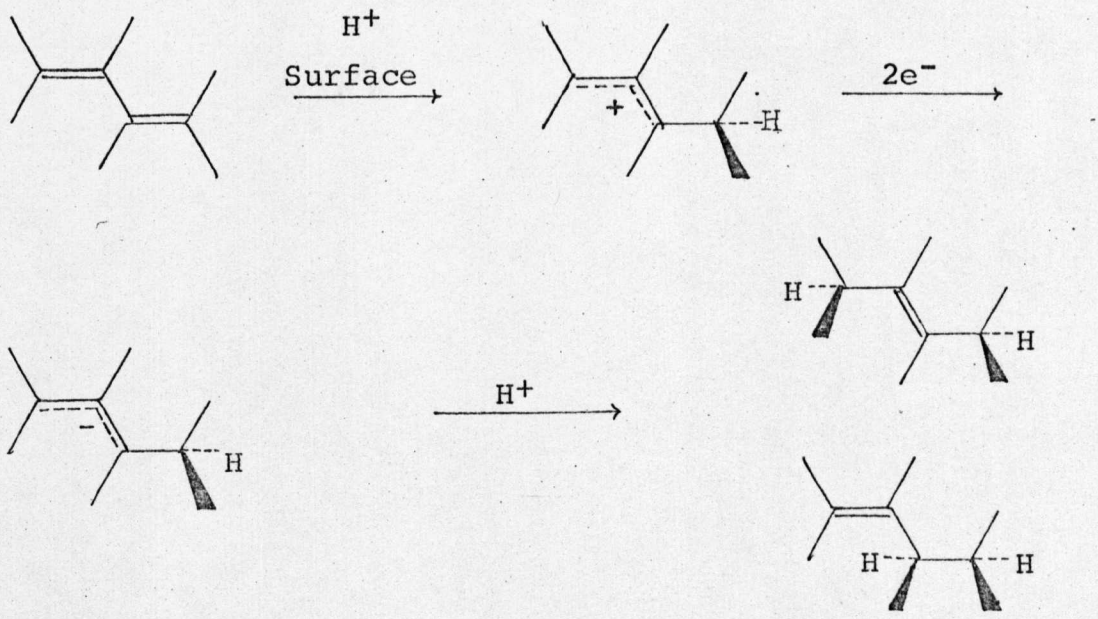

The mechanism, which accounted for 1, 2- and 1, 4- addition could also explain the production of bimolecular reduction products. The initial protonation, however, is not a very feasible step in such a basic solvent as liquid ammonia.

Hückel and Bretschneider[23], noting the similarity between reductions with sodium and calcium, put forward the view that Willstätter's Salts (I) were ionic and that the whole reduction process itself is ionic in nature.

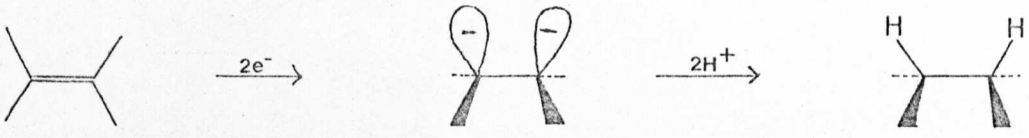

Much support has been found for this theory and many others similar in nature have been proposed[24].

The extrapolation of Willstätter's theory by Michaelis and Schubert[25] has now gained the widest acceptance. From their theoretical treatment of reduction they were able to distinguish between two possible initial stages.

(a) reversible addition of an electron to the substrate to form the radical-anion which then becomes protonated to either dimerise, or undergo further consecutive addition of an electron and a proton,

$$R \rightleftharpoons R^{\cdot-} \overset{H^+}{\rightleftharpoons} RH^{\cdot} \rightleftharpoons \tfrac{1}{2}(RH)_2$$

$$\Big\Vert e^-$$

$$RH^- \xrightarrow{H^+} RH_2$$

(b) reversible addition of two electrons to the substrate, either simultaneously or consecutively, followed by the addition of two protons.

$$R \overset{2e^-}{\rightleftharpoons} R^{2-} \xrightarrow{H^+} RH^-$$

$$\Big\Vert e^- \quad \Big\Vert e^- \qquad 2H^+ \searrow \quad \swarrow H^+$$

$$R^- \qquad\qquad RH_2$$

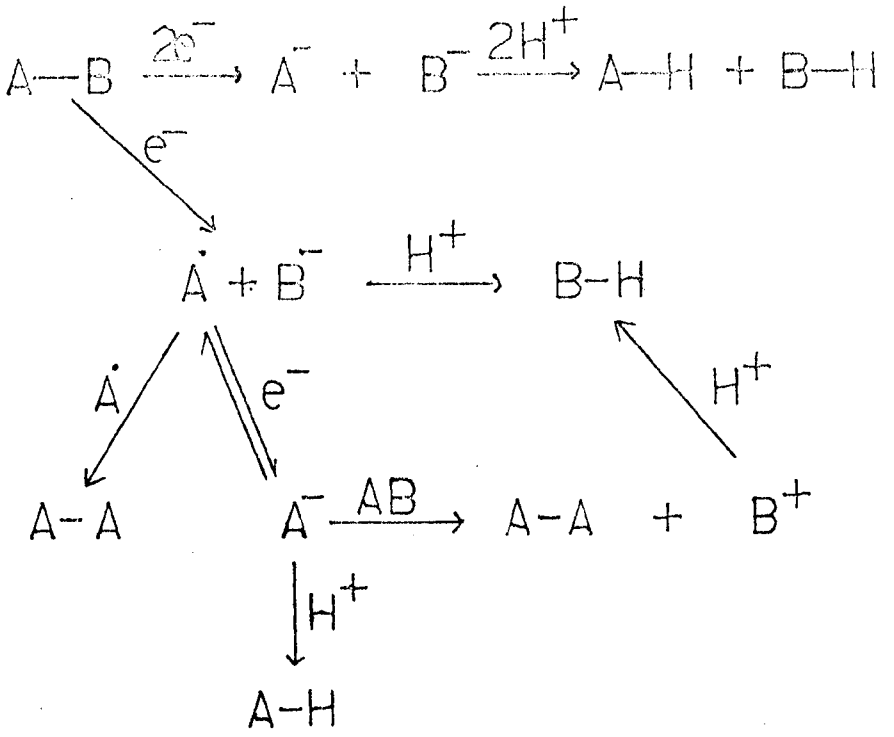

a)

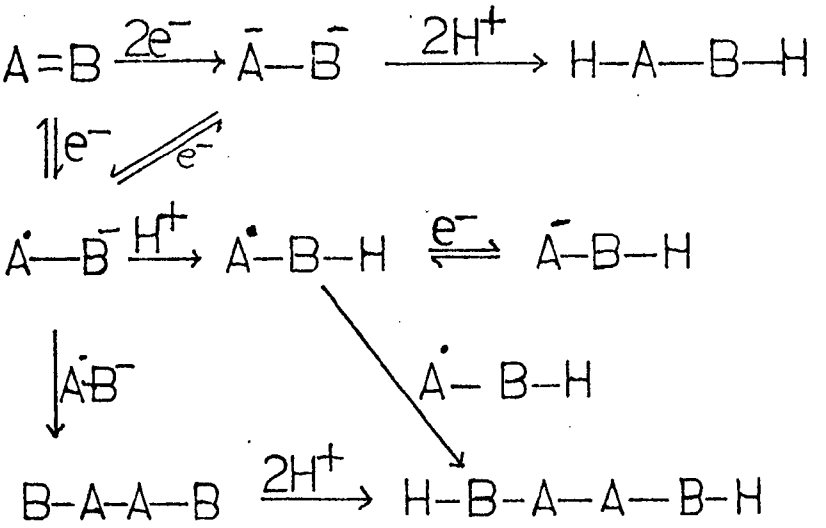

b)

Scheme 1.1

a) Reductive Fission

b) Saturation of a Double Bond

Birch[26] has further elaborated on this theory, systematising reductive fission and reduction, or partial reduction of unsaturation in molecules of the type A-B and A=B (Scheme 1.1). More recently these mechanisms have been discussed by Buick[27], Neal[28] and Jolly[29].

1.3 Kinetics of reactions of the Solvated Electron

Despite the fact that the ammoniated electron has been known for over a hundred years, the availability of kinetic data is minimal[30]. On the other hand such data for the aquated electron, whose existence was postulated some twenty years ago and demonstrated ten years later, is abundant[31].

Metal-ammonia systems are metastable, decomposing slowly under the most stringent conditions[32] and rapidly in the presence of various catalysts to form hydrogen and the corresponding amide.

$$e^-_{(NH_3)_x} \rightarrow \tfrac{1}{2}H_2 + NH_2^- + (x - 1)\ NH_3 \qquad 1\cdot2$$

Many workers have attempted to calculate the rate constant for this reaction but have observed different rates in different vessels. It is believed that it is catalysed by the vessel walls. The homogeneous rate constant for reaction 1.2, estimated[33] as being $< 1\cdot5 \times 10^{-5}s^{-1}$, may be compared with the same reaction with water[34]

$$e^-_{(H_2O)_x} \rightarrow \tfrac{1}{2}H_2 + OH^- + (x - 1)H_2O \quad k < 4\cdot4 \times 10^4 s^{-1}$$

One of the most significant differences between the kinetics of e^-_{amm} and e^-_{aq} is shown by the rate constants for reactions 1·3 and 1·4

$$e^-_{aq} + e^-_{aq} \rightarrow H_2 + 2OH^- \quad k_{1.3} = 6\cdot0 \times 10^9 \text{ l mol}^{-1}s^{-1} \ [34] \qquad 1\cdot3$$

$$e^-_{amm} + e^-_{amm} \rightarrow H_2 + 2NH_2^- \quad k_{1.4} \quad \text{negligible} \qquad 1\cdot4$$

Were it not for the value of $k_{1.4}$ metal-ammonia systems would decolourise in microseconds.

The rate of formation of radical-anions is rapid at even moderate substrate concentrations. The rate constants for the reaction 1·5 have been measured

$$e^-_{solv} + R \rightarrow R^{\cdot -} \qquad 1\cdot5$$

by observing the rates of the first order-decay of the absorption spectrum of e^-_{solv} in the presence of varying quantities of solute in either aqueous, aqueous-alcoholic, or alcoholic solution and vary from $1\cdot4 \times 10^7$ 1 mol $^{-1}s^{-1}$ for benzene to $1\cdot8 \times 10^{10}$ 1 mol $^{-1}s^{-1}$ for acetamide[31]

It is necessary, in reductions by metal-ammonia solutions, to provide a proton source because of the low autoionisation constant ($pK_a = 34$) of ammonia. This is normally achieved by the addition of ammonium ions or compounds which behave as strong acids in ammonia (e.g. ethanol). Doing so, however, introduces a competitive reaction for the solvated electron

$$NH_4^+ + e^-_{amm} \xrightarrow{k} NH_4^{\cdot} \quad \text{PRODUCTS} \quad k \simeq 10^{10} \text{ 1 mol}^{-1}s^{-1} \ [35] \qquad 1\cdot6$$

CHAPTER 2

RADICAL-ANIONS

2 RADICAL - ANIONS

Reactions involving radical-anion intermediates were investigated as early as 1867 by Bertholet[36], but it is only recently that they have been recognised as such. Schlenk[37] in 1914 proposed the earliest enlightened description of the structure of radical-anions, but even so it was not until 1953 that Lipkin and Weissman[38] provided conclusive evidence about their exact nature. They showed by means of esr that for compounds like sodium anthracene, an electron is transferred from the alkali-metal to the aromatic hydrocarbon and is delocalised in its lowest antibonding π-orbital. Organic radicals tend to undergo reactions to form singlet diamagnetic states, and for this reason are generally highly reactive and short lived.

Extensive coverage of the subject of radical-anions has been made by Szwarc[39] and Kaiser and Kevan[40].

2.1 Formation and Study of Radical-Anions

In solution radical-anions may be formed by many processes for example by (a) attachment of solvated electrons, produced in radiolysis or photolysis, to electron acceptors, (b) by reduction of electron acceptors by certain metals (e.g. alkali-metals, or alkaline earth-metals) in suitable solvents, (c) by reduction at the cathode of electrolytic cells, (d) by electron transfer from another radical-anion or (e) in processes involving change-transfer complexes (where they are produced simultaneously with a radical-cation).

Radical-anions possess two important properties which facilitate their study. They are paramagnetic and usually coloured, having intense absorptions in the visible and near

uv parts of the spectrum. These properties enable the techniques of pr and fp to be applied and indeed many kinetic data have been made available by these methods[31,41].

The fact that the unpaired spin in radical-anions tends to make them highly reactive is more than compensated for by the fact that it provides an extremely sensitive probe into their electronic structure. However, methods have had to be devised whereby their lifetimes can be increased. These methods are numerous and more comprehensive reviews may be found elsewhere[42(a)-(k)]. In general they may be studied by matrix isolation methods or by methods which produce them in a steady state concentration (e.g. continuous flow or electrolysis).

2.1.1 Matrix Isolation Methods

In order that a matrix isolation method may be used successfully, the matrix must fulfil the requirements that (a) it is sufficiently rigid to prevent diffusion of the radicals (necessitating use of low temperatures, well below the freezing point of the matrix), that (b) it is inert, interacting with neither the free radicals being studied nor the radiation producing them, that (c) for uv and ir studies it is transparent and that (d) in cases where the radicals are trapped by condensation, it is volatile. Fluorocarbon, hydrocarbon and inert gas matrices are by far the most extensively used. In the case of esr studies, matrices in which the radicals are trapped in relatively large cavities have the added advantage of allowing the trapped radical to undergo extensive "tumbling" motions to average out any anisotropic contributions to their esr spectra (e.g. adamantane) (section 3.1 (b)). There are two

distinct ways of preparing trapped radicals - (a) production in situ by radiolysis or photolysis or (b) by forming them in the gas phase and then co-condensing them with molecules of the matrix. Of all the solid state methods one of the most elegant is the rotating cryostat method of Bennett[43]. Alternate layers of two reactants (e.g. Sodium and alkyl halides) are condensed from the gas phase on the surface of a rapidly rotating cold finger (77 K) at low pressure ($< 10^{-5}$ Torr). The 'swiss roll' of radicals so formed may then be transferred under the same conditions to the cavity of an esr spectrometer.

Solid state methods are subject to the limitation of broad resonance lines (section 3.3) and in general only low resolution specta may be obtained.

2.1.2 Steady-State Methods

Steady-state concentrations of radical-anions may be produced either electrolytically or in flow systems or by continuous irradiation.

In electrolytic processes, the cathode acts as a continuous electron donor and attachment of single electrons to suitable acceptors in its vicinity results in the production of a steady state concentration of the corresponding radical-anion. Electrochemical generation of radical-anions has several advantages over other methods in that it requires the use of small amounts of substrate and reduction may be carried out in a variety of solvents. Suitable control of the reduction potential can be used to prevent the formation of diamagnetic dianions. Clearly interference may arise from secondary products formed in the vicinity of the cathode as the reduction process continues.

The use of flow techniques to produce steady-state concentrations of transient intermediates in the gas phase is a long-established technique[44] and was first applied to reactions in the liquid phase by Roughton[45]. Stone and Waters[46], and Norman[47] were the first workers to use the method to study transient free radicals in aqueous solution, and more recently it has been used by Buick et al.[48] to study the reactions of e^-_{amm} in liquid ammonia. In order that intermediates might be observed, the flow system must provide a mixing time which is short by comparison with the life-time of the intermediate. Aqueous flow systems have the disadvantage that the high dielectric constant for water necessitates mixing outside the cativy of the esr spectrometer and the time between mixing and observation is not less than 0·02 s. In liquid ammonia this is not so, and suitable mixer design[48] has enabled mixing to be performed within the cavity in a few ms. Rapid mixing techniques have the disadvantage that they require fairly large amounts of substrate.

Techniques employing continuous irradiation of samples in the esr cavity can also produce transient intermediates in sufficiently high steady-state concentrations for observation by esr. The method has a similar advantage to electrolysis in requiring only small amounts of substrate. Radiolytic methods tend to be rather less selective than photolytic ones, but a single radical is often obtained.

2.1.3 Indirect Magnetic Resonance Methods

Allied to the direct observation of transient free radicals are the techniques of spin trapping[49] and Chemically Induced Dynamic Nuclear Polarisation (CIDNP)[50].

Spin trapping involves the capture of transients by an

additive to produce a more stable radical, detectable by esr, whose hyperfine coupling constants permit the identification of the initial radical trapped.

$$\underset{\text{(transient)}}{R^{\cdot}} + \underset{\text{TRAP}}{\text{SPIN}} \rightarrow \underset{\text{(stable)}}{\underset{\text{ADDUCT}}{\text{SPIN}}}$$

Spin traps are usually of the nitroso or nitrone type of compound. t-Butylnitrone for example has been used to trap the secondary radicals in the reaction of hydroxyl radicals with methanol[51]

$$H_2O_2 \xrightarrow{h\upsilon} 2HO^{\cdot}$$

$$HO^{\cdot} + CH_3OH \rightarrow H_2O + \dot{C}H_2OH$$

$$HOCH_2^{\cdot} + (Me)_3C\text{-}N{=}O \rightarrow HOCH_2\text{-}\underset{\underset{O^{\cdot}}{|}}{N}\text{-}C\text{-}(Me)_3$$

CIDNP is itself only diagnostic of short lived free radicals in a system. The phenomenon depends on strong polarisation of certain nuclear spins by the unpaired electron during the molecule's existence as a free radical and is manifested by emission or enhanced absorption lines in nmr spectra. The absence of any CIDNP effect does not imply the absence of free radicals.

2.2 Electron Spin Resonance in the Study of Radical-Anions

As instrumentation became more refined towards the end of the 1950's, the wealth of publications on esr studies of organic free radicals increased markedly. Much of the work around this time was concerned with stable free radicals of aromatic hydrocarbons, and contributions by Weissman and his collaborators[52,53] are of particular significance. With reliable data becoming available, much work was initiated on theoretical aspects of hyperfine splitting (section 3.2) and presently-accepted theories have their foundations in

these studies. Some of the more important contributions to the study of free radicals and their reactions are now discussed.

Although observation of trapped alkyl radicals at cryogenic temperatures had been reported by several workers[54,55] it was not until the classical work of Fessenden and Schuler[56] that these unstable intermediates were fully characterised. Using continuous irradiation with 2·8 Mev electrons, they were able to produce steady state concentrations of alkyl radicals in liquid hydrocarbons at low temperatures. Their well-resolved spectra enabling γ-proton couplings and second-order splittings[57] to be resolved. Radiolysis in liquid systems has since allowed reactions of O^- [58], $OH^\cdot$ [58,59] $H^\cdot$ [60], and e^-_{solv} [61] to be studied. Studies of other radiolytic processes have been made on carboxylic acids[62,63,64], esters[64], amides[65], and amino acids[62,65], both in the crystalline and polycrystalline state.

Despite the fact that polarographic reductions had been studied for many years, it was not until 1960 that it was first used by Maki and Geske[67] to characterize the radical-anions of nitro aromatics by esr. The technique has since found wide application, for example in the study of nitriles[68], ketones[69,70], ferrocenes[71], and thiobenzamides[72-74]. Electrolysis in liquid ammonia, where homogeneous reduction is effected by e^-_{amm} produced at the cathode, has accounted for the characterization of the radical-anion of butadiene[75] and its alkyl homologues[76], and nitrogen containing heteroaromatics such as pyridine and pyrimidine and their derivatives[77]. A more recent development of the electrolytic method is that of Konishi et al.[78] where studies of acridine and its halogen

derivatives were facilitated by the inclusion of a slow flow modification. The work of Waters on the production of aryloxy[46], meta-semiquinone[79] and anilino radicals[80], and the reduction of nitro-compounds[81], describes the application to esr spectroscopy of the Dixon and Norman flow technique[47]. This technique has been more widely applied to the study of the reactions of the hydroxyl radical, produced by the $Ti(III)/H_2O_2$ couple.

$$Ti^{3+} + H_2O_2 \rightarrow Ti^{4+} + OH^- + OH^{\cdot}$$

In general the hydroxyl radicals formed undergo hydrogen abstraction reactions 2·1 or addition 2·2.

$$OH^{\cdot} + CH_3OH \rightarrow {}^{\cdot}CH_2OH + H_2O \qquad 2\cdot1$$

$$OH^{\cdot} + CH_2{=}\underset{\displaystyle CN}{\underset{|}{C}}H \rightarrow HO{-}CH_2 - \underset{\displaystyle C\dot{N}}{\overset{\displaystyle H}{\overset{|}{\underset{|}{C}}}} \qquad 2\cdot2$$

In cases where both are possible, the latter is favoured and in saturated systems such as alcohols[47], ethers[47], ketones[82] and acids[82] abstraction from the α-position is favoured. The use of Fe(II) in the couple gives in many cases the same radicals as Ti(III) but in certain cases differences in the relative concentration of radicals are observed and are attributed to the difference in the oxidising powers of Fe(III) and Ti(IV)[83] and in this respect the selectivity of Fe(III) between tetravalent carbon atoms in different environments. Ti(III) coupled with hydroxylamine[84], formic acid[85] or hydrogen peroxide and persulphate[86] has been used to study the reactions of $NH_2^{\cdot}$, $CO_2^{\bar{\cdot}}$, $HCO_2^{\cdot}$ and $SO_4^{\bar{\cdot}}$.

The ability of liquid ammonia to dissolve alkali metals to produce e^-_{amm} has been utilised by Buick et al., and in the present work in liquid ammonia flow systems (Chapter 4). It has hitherto been used to study electron attachment to aryl halides[48], aromatic carboxylic acids[87], pyridines[88] and styrenes[89].

Many free radicals and free radical reactions have been examined by the continuous liquid photolysis methods of Kochi and Krusic[90]. Radicals are generated by uv irradiation of static solutions of peroxides in the cavity of an esr spectrometer. Di-t-butylperoxide is irradiated (250-300 nm light) in the presence of appropriate substrates. Only the products of the reactions of the t-butoxy radicals are observed, arising principally by hydrogen abstraction, addition and displacement, and to a lesser extent by rearrangement and fragmentation. The transparency of di-t-butylperoxide in this region of the uv (ε = 20 l mol $^{-1}$cm^{-1} at 253·7 nm) requires an intense source of radiation, and this tends to limit the variety of substrates that can be used. Diacyl peroxides and peresters on the other hand have larger extinction coefficients in the same region (20-40 l mol $^{-1}$cm^{-1} and 50-60 l mol $^{-1}$cm^{-1} respectively), and have the further added advantage that unlike di-t-butylperoxide the solution quantum yield for decomposition is unity and independent of the viscosity of the medium. These methods have been extensively applied to structural problems and reaction mechanisms, for example the study of allylic radicals and isomerisation[91] methylcyclopropyl radicals[92] the 7-norbornenyl radical[93] group IV organometallic alkyl radicals[94] and the study of hindered interal rotation and equilibrium conformation of

alkyl radicals[95].

A method involving both continuous irradiation and slow flow has been used by Kemp and Greatorex to study free radicals produced in solution during photo-oxidation by transition metal ions. The photo-reactions between cerium (IV) and uranium (VI) and alcohols being studied[96]

The study of radical-anions of diones by Russel et al.[97] has made a major contribution to the field of conformational analysis. The radical-anions are produced by electrolytic reduction or reaction of the appropriate α-hydroxy ketone in DMSO containing an excess of potassium t-butoxide

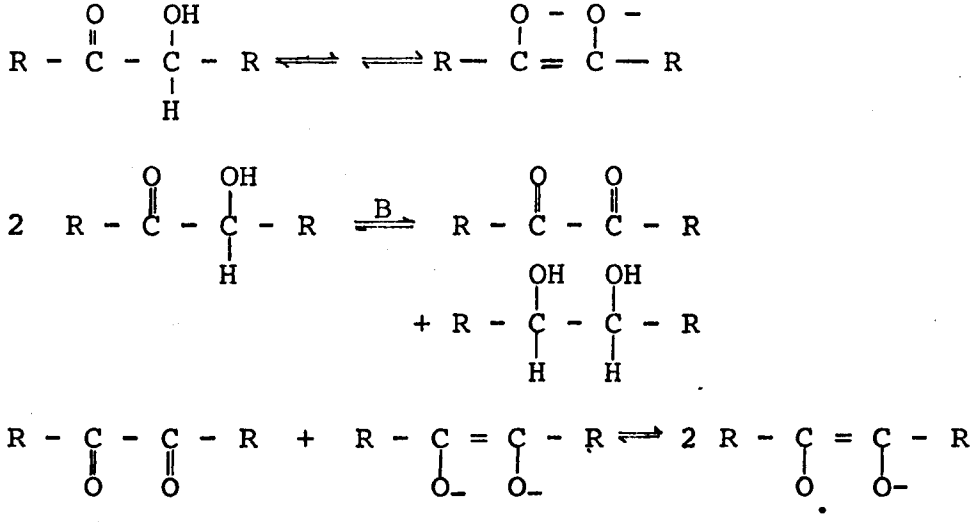

Semidione radical-anion

Many acyclic[98a)-c)] and monocyclic semidiones[98c)] produced by these methods are very stable, even when R is alkyl or hydrogen, and have been studied extensively. Particular attention has been paid to the conformational equilibria in semidiones derived from cyclic systems.

2.3 Reactions of Radical-Anions

(i) Reduction

$$AB^{\cdot-} + e^- \longrightarrow AB^{2-} \cdot \qquad 2\cdot3$$

The ability of a molecule AB to take up a single electron

depends on the availability of low energy antibonding MO's. The addition of two electrons to such an orbital would not be considered as being energetically unfavourable, and in certain cases, polarographic reduction of organic compounds show two characteristic waves corresponding to the consecutive uptake of two electrons to form the radical-anion and diamagnetic dianion respectively[99]. Reaction 2·3 has been discussed in the reduction of organic compounds by metal-ammonia systems (section 1.2.2).

(ii) Dissociation

$$AB^{\cdot-} \rightarrow A^{\cdot} + B^{-} \qquad 2\cdot4$$

Dissociation reactions can be very fast ($k > 10^7 s^{-1}$) depending on the bond strength of A-B and the electron affinity of B. Pr of Benzyl chloride leads to the formation of benzyl radicals[100] arising from the dissociation of the parent radical-anion.

$$PhCH_2Cl \xrightarrow{e^-} PhCH_2^{\cdot}Cl^{-} \rightarrow PhCh_2^{\cdot} + Cl^{-}$$

Dissociation reactions have been proposed as intermediate steps in such reactions as C-alkylation of p-nitrobenzyl-chloride[101] and in the dehalogenation of aryl halides by solvated electrons[48].

(iii) Disproportionation

$$2AB^{\cdot-} \rightleftharpoons AB + AB^{-}$$

There is little evidence in the extant literature for reactions of this type. Dissociation constants have been measured[102] in various polar solvents for the equilibrium

$$2[R_2C = CR_2]^{\cdot-} M^{+} \rightleftharpoons [R_2\dot{C} - \dot{C}R_2]^{2-} 2M^{+} + R_2C = CR_2$$

the disproportionation being strongly dependent on the nature of the solvent, cation and radical-anion. Rate constants, measured by pr, are found to be fast

$2I_2^{\cdot-} \rightarrow I^- + I_3^-$ $\quad k \simeq (7{\cdot}7 \pm 1{\cdot}5) \times 10^9$ l mol^{-1}s^{-1}

(iv) Dimerisation and Polymerisation

$2AB^{\cdot-} \rightleftharpoons {}^-ABAB^-$ 2·5

Radical-anions of aromatic hydrocarbons, such as naphthalene and anthracene, do not undergo dimerisation. The loss of resonance energy in such a process is not compensated for by the formation of a new C-C bond. On the other hand hetero-aromatics will undergo reaction 2·5, particularly if they are present as ion-pairs. The pyridine radical-anion shows a marked tendancy to dimerise in HMPA solution, but small amounts of monomer can be detected by esr[103]. Stopped flow techniques have been used to study the dimerisation of the 1,1-diphenylethylene radical-anion in HMPA[104]. The rate constant in this solvent ($k \simeq 10^5$ l mol^{-1}s^{-1}) is considered as corresponding to the free ion dimerisation. The rate for the same reaction in THF where the radical-anion is in its ion-paired form is an order of magnitude larger[105].

The dimerisation of vinyl and vinylidine radical-anions is proposed as the initial stage of polymerisation by an electron transfer process[106]. The styrene radical-anion will for example react rapidly with another styrene radical-anion, 2·6, or with another styrene molecule, 2·7, to form either a diamagnetic-anion, or a dimeric radical-anion, both of which can undergo polymerisation in the presence of excess monomer.

$$2Ph - \dot{C}H - CH_2 \rightleftharpoons Ph - \bar{C}H - CH_2 - CH_2 - \bar{C}H - Ph \qquad 2{\cdot}6$$

$$Ph - \dot{C}H - CH_2 + Ph - CH = CH_2 \rightleftharpoons Ph - \dot{C}H - CH_2 - CH_2 - \bar{C}H - Ph \qquad 2{\cdot}7$$

(v) Protonation

Dorfman et al.[107] have studied the lifetimes of aromatic hydrocarbons in aliphatic alcohols and have attributed their fast first order decay to the reaction,

$Ph^{\cdot -} + ROH \rightarrow PhH^{\cdot} + RO^{-}$

the rate constants correlating well with the acidity measurements of the various alcohols.

Photolysis of benzophenone in toluene/N,N-dimethylaniline solution leads to the formation of the protonated benzophenone ketyl[108(a)]. Wilkinson and Porter[108(b)] have calculated the pK value for this species, produced by fp in isopropanol/water mixtures, to be 9·2 ± 0·1.

Buick et al.[88] have observed by esr the protonated radical-anions of pyridine and some carboxy pyridines.

(vi) Electron-transfer

The simplest case of electron-transfer reactions is represented by exchange between a radical-anion and its parent molecule

$AB^{\cdot -} + AB \rightleftharpoons AB + AB^{\cdot -}$

and rates have been measured in several instances by esr line-broadening[39,109].

Electron transfer may also take place between a radical-anion and another molecule

$AB^{\cdot -} + XY \rightleftharpoons AB + XY^{\cdot -}$

The nature of $XY^{\cdot -}$ may vary markedly. On the one hand it can represent a fairly stable radical-anion, as in the reaction of tolan with sodium naphthalenide[110] or one of extremely short lifetime, as in the reaction of alky halides with sodium naphthalenide[111].

CHAPTER 3

ELECTRON SPIN RESONANCE

3 ELECTRON SPIN RESONANCE

3.1 The Resonance Condition

The electron has a non-classical angular momentum called spin which gives rise to a magnetic moment

$$\vec{\mu} = \gamma_e \hbar \vec{S} = - g_e \beta_e \vec{S}$$

where $\hbar S$ is the spin angular momentum vector of the electron. The number of allowed spin states is restricted by quantum mechanics such that the component, m_s, of the spin angular momentum vector in any given direction can only take the values S, S - 1, ..., -S, where S is the total spin quantum number. For the electron $S = \frac{1}{2}$ and hence the only allowed quantum states are $m_s = -\frac{1}{2}$ or $|\beta\rangle$, or $m_s = \frac{1}{2}$ or $|\alpha\rangle$. Application of a magnetic field results in an interaction between the magnetic moment and the applied field (Zeeman effect) which may be represented by the Hamiltonian

$$H_S = - \vec{\mu} \cdot \vec{H}$$

which on substituting for $\vec{\mu}$ becomes,

$$H_S = g_e \beta_e H m_s$$

if the field is applied in the z direction. If an oscillating field, perpendicular to H, is applied then transitions between the lower energy state $|\beta\rangle$, and the higher energy state $|\alpha\rangle$ may be induced, providing the frequency, υ, of the oscillating field satisfies the resonance condition

$$\Delta E = h\upsilon = g_e \beta_e H \qquad 3\cdot1$$

In the case of paramagnetic molecules where the component atoms have nuclear spin, an interaction between the nuclear magnetic moment and the applied magnetic field also occurs and a similar Hamiltonian may be derived to represent this interaction,

$$H_I = g_N\beta_N H m_I$$

where m_I is the allowed component of the nuclear spin in the z direction. Although transitions between these energy levels are not seen in the normal esr experiment, coupling between the two spin vectors does give rise to hyperfine structure in the esr spectrum. This coupling may take place in two ways.

(a) Isotropic Hyperfine Coupling

The magnetic moments of the electron and the nucleus are coupled by the contact interaction. This interaction first formulated by Fermi[112], is represented by the operator

$$H_C = a\vec{I} \cdot \vec{S} = \frac{8\pi}{3} g_e\beta_e g_N\beta_N \delta(\vec{r})\vec{I} \cdot \vec{S} \qquad 3\cdot2$$

The coupling constant, a, has the dimensions of energy and is subject to the restrictions of the Dirac delta-function in that it is zero unless $(\vec{r})$ is zero, i.e. isotropic coupling only takes place if there is a finite electron spin density at the nucleus.

(b) Anisotropic hyperfine interaction

Coupling also occurs in an analogous manner to the classical dipolar coupling between two bar magnets and is represented by the quantum mechanical operator

$$H_D = - g_e\beta_e g_N\beta_N \left\{\frac{\vec{I} \cdot \vec{S}}{r^3} - \frac{3(\vec{I} \cdot \vec{r})(\vec{S} \cdot \vec{r})}{r^5}\right\}$$

where $\vec{r}$ is the radius vector of the two moments. In the case of molecules with spherical symmetry this interaction averages to zero. Weissman[113] has shown that in solution rapid tumbling gives molecules an effective spherical symmetry.

The complete Hamiltonian, referred to the z direction, for a molecule with spherical symmetry may then be written

$$H = g_e\beta_e H m_S - g_N\beta_N H m_I + a m_I m_S$$

In the high-field limit where the electron-nuclear inter-

actions may be considered as a small perturbation on the Zeeman levels, this "spin" Hamiltonian gives rise to the energy levels

$$E = (g_e\beta_e m_S - g_N\beta_N m_I)H + a m_I m_S \qquad 3\cdot3$$

and the selection rules

$$\Delta m_I = 0,\ \Delta m_S = \pm 1$$

For a single electron interacting with n nuclei of spin m_I^n and coupling constants a^n, and neglecting the nuclear Zeeman interactions, the resonance condition may be formulated,

$$h\upsilon = [\underline{g}\ \beta_e H + \sum^{n} a^n m_I^n] \qquad 3\cdot4$$

For the systems studied in this work the orbital momentum is almost entirely quenched and so $\underline{g}$, in equation 3·4, which is a measure of the coupling between spin and orbital angular momenta, is very close to the value for the free electron g_e. The $\underline{g}$-factor is characteristic of a particular system.

3.2 The Mechanism of Hyperfine Splitting

The condition for isotropic coupling to occur between the electron and nuclear spin vectors is that there should be a finite spin density at the nucleus, equation 3·2, i.e. the orbital containing the unpaired spin should possess some s-character. In conjugated π-radicals the unpaired electron is delocalised in a π*-antibonding orbital. Since this orbital has a node in the molecular plane, no hyperfine splitting would be expected from aromatic ring protons. This is not what is observed experimentally and many theories have been put forward to account for this paradox, including zero point vibrations[38(b)] and indirect coupling through chemical bonds[114]. The problem is resolved when interactions between σ-and π-electrons are considered. This approach has been used successfully by several authors[115]. The unpaired

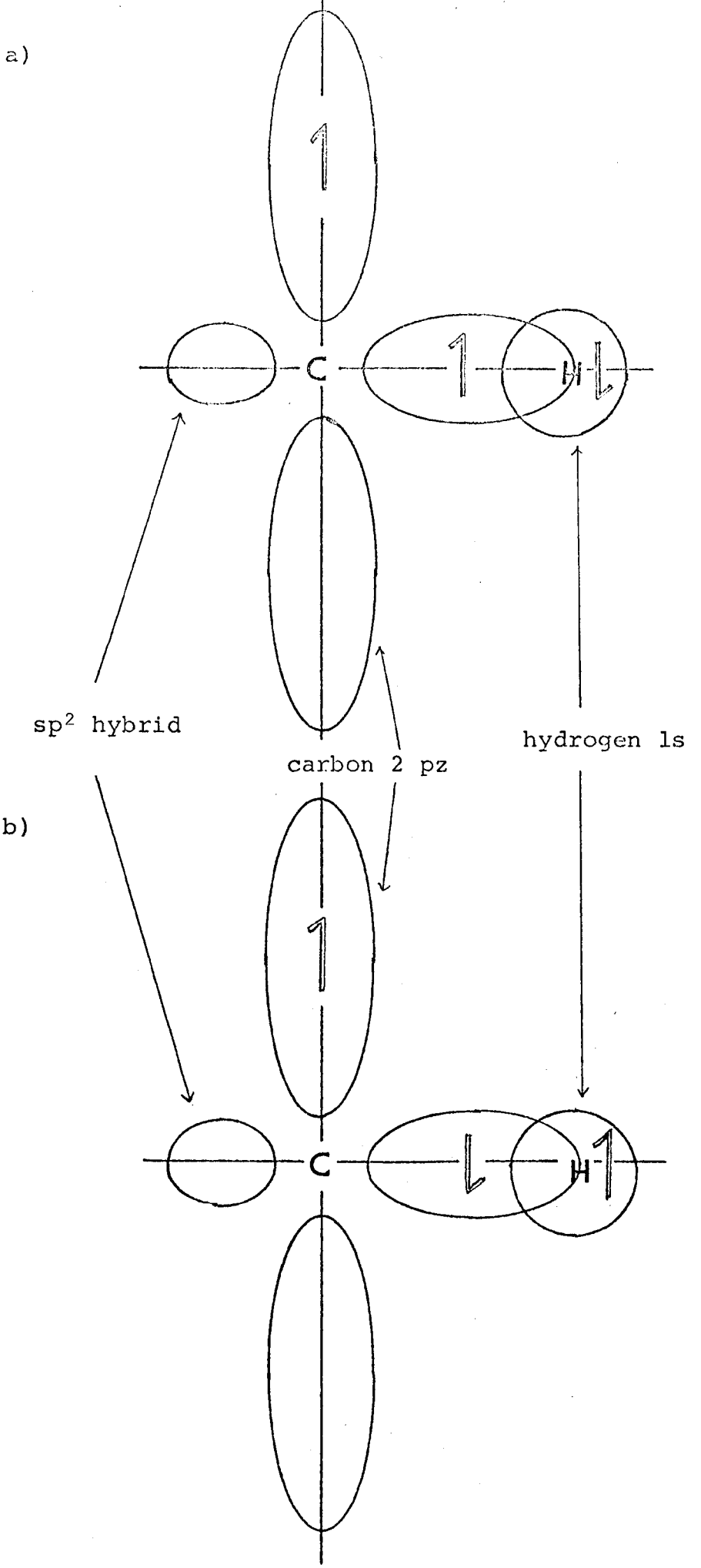

Fig. 3.1 Spin Polarisation in an Isolated C-H fragment

spin of the electron in the carbon $2p_z$ orbital polarises the spins of the electrons in the C-H bond and thereby induces some unpaired spin in the hydrogen 1s orbital. The concept of spin polarisation may be realised more fully be examination of an isolated C-H fragment of a conjugated system (Fig. 3.1). If the unpaired electron in the carbon $2p_z$ orbital is described by the state $|\alpha\rangle$ then the configuration of the electrons in the C-H bond may then be either $|\alpha\rangle|\beta\rangle$ or $|\beta\rangle|\alpha\rangle$, Fig. 3.1 (a) and (b) respectively. Of these two configurations (a) is the more probable (Hund's rules) and as a result an excess of β spin is induced in the 1s orbital. McConnell[115(a)] proposed that the coupling constant, a_{CH}^{H}, of the proton is directly proportional to the unpaired spin density, ρ_C, in the Π-atomic orbital of the carbon atom to which it is attached,

$$a_{CH}^{H} = Q_{CH}^{H}\rho_C \qquad 3\cdot5$$

where Q_{CH}^{H} is the σ-Π-interaction parameter. Detailed MO and VB calculations have confirmed both the form of this equation and the sign of Q_{CH}^{H}. The value of Q_{CH}^{H} has been calculated as -2·37 mT which is in excellent agreement with experimental observations. The value however appears to vary slightly with excess charge on the carbon atom and is clearly dependent on its hybridisation.

The coupling of methyl protons in conjugated systems (and substituted methyl) is readily understood in terms of a hyperconjugative mechanism, and McLachlan[116] using a VB technique has shown that

$$a_{CH_3}^{H} = Q_{CCH_3}^{H}\rho_C \text{ where } Q_{CCH_3}^{H} = 2\cdot8\text{mT} \qquad 3\cdot6$$

The direct interaction of the protons with the Π-system implies the $Q_{CCH_3}^{H}$ will have the opposite sign to Q_{CH}^{H}.

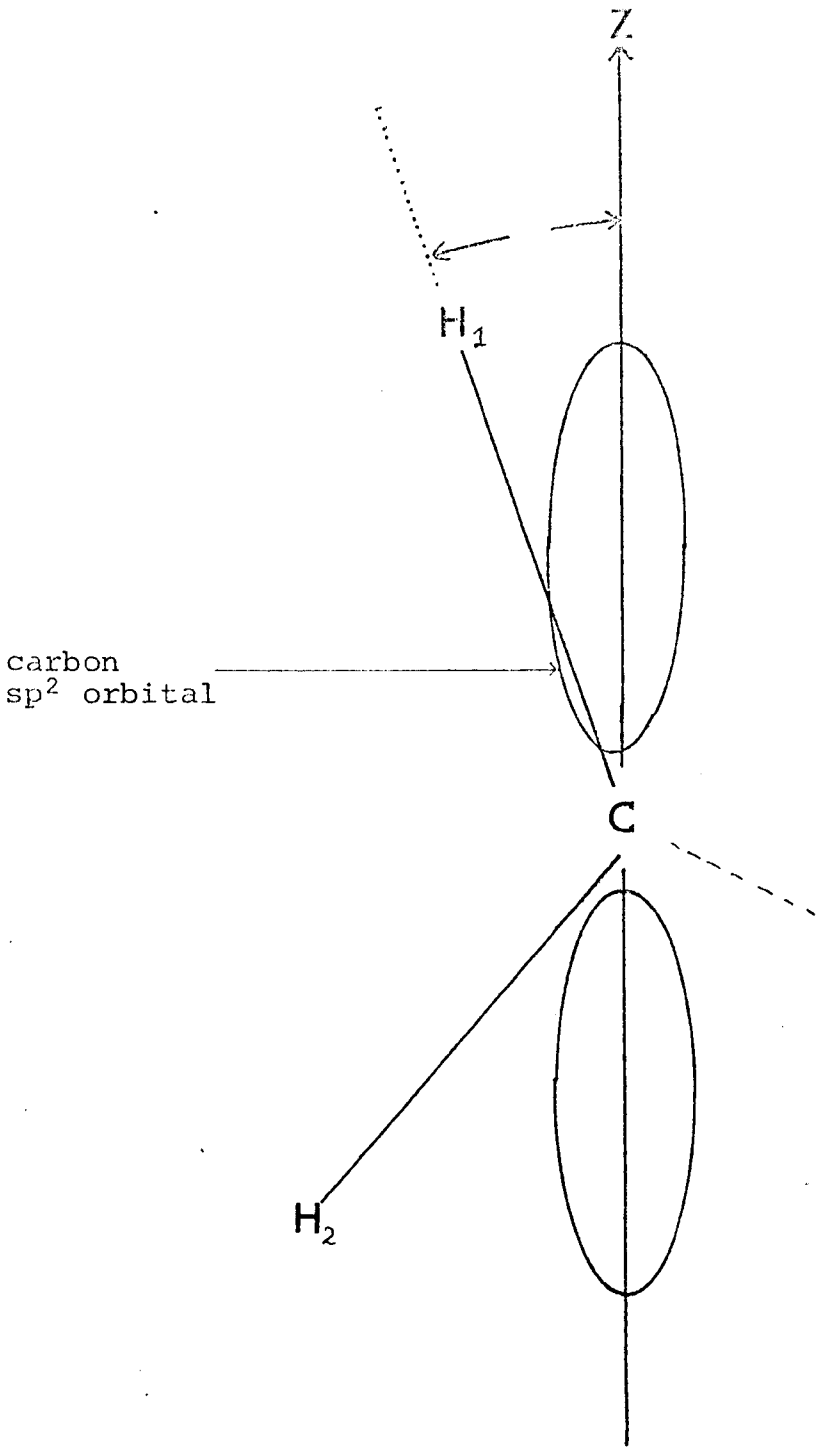

Fig. 3.2 View along C'-C bond of the fragment C'-C$\begin{smallmatrix}H\\H\end{smallmatrix}$

Applying similar configuration interaction techniques Karplus and Fraenkel[117] have derived similar expressions for ^{13}C and ^{14}N atom splittings.

3.2.1 Coupling of Conformationally Fixed β-Protons

Fig. 3.2 represents a view along the C'-C bond of the fragment $C'-C\langle^{H_1}_{H_2}$ where C' is an sp^2 carbon atom and $-C\langle^{H_1}_{H_2}$ is a conformationally fixed methylene group. θ is the angle between the z axis and the projection of the C-H_1 bond on the plane through the $2p_z$ orbital, perpendicular to the C'-C bond. The wave function for the $2p_z$ orbital indicates that the distribution of the spin density in this plane is of the form

$$\psi^2_\theta(0) = \psi^2_0(0)\cos^2\theta$$

where $\psi^2_\theta(0)$ and $\psi^2_0(0)$ are the spin densities corresponding to the angles θ and 0°. On the assumption that the isotropic hyperfine interaction follows a similar relationship, the maximum coupling would arise when $\theta = 0^\circ$ and zero when $\theta = 90^\circ$. The coupling constants for protons H_1 and H_2 may then be written

$$a^{H_\theta}_{CCH_2} = Q^{H}_{CCH}\rho_c\cos^2\theta \qquad 3\cdot7$$

$$a^{H_{\theta+120}}_{CCH_2} = Q^{H}_{CCH}\rho_c\cos^2(60-\theta) \qquad 3\cdot8$$

where ρ_c is the spin density in the carbon $2p_z$ orbital and Q^{H}_{CCH} is a constant characteristic of the C'-$C\langle^{H}$ system. For a system which is free to rotate about the C'-C bond 3·7 reduces to

$$a^{H}_{CCH}{}_{av} = Q^{H}_{CCH}\rho_c \cdot \frac{1}{2\pi}\int_0^{2\pi}\cos^2\theta d\theta = \tfrac{1}{2}Q^{H}_{CCH}\rho_c$$

which for the ethyl radical, assuming $\rho_c = 1$ gives $Q^{H}_{CCH} = 54$.

An empirical relationship has been developed to account for angular dependence of β-couplings viz.,

$$a^{H\theta} = [B + B_0 \mathrm{Cos}^2\theta]\rho_c \qquad 3.9$$

where $B \simeq 0{\cdot}4$ mT and $B_0 \simeq 5{\cdot}0$ mT. The introduction of B, which may be interpreted as a spin polarisation term, is to account for non-zero couplings when $\theta = 90^o$.

3.3 Spin Relaxation and Line Shape

Calculation of transition probabilities shows that transitions in either direction between the two states $|\alpha\rangle$ and $|\beta\rangle$ are equally probable. Whether or not absorption or emission will occur is therefore determined by the relative population of the two states. Application of the Boltzmann distribution law shows that since at ordinary temperatures $kT >> g_e\beta_e H$, the ratio of the populations in the two states $N_\beta : N_\alpha$ is only slightly less than unity, and application of a resonant rf field would rapidly saturate (section 4.5) the upper level and absorption of energy would cease. However non-radiative transitions between the two states do arise by transference of the excess magnetic energy to other degrees of freedom. This is called spin-lattice relaxation, denoted by T_1, and is the time to decrease N_α by $^1/_e$. Since relaxation time determines the lifetime, Δt, of a spin state, it is related to the uncertainty in the energy of the Zeeman levels, ΔE, by the Heisenberg relationship

$$\Delta E \,.\, \Delta t \simeq \frac{h}{2\pi}$$

and thereby affects the shape of the esr line. However the width of the esr line is usually much greater than would be expected from the value of T_1, and a new relaxation time, T_2, based on the width at half height, Γ^*, of a normalised line

* Referred to as linewidth.

may be defined

$$^1/_{T_2} = K\gamma_e\Gamma$$

K = 1 for Lorenzian shaped lines and $(\pi \ln 2)^{\frac{1}{2}}$ for Gaussian*.

T_2 is a linear function of linewidth and includes both lifetime broadening (T_1) and other broadening processes, usually homogeneous in nature. T_2 may therefore be written

$$\frac{1}{T_2} = \frac{1}{T_2'} + \frac{1}{2T_1}$$

where T_2' is the spin-spin, or transverse, relaxation time. (The factor of 2 appears because $2T_1$ is the mean spin lifetime.) For many systems $T_1 >> T_2'$ and so $T_2 \simeq T_2'$ i.e. the linewidth is a measure of $^1/_{T_2'}$. The processes which contribute to line-broadening are numerous and include electron-electron and electron-nuclear, spin - dipolar interactions, and chemical processes if they alter the magnetic environment of the unpaired spin.

3.3.1 General Model for Chemical Line-Broadening Mechanisms

Theoretical explanations of chemical line-broadening mechanisms have been made using both the Modified Bloch equations[118] and the relaxation matrix treatments[119]. The former method is more generally applicable in that it covers a wider range of rates but it is a secular treatment and does not consider changes in nuclear and/or electron spin states during the reaction. While the relaxation method does take account of secular processes, it is only applicable to the

* In solution lineshapes are best approximated to by Lorenzian shaped lines. Gaussian shaped lines are usually found in the solid state where in-homogeneous broadening occurs. This arises from the unpaired spin being subjected to slightly different effective magnetic fields and hence at any one time, only a few spins resonate as the magnetic field sweeps through the line. The line is then a superposition of a large number of individual components slightly shifted from one another. The component line shapes are Lorenzian, but the overall shape is Gaussian.

fast rate region.

As the rate of interconversion between the two forms increase from the slow limit, where the lines observed are attributable to two distinct species, to the fast limit where the lines coalesce to positions that are the weighted means of the original line positions, five distinct stages may be distinguished. Consider a free radical that can exist in two interconverting forms A and B. When the rate of interconversion is slow then these two forms are distinguished during the time of the esr experiment and, for example, if they have different single line esr spectra, a simple two line spectrum will be observed where the linewidth $\Gamma = \Gamma_0$. As the lifetimes of the species decrease the mean lifetime, τ, for line broadening to be significant can be calculated from the Uncertainty Principle ($\Gamma = 0{\cdot}01\text{mT} \equiv \tau = 5 \times 10^{-7}\text{s}$). At the limit of slow interconversion the relationship between the linewidth Γ and the mean lifetime is[120]

$$\Gamma = \Gamma_0 + \frac{1}{2\tau\gamma_e} \qquad 3{\cdot}10$$

where 2τ is the mean lifetime of species A or B, (τ is defined as $\frac{\tau_A\tau_B}{\tau_A + \tau_B}$, so for equal lifetimes $\tau_A = \tau_B = 2\tau$).

When the interconversion rate approaches the difference in the resonance frequencies for the two species, the lines continue to broaden and shift towards their midpoint, the shift being given by[121]

$$(\delta H_0^2 - \delta H_e^2)^{\frac{1}{2}} = \frac{\sqrt{2}}{\gamma_e\tau}$$

where δH_0 is the separation in the absence of interconversion and δH_e is the separation when interconversion is taking place.

For very fast rates of interconversion the width of the

esr line is proportional to τ and the mean square of δH_0, and is given by[122]

$$\Gamma = \Gamma_0 + \gamma_e \tau \frac{<(\delta H_0)^2>}{4}$$

In the limit the two lines coalesce and clearly as the rate increases towards its limit the single line will narrow to $\Gamma = \Gamma_0$.

If the two forms are not equally probable then the position of convergence is given by

$$H = \frac{P_A H_A + P_B H_B}{P_A + P_B}$$

where P_A and P_B are the probabilities of the two forms and H_A and H_B are the field values at which they resonate. The linewidth is given by[122]

$$\Gamma = \Gamma_0 + \gamma_e \tau P_A P_B (\delta H_0)^2 \qquad 3\cdot11$$

3.3.2 Mechanisms contributing to line-broadening

Bimolecular electron exchange between two colliding free radicals can result in line-broadening, but only when the electrons are exchanged between non-equivalent magnetic states. Electron transfer reactions (section 2.3 (vi)) also cause line-broadening, but in this case the extent of the broadening is different for lines of different degeneracy, since the probability of jumps between molecules with the same resonant field is greater in these cases.

Under certain conditions linewidths may vary from one line to another in a given esr spectrum, but unlike electron transfer broadening, alternate lines (or groups of lines) have alternate linewidths. The cause of these alternations is the time dependence of certain hyperfine splittings arising from chemical processes or from internal molecular rearrangements e.g. restricted rotation[56], solvent inter-

actions[123], alkali-metal counter-ion interactions[124], or conformational interconversions[125]

3.3.3 Alternating linewidths arising from conformational interconversions

In certain situations, modulation of the hyperfine splittings may be out of phase, i.e. the hyperfine splitting of the nuclei are being interconverted such that they are not instantaneously equivalent, but have the same time averaged value. The fact that they are not instantaneously equivalent gives rise to the phenomenon frequently referred to as an alternating linewidth effect. When two forms A and B containing n nuclei with spin $M_I(A)$ and $M_I(B)$ respectively, are rapidly interconverting, from equations 3·4 and 3·11, it can be shown that the contribution to the linewidth is given

$$\Delta\Gamma = \left[\tau\gamma_e{}^2 P_A P_B (a_A - a_B)^2\right]\left[\sum^{n} m_I(A_i) - \sum^{n} m_I(B_i)\right]^2 \qquad 3\cdot12$$

where a_A is the coupling constant for the n nuclei of A and a_B is the coupling constant for the n nuclei of B

When A and B are two equally probable conformations of one molecule and a_A and a_B refer to the axial and equatorial protons of a constituent methylene group, which are being interchanged by a ring flipping mechanism, then equation 3·12 may be simplified to

$$\Delta\Gamma = \left[\frac{\tau}{8}\gamma_e{}^2 (a_A - a_B)^2\right]\left[m_I(A) - m_I(B)\right]^2 \qquad 3\cdot13$$

Since the first bracket is constant for a given esr spectrum, the contribution to the linewidth, $\Delta\Gamma$, will be determined by the square of $[m_I(A) - m_I(B)]$, and when $m_I(A) = m_I(B)$ the hyperfine lines remain narrow. Two distinct situations may arise depending on the signs of the coupling constants. If they are the same sign then the separation of the sharp lines is given by the sum of the coupling constant, but by their

difference when they are opposite in sign. For conformational changes, the coupling constants of axial and equatorial protons attached to the same carbon atom will have the same sign and the former situation is observed.

3.4 Calculation of Theoretical Spin Densities in Conjugated Π-Radicals

Once experimental coupling constants have been measured and experimental spin densities have been calculated from equations 3·5 and 3·6, in many cases ambiguities arise in their assignment to particular carbon atoms. These may be overcome by comparison of the experimental values with values calculated by theoretical methods. The methods used throughout this work are the Hückel Molecular Orbital (HMO) method,[126] and the approximate configuration interaction treatment of McLachlan.[127] The HMO method applies to planar molecules in which the sp^2 hybrid orbitals on adjacent carbon atoms overlap to form a σ framework, while the corresponding $2p_z$ orbitals overlap to form MOs over the whole molecule. σ-Π-interactions are specifically excluded.

Each MO is formulated as a linear combination of the $2p_z$ atomic orbital in the form

$$\Phi_j = \sum_i^n c_{ij}\Psi_i$$

where Φ_j is the jth MO, Ψ_i is the atomic orbital on the ith atom, and c_{ij} is the coefficient of the ith atomic orbital in the jth MO. The energy, ε, corresponding to this MO, and approximately to the true energy E, is given by

$$\varepsilon \geq \frac{\int \Phi_j^* H \Phi_j d\tau}{\int \Phi_j^* \Phi_j d\tau} \qquad 3\cdot14$$

Where H is the Hamiltonian operator which in the HMO treatment is not specified. The solution of equation 3·14 which

is obtained by applying the Variation principle to give a set of coefficients, c_{kj}, which afford the best value of ε for the jth MO, reduces to a set of secular equations of the form

$$\sum c_{rs}(H_{rs} - E.S_{rs}) = 0$$

where H_{rs} and S_{rs} are the abbreviated integrals $\int \Psi_r H \Psi_s d\tau$ and $\int \Psi_r \Psi_s d\tau$ respectively. The diagonal matrix elements, H_{rr}, are the coulomb integrals and the off-diagonal elements, H_{rs} $(r \neq s)$, are the resonance integrals. S_{rs} are the overlap integrals. In the HMO theory $H_{rr} = \alpha^{\ddagger}$ and H_{rs} is taken as zero for non-bonded atoms and is represented by $\beta^{\ddagger}$ for bonded atoms. The overlap integrals, S_{rr}, are set equal to unity and S_{rs} $(r \neq s)$ to zero. E is the energy of the rth MO. The n values of the energy are obtained by solving the secular equations and are given in the form

$$E = \alpha + m_j\beta$$

where α represents the energy of an electron in an isolated carbon $2p_z$ orbital and β represents the energy of interaction of two carbon $2p_z$ orbitals in benzene. Despite the fact that both these quantities are negative, α is chosen as an arbitrary zero and bonding MO's correspond to positive values of m_j and antibonding MO's to negative values. In cases where m_j is zero, the MO is termed a non-bonding orbital. In alternant systems, such as those described in this work, the bonding MO's contain pairs of electrons in the neutral molecule and the radical-anion has the additional electron delocalised in the lowest anti-bonding MO(s). If Φ_k is the MO occupied by the unpaired electron

$$\Phi_k = c_{k1}\Psi_1 + c_{k2}\Psi_2 + \ldots c_{kn}\Psi_n$$

‡ Not to be confused with the spin states of the electron $|\alpha\rangle$ and $|\beta\rangle$

and Φ_k is normalised ($c_{k1}^2 + c_{k2}^2 + \ldots c_{kn} = 1$), the square of the coefficients c_{kj} gives the probability of finding the unpaired electron on atom j in the kth MO i.e.

$$\rho_j = c_{kj}^2$$

is a measure of the unpaired Π-electron density on atom j. Good agreement between experiment and theory is obtained by this method for many even alternant systems[128(a)-(d)], but for odd alternant systems agreement is rather poor. The HMO method predicts zero spin densities in certain positions but experiment shows this not to be the case. The method also fails to account for negative spin densities indicated by some experiemntal results[129]. The observations can be accounted for if the Hückel theory is modified to take into account electron correlation. There are several methods for doing this and the one employed in the work is due to McLachlan[127]. Although the method is based on Self-consistent Field Theory it employs Hückel MO's as unperturbed functions and for an n-atom conjugated system the approach leads to an expression for the spin density at atom j

$$\rho_j = c^2_{kj} - \lambda \sum_{r=1}^{n} \Pi_{rj} c^2_{kr} \qquad 3\cdot15$$

where c_{kj} is the coefficient of atom j in the kth MO which contains the unpaired electron. λ is an adjustable parameter derived from theory, usually having values between 1·0 and 1·2, but values have been reported as low as 0·75[77].

Π_{rj} is the dimensionless mutual atom-atom polarisability defined by

$$\Pi_{rj} = -4\beta \sum_{s}^{\text{bonding}} \sum_{t}^{\text{antibonding}} \frac{(c_{sr}c^*_{tr})(c^*_{sj}c_{tj})}{E_t - E_s} \qquad 3\cdot16$$

where E_j and E_t are the Hückel energies of the

levels. This method does predict negative spin densities where the Hückel method predicts zero, and gives rise to a corresponding increase in positions of positive spin density in preserving the relationship

$$\sum_j \rho_j = 1$$

One of the assumptions of the Hückel theory is the equality of all the resonance integrals ($\beta = 1$) which is tantamount to suggesting the equality of all bond lengths, whereas carbon-carbon "aromatic" bond lengths are known to vary. Similarly α was defined in terms of a core Hamiltonian, but α will vary from carbon to carbon depending on the effect of other electrons. These variations in α and β will be more significant when heteroatoms are included in the conjugated system, and can be accounted for in the theory by relating α and β for sp^2 bonded carbon π-systems to new empirical values by the dimensionless numbers $\underline{h}$ and $\underline{k}$

$$\alpha_X = \alpha + \underline{h}\beta$$

$$\beta_{C-X} = \underline{k}_{C-X}\beta$$

where α_X and β_{C-X} are the integrals relating to the heteroatom X.

The calculation of spin densities by the HMO method and the McLachlan procedure are greatly facilitated by the use of high speed computing. Eigenvalues and eigenvectors being obtained by matrix solution of the secular equations (see Appendix I).

CHAPTER 4

EXPERIMENTAL TECHNIQUES

4 EXPERIMENTAL

4.1 Multicapillary Mixer

The multicapillary mixing chamber used (Fig. 4.1) throughout this work is essentially the same as that described by Buick *et al.*[48], the design being such that mixing can be performed in the resonant cavity of the esr spectrometer, with the minimum amount of dead space (*ca.* 0·1 cm^3). Using maximum flow rates (up to 8 cm^3 s^{-1}) the time between mixing and observation can be reduced to *ca.* 2 ms. The only modification to the cell arose from a new construction technique. Whereas in earlier designs the mixing tube (MT) was 'Araldited' onto the mixer jacket (MJ) in the final stages of construction the most recent design involves MJ and MT being glass-blown together in the earlier stages.

The mixer jacket (*ca.* 6 mm i.d.) is blown to the required shape and drawn to 2·4 mm at the outlet end. The mixing tube is then glass-blown into place, so that the tapered section (TS) is not less than 10·0 mm in length. (Sharper tapers than this lead to poor mixing properties.) Bundles of 10-15 capillary tubes (CT) (*ca.* 0·5 mm i.d.) are then inserted through the jacket into the mixing tube and sealed together in a flame at the inlet end. The bundle so formed is then withdrawn and the open ends set in paraffin wax and cut off on a diamond saw, to the correct length. It is fixed into the jacket by first holding in position at the inlet end with paraffin wax, and then introducing Araldite (A) through the side arm (SA). After allowing 24 hours for this to set, the closed ends of the capillaries are cut off and any remaining paraffin wax removed by immersion in

Figure 4.1

The multicapillary mixing chamber

Key: See section 4.1

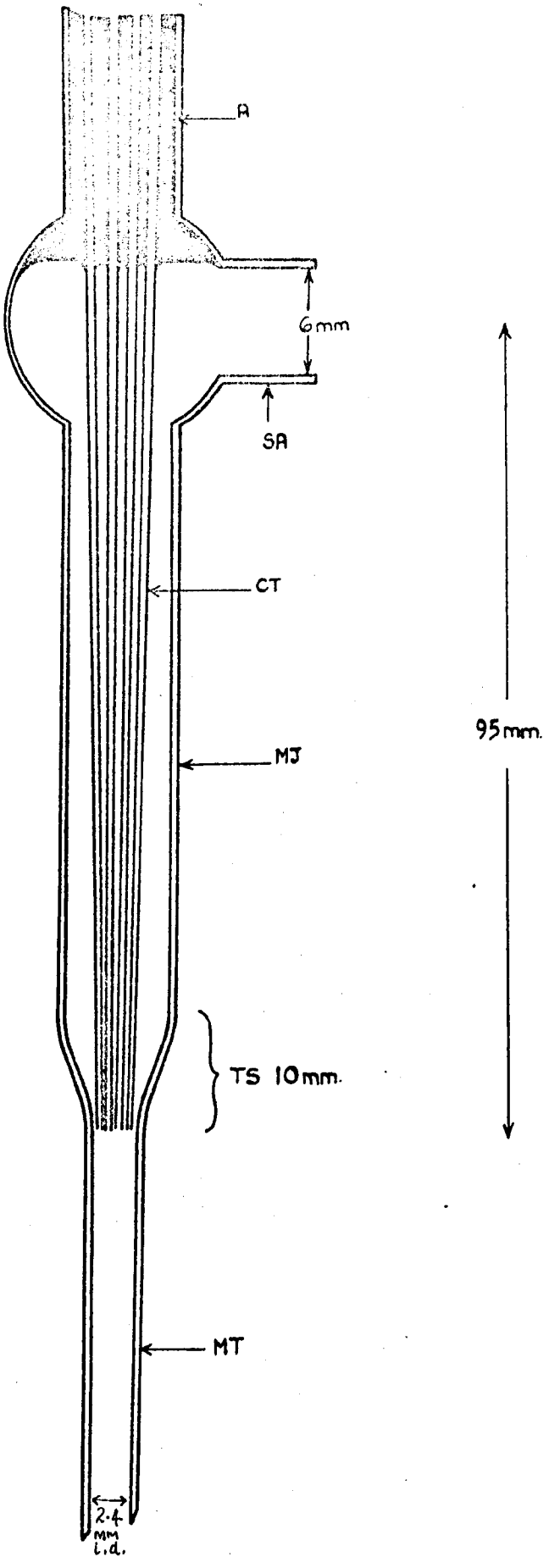
A
6mm
SA
CT
MJ
TS 10mm.
MT
2·4 mm i.d.
95mm.

boiling water.

4.2 Continuous flow experiments

Considerable modification of the equipment previously utilised[48] resulted in much improved signal-to-noise ratios (cf. Fig. 6.3 (a) and 6.3 (b)), largely as a result of achieving temperatures as low as 198 K of the reactant solutions prior to mixing, and maintaining their temperatures during transfer to the mixing chamber (Fig. 4.2). Two similar cryostatic systems are used to supply the multi-capillary mixing cell with reactants. The whole apparatus is constructed from pyrex glass jointed with 'locked' spring-loaded, greaseless, ball and socket joints.

The liquid ammonia is stored in a 2l round bottomed flask (F) maintained ca. 10 K below its boiling point by surrounding with chips of solid carbon dioxide. Heating of the ammonia while it is is flowing is prevented by the use of vacuum jacketing (VJ) and fracture of the glass on cooling by the incorporation of expansion coils (EC) in the line. The spring-loaded flask top (SV) acts as a safety valve. Cryostating is achieved by forcing the solutions, just prior to mixing, through ca. 6 m of coiled 8 mm o.d. thin walled glass tubing (C) immersed in a refrigerant (R) contained in a Dewar vessel (D). The temperature is registered (± 2 K) by means of a thermocouple placed in the eluate immediately below the mixing point in the cell. For work just above the freezing point of ammonia methanol/CO_2 is employed as refrigerant. Freezing of the ammonia is prevented by commencing the flow before the final cooling of the bath.

4.3 Static reductions

Static reduction experiments were performed by preparing

Figure 4.2

Low temperature modification to the continuous flow apparatus for reduction of compounds in liquid ammonia solution by e^-_{amm} (one section only displayed)

Key: See section 4.2

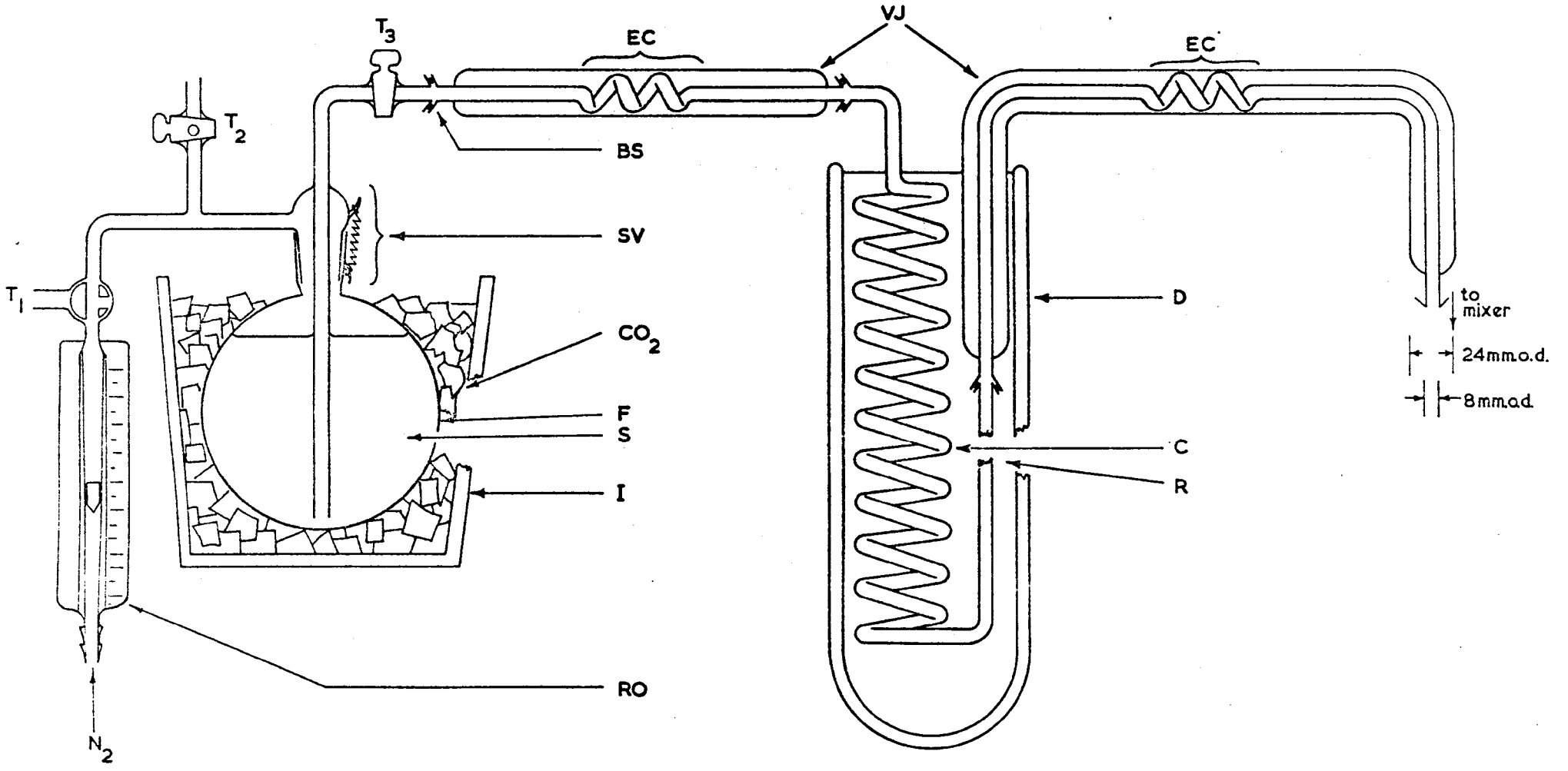
T3
EC
VJ
EC
T2
BS
SV
T1
CO2
D
to mixer
24mm.o.d.
8mm.o.d.
F
S
C
I
R
RO
N2

solutions in the absence of air on a vacuum line. The cell (Fig. 4.3) consisted of a standard 2·4 mm i.d. esr tube (T) with a 6 mm i.d. side arm (SA), fitted with a "greaseless" high vacuum stop-cock (SC), and a B_{14} standard taper 'Quickfit' cone (C). Solid substances were added directly to the cell and liquids were introduced by bulb-to-bulb distillation. Reducing solutions were made up in the side arm by distilling degassed ammonia off sodium metal onto preformed sodium mirrors. Mixing was effected by shaking and observations were made within one minute, normally at 198 K.

4.4 The esr spectrometer

The esr spectrometer used throughout this work was a Decca X-1 model with a Newport Instruments 7 inch magnet employing 100 kHz frequency modulation of the magnetic field. The klystron oscillator generates a constant monochromatic microwave frequency of 9270·387 MHz which is applied to the sample in the resonant cavity of the spectrometer, by means of a waveguide connected to one arm of a microwave bridge. Before resonance can be observed the microwave bridge is balanced so as to produce a zero current in the crystal detector. The cavity, which is placed centrally between the poles of the electromagnet is then subjected to a uniformly varying, homogeneous magnetic field (ca. 330 mT for $g \approx 2$) and the resonance observed. Sweep times for continuous flow experiments are limited by the flow rates employed. At the maximum rate (8 cm^3 s^{-1}) cohtinuous flow can only be maintained for 600 s, and under these conditions sweep rates less than 0·01 mT s^{-1} could not be used. Modulation of the magnetic field enhances the

Figure 4.3

Static reduction cell

Key: See section 4.3

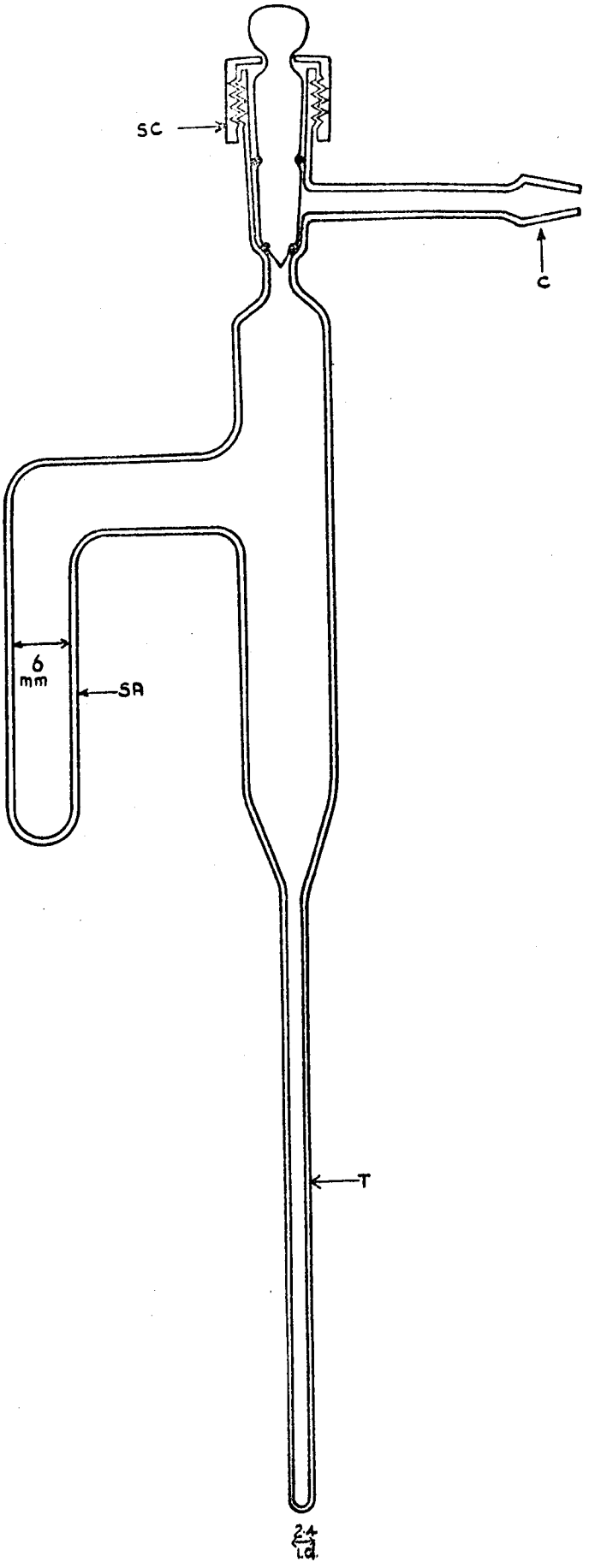
SC
C
6
mm
SA
T
24
Lg

sensitivity of the spectrometer and in so doing transforms the D.C. absorption into an alternating current. The amplitude of this alternating current is proportional to the slope of the absorption curve, and as a result the signal appears as its first derivative. Spectra were recorded on a Hewlett-Packard X-Y and Smith's "Servoscribe" Y-t chart recorders. For static reduction experiments samples were maintained at low temperature by the use of a variable temperature probe (Decca Radar Ltd.) which allowed a controlled flow of cold nitrogen gas to pass over the sample tube. The temperature was maintained ($\pm$ 0·5° K) by a feedback circuit consisting of a platinum resistance thermometer and a heating element in the nitrogen gas flow.

4.5 Recording spectra

In recording esr spectra it is necessary to avoid undesirable effects arising from saturation and overmodulation. Saturation occurs when the microwave power is increased to such an extent that the population difference between the lower and upper spin states ($N_\beta - N_\alpha$) is reduced by intensified upward transitions, faster than it can be re-established by relaxation processes. The resultant decrease in the population excess both weakens and distorts the hyperfine lines. Saturation was prevented by attenuating the microwave power. The signal to noise ratio was enhanced by raising the modulation amplitude, but when this was approximately equal to the linewidth, resolution deteriorated.

4.6 Spectral analysis

In most free radicals the magnetic nuclei may be grouped in equivalent sets. This equivalence may arise through molecular symmetry or though accidental degeneracy.

Nuclear hyperfine coupling with a nucleus of spin I gives rise to (2I + 1) allowed esr transitions and if a radical contains groups of p_n equivalent nuclei with spin I_n then the total number of allowed transitions is given by

$$N_{TOT} = \prod_n (2I_n + 1)^{p_n}$$

Although this gives the total number of lines possible it says nothing about the multiplicity of certain lines arising from the equivalence of p_n nuclei, and therefore does not necessarily give the number and degeneracy of lines that will appear in the spectrum. Most organic free radicals contain groups of equivalent protons and the relative intensities of esr lines arising from these are given by the coefficients of the binomial expansion of $(1 + x)^n$ which may be readily calculated by the construction of Pascal's triangle. Other magnetic nuclei, rarely found in equivalent groups in organic free radicals, include ^{2}H, I = 1: ^{14}N, I = 1: ^{23}Na, I = $\frac{3}{2}$: ^{39}K, I = $\frac{3}{2}$: ^{19}F, I = $\frac{1}{2}$: ^{35}Cl, I = $\frac{3}{2}$. In simple cases where there are few interacting magnetic nuclei analysis of spectra is relatively simple, particularly when no accidental degeneracy arises and equivalence of certain nuclei is produced through molecular symmetry. However, in systems of low symmetry containing several non-equivalent nuclei, the situation becomes very complex and analysis can only be made by a process of trial and error. A computer simulation of such a spectrum is made on a basis of a trial analysis, and compared with the experimental spectrum for correct line positions, widths and intensities. The input data is then adjusted until the simulated and experimental spectra are exactly superimposable.

The computer program used for this purpose, is given in

Appendix II. Mixed spectra were simulated using the program given in Appendix III. In all cases the magnetic field was calibrated using dilute solutions of potassium nitrosyl disulphonate, Frémy's salt. The radical-dianion $.NO(SO_3)_2^{2-}$ produces a three line spectrum separated by 1·307 mT.

g-factors were calculated from equation 3·1

$$g_x = \frac{h\upsilon}{H_x\beta_e}$$

Since all continuous flow spectra show the characteristic singlet of the ammoniated electron ($g = 2{\cdot}0011$[28]) it was possible to calculate the value of H_x (the field value at the centre of the esr spectrum of the radical X) by subtracting its separation in millitesla from the value H_e for the solvated electron. g-factors calculated by this method are estimated as being accurate to ±0·0001.

4.7 Activation Parameters

The computer program given in Appendix IV was used for the calculations. The Arrhenius factors, E_a (activation energy) and A (frequency factor) from the relation $k = A\exp(-E_a/RT)$ were calculated from a linear least squares best fit line to a plot of values of ln k versus 1/T. Values of $\Delta H^{\ddagger}$ and $\Delta S^{\ddagger}$ from the transition-state theory equation, $k = k'T/h.\exp(\Delta S^{\ddagger}/R).\exp(-\Delta H^{\ddagger}/RT)$, were derived for 298·1 K by means of the relations:

$$\Delta H^{\ddagger} = E_a - RT$$

$$\Delta S^{\ddagger} = R(\ln A - \ln(k'T/h) - 1)$$

PART B

EXPERIMENTAL RESULTS

CHAPTER 5

REDUCTION OF AROMATIC AMIDES AND THIOAMIDES

5 AROMATIC AMIDES AND THIOAMIDES

5.1 Introduction

It has been shown by earlier workers[87] in this field that solutions of carboxylic acids in liquid ammonia could be reduced by the ammoniated electron, e^-_{amm}, in the liquid ammonia flow system to give the esr spectra of the corresponding radical-dianions, and in view of the very fast reduction rate for benzamide by e^-_{aq} ($k = 1{\cdot}7 \times 10^{10}$ $l\ mol^{-1}s^{-1}$)[130], it seemed probable that analogous behaviour would be exhibited by aromatic amides. The radical-anions of the latter have only been observed in solution by esr spectroscopy in those instances where the molecule has borne a second, highly electronegative substituent such as $-NO_2$[131], or a second $-CONH_2$ group[70], although Sevilla[132] has obtained the esr spectrum of CH_3COND_2 in an alkaline glass at 77 K. Conventional reduction of benzamide at 240 K with two moles of sodium yields a mixture of products from which benzyl alcohol and dihydrobenzamide were isolated[133].

Electrolytic reduction of several N,N-dialkylthiobenzamides in acetonitrile solution to give esr spectra of the radical-anions has been accomplished by Voss and Walter[72-74] but there is no record of a spectrum derived from thiobenzamide itself.

Although Buick has reported[27] the coupling constants for several aromatic amide radical-anions, produced at $\sim$ 230 K in the continuous liquid ammonia flow system, such difficulty was experienced in certain instances in trying to correlate experimental values of unpaired spin densities with

calculated values, that the radical-anions were prepared again at ∿ 200 K, in order to check Buick's analysis against more highly resolved spectra. In this chapter are reported the esr spectra of semi-reduced benzamide and thiobenzamide and a variety of their substituted derivatives together with assignments of coupling constants based on comparison with calculated spin densities obtained by simple MO methods.

5.2 Experimental

Low temperature continuous flow experiments were carried out in the system described in section 4.2. In most cases sufficiently well-resolved spectra were obtained with substrate concentrations of ca. 10^{-2} M. However, the increased lifetime of the radical-anions at low temperature sometimes made it necessary to use 10^{-3} M solutions to avoid concentration broadening of the spectral lines. 3,5-Dimethyl-, 2,4,6-trimethyl- and 4-t-butyl-N,N-dimethylbenzamides required the addition of 10% (V/V) of tetrahydrofuran to effect solution. The concentration of sodium was always slightly greater than that of the substrate. Maximum flow rates of 8 ml s^{-1} were employed throughout this work.

Materials

Commercially available materials were recrystallised before use. N,N-dialkylbenzamides were prepared by the method in Ref. 134 and N,N-dimethylthiobenzamide by the method of Okomuru[135].

5.3 Results and Analysis of Spectra

5.3.1 Benzamide and Ring-substituted Benzamides

Benzamide dissociates in liquid ammonia[136]

$$C_6H_5CONH_2 + NH_3 \rightleftharpoons C_6H_5CONH^- + NH_4^+$$

and the initial product of electron capture by benzamide anion

is expected to be the species $C_6H_5CONH^{2-}$. This expectation is borne out by the observed esr spectrum (Fig. 5.1) obtained at 203 K and analysed in terms of six inequivalent protons and one nitrogen nucleus (Table 5.2). This pattern of inequivalent ring protons contrasts with the symmetrical distribution of spin densities in the $ArCO_2^{2-}$ series and indicates hindrance of rotation about the C_1-C_7 bond, a characteristic of several benzamide[137] and dialkylbenzamide[138-141] molecules as evidenced by their nmr spectra.

The radical-anion derived from 4-methylbenzamide also displayed inequivalent ortho- and meta-protons (Table 5.2) but 2-methylbenzamide produced a spectrum analysed in terms of a single species and not a mixture of two rotational conformers which might have been expected; this results presumably from a marked preference for one of the two forms, originating in some interaction between the two substituents. 3-Methylbenzamide produced a spectrum which could not be analysed but which exhibited broadening of certain lines, suggesting the presence of two radical-anions of generally similar coupling constants, i.e. probably two rotational conformers.

4-Fluorobenzamide gave a spectrum consisting mainly of the expected radical-dianion, but with a minor component due to the benzamide dianion; loss of nuclear fluorine on the time-scale of these experiments has been a consistent feature of this work, e.g. with 4-fluorobenzoic acid[87] and 4-fluorobenzonitrile[48]. Again, an unsymmetrical spin distribution was found in the fluorine-substituted radical-dianion (Table 5.2). Only a partial analysis of the spectrum from 3-fluorobenzamide is possible but it is suspected that

Figure 5.1

a) Low-field half of the esr spectrum of the benzamide radical-anion measured at 203 K

b) Computer simulation

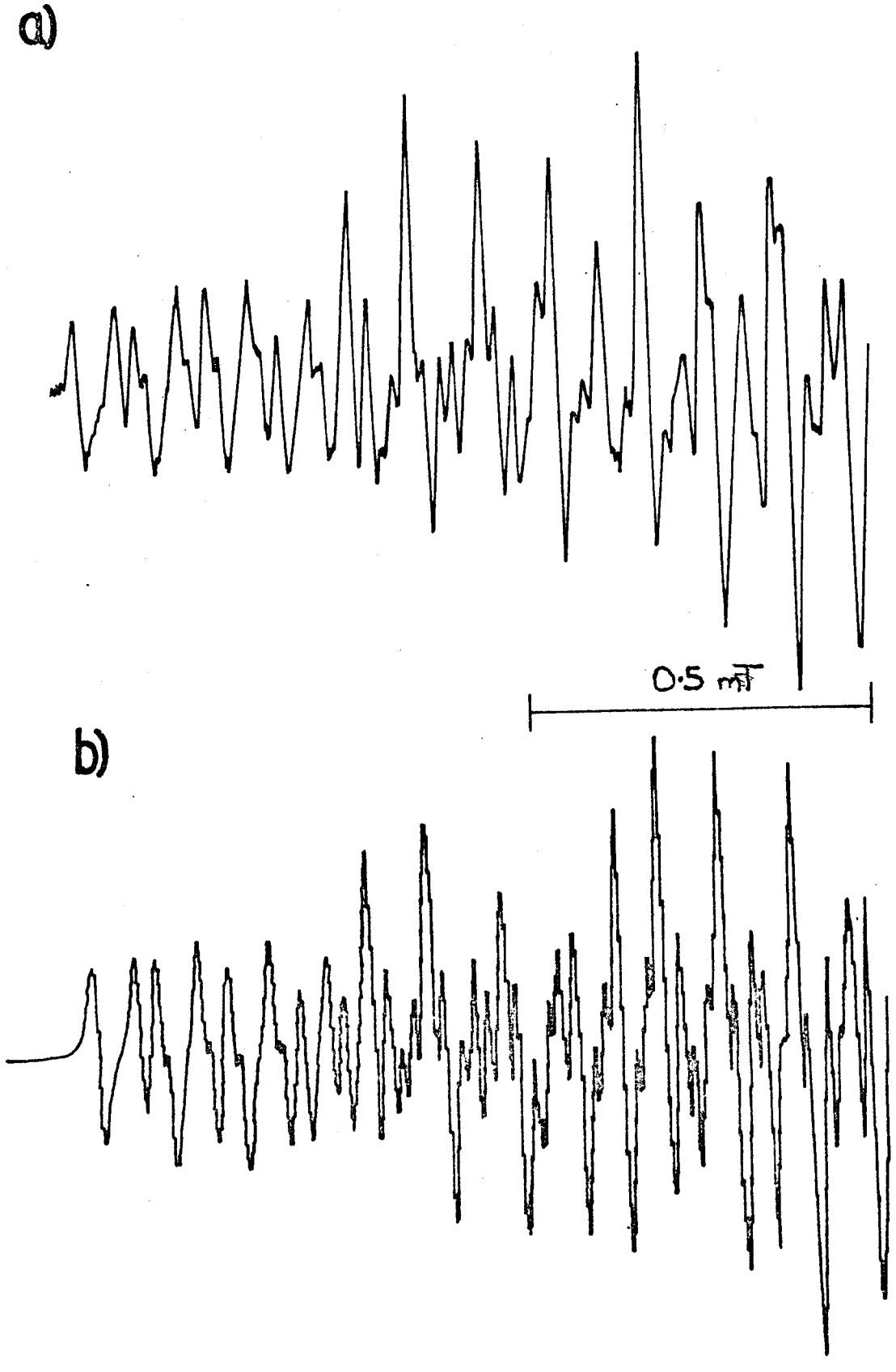
a)
0.5 mT
b)

a mixture of conformers is present. 2-Fluorobenzamide gave a spectrum analysed in terms of a single species with couplings from ^{19}F and ^{14}N nuclei and six protons, i.e. one proton additional to those expected from $FC_6H_4CONH^{2-}$ (Table 5.2). This result is anomalous; the other aromatic amides exhibit spectra attributable to $ArCONH^{2-}$ with the exception of N-methylbenzamide, which also behaves like 2-fluorobenzamide radical-anion in displaying coupling from one proton extra to those expected from the species $ArCONH^{2-}$.

4-Nitrobenzamide gave a spectrum closely similar to that described by Maki and Geske[131] and analysed in terms of one ^{14}N nucleus and two pairs of equivalent protons (Table 5.2). The large difference in the ^{14}N coupling is attributable to solvent effects characteristic of nitroaromatic radical-anions. The broad nature of the lines obscured the smaller coupling constants, and the small difference between pairs of ortho- and meta-couplings could not be detected. A spectrum which could not be analysed was obtained from phthalamic acid (2-carboxybenzamide).

5.3.2 N-Methylbenzamides

N-Methylbenzamide yielded a spectrum analysed in terms of six inequivalent protons, three equivalent protons and a ^{14}N nucleus (Table 5.2). It appears therefore, that the species responsible is $C_6H_5CON(CH_3)H^-$, i.e., that the unionised form is prevalent. The 4-methyl derivative produced no appreciable resonance, but 4-fluoro-N-methylbenzamide yielded a broad spectrum of many lines which has not been analysed.

Hippuric acid (N-carboxymethylbenzamide) also gave a highly complex but symmetrical spectrum which has not yet

been interpreted.

5.3.3 N,N-Dimethylbenzamides

N,N-Dimethylbenzamide gave identical spectra both by the continuous flow and static reduction methods (Table 5.2 and Fig. 5.2): these indicate the presence of six equivalent protons, two sets of two equivalent protons and a single proton but the coupling from ^{14}N was so small as to be unresolved; however it is clear that $C_6H_5CON(CH_3)_2^{\cdot-}$ is formed. The most significant feature is the symmetry of the spectrum which distinguishes it from those of radical-anions derived from benzamide and N-methylbenzamide.

N,N-Dimethylbenzamide radical-anion showed remarkable stability compared with the other radicals in this series, remaining stable for over an hour in liquid ammonia at 195 K.

4-Methyl- and 4-fluoro-N,N-dimethylbenzamides gave all the couplings expected (Table 5.2) but 4-butyl-N,N-dimethylbenzamide produced an overall 1:2:1 spectrum with lines broadened by the t-butyl protons. Whilst the latter spectrum was also obtained by static reduction, the 4-methyl-and 4-fluoro-substituted radicals were obtained only in the flow system. 4-Chloro-N,N-dimethylbenzamide gave the esr spectrum of N,N-dimethylbenzamide radical-anion both in flow and static systems. 3,5-Dimethyl-N,N-dimethylbenzamide and 2,4,6-trimethyl-N,N-dimethylbenzamide were sparingly soluble both in liquid ammonia and the cosolvent system and only weak resonance was obtained from these. The 4-ethoxy derivative gave a spectrum consisting of many broad lines which could not be interpreted.

5.3.4 Nicotinamides

Even at the lowest solute concentrations, nicotinamide

Figure 5.2

a) Esr spectrum of the radical-anion of N,N-dimethylbenzamide

b) Computer simulation

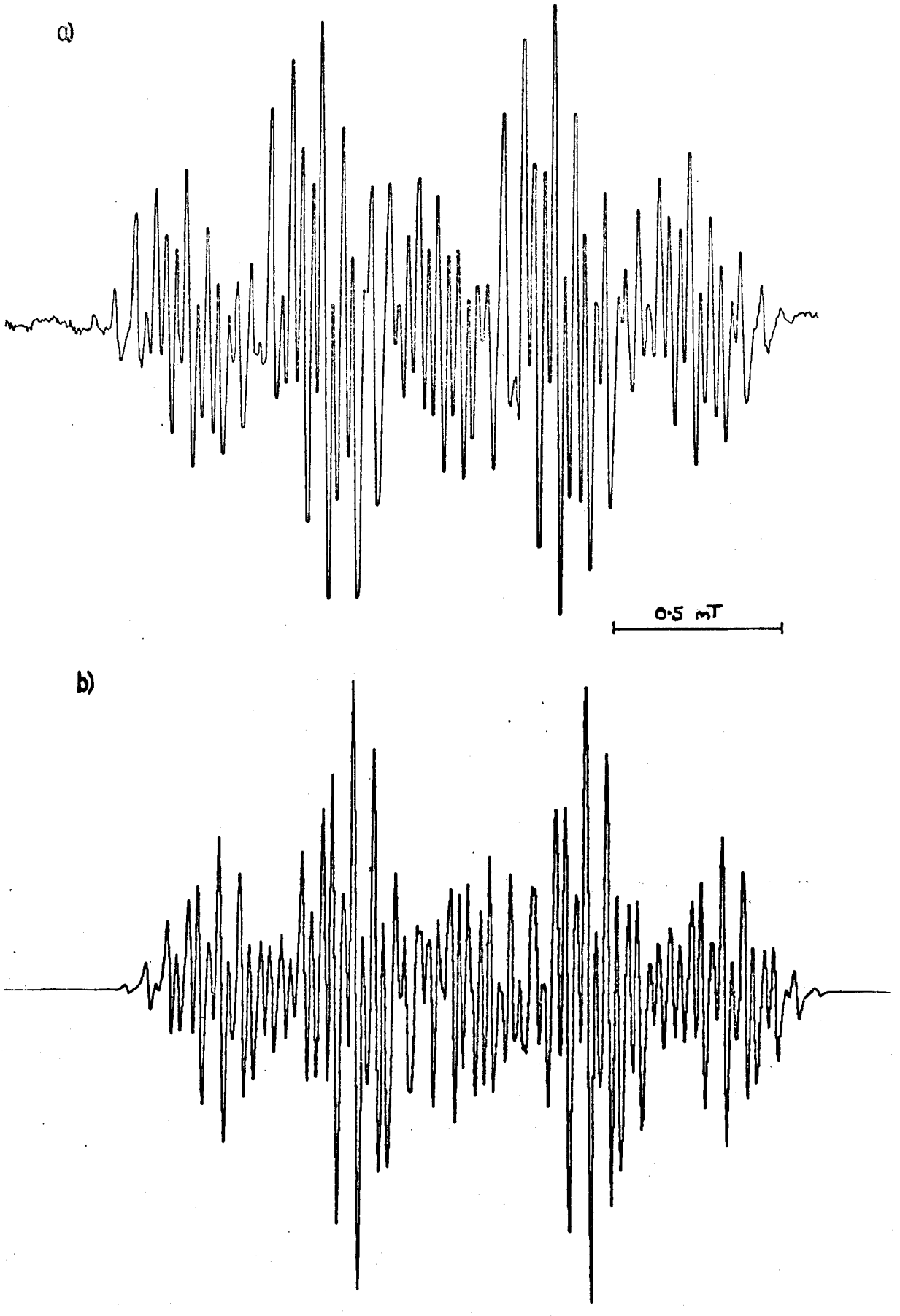
a)
0·5 mT
b)

itself gave a broad triplet spectrum showing only the slightest resolution of other peaks. However, while N-ethylnicotinamide produced a similar featureless spectrum at 10^{-2}M concentration, at ca. 10^{-3}M concentration the spectrum shown in Fig. 5.3 was obtained. Only the coupling constants shown in Table 5.2 have been determined with certainty and these compare favourably with those of the parent acid. Attempts to facilitate a complete analysis through increasing spectral intensity by using higher substrate concentrations have resulted in a prohibitive degree of line-broadening. Nonetheless, this spectrum is of interest as the first example of that of a semi-reduced nicotinamide.

5.3.5 Thiobenzamides

Thiobenzamide itself gave the spectrum illustrated in Fig. 5.4 and corresponding to the species $C_6H_5CSNH^{2\cdot}$ which clearly displays an asymmetric distribution of spin density similar to that found with its benzamide analogue. N,N-Dimethylthiobenzamide produced a spectrum generally similar to that reported by Voss and Walter[72,73] but rather better resolved, and affording more accurate coupling constants (Table 5.2). The spectra of thiobenzamides are rather narrower than those of their oxygen analogues, and are centred at lower field (sulphur-containing radicals generally show higher g-factors than their oxygen analogues).

The g-factors of unanalysed radical-anions are given in Table 5.3.

5.4 Discussion

5.4.1 MO Calculations and Assignment of Coupling Constants

By setting h_C and k_{C-C} for the aromatic ring equal to zero and one respectively, the Hückel parameters for the amide

Figure 5.3

a) Esr spectrum of the radical-anion of N-ethylnicotinamide

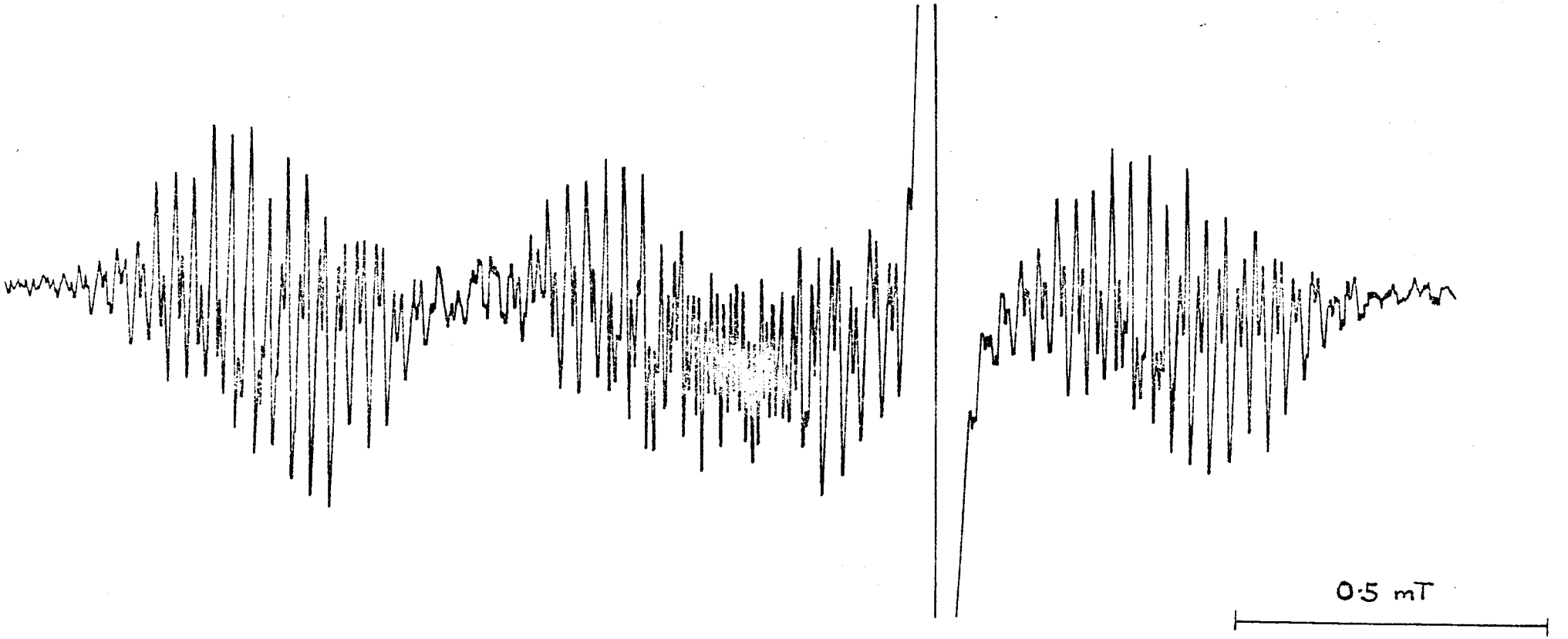
0·5 mT

Figure 5.4

a) Spectrum of the radical-anion of thiobenzamide

b) Computer simulation

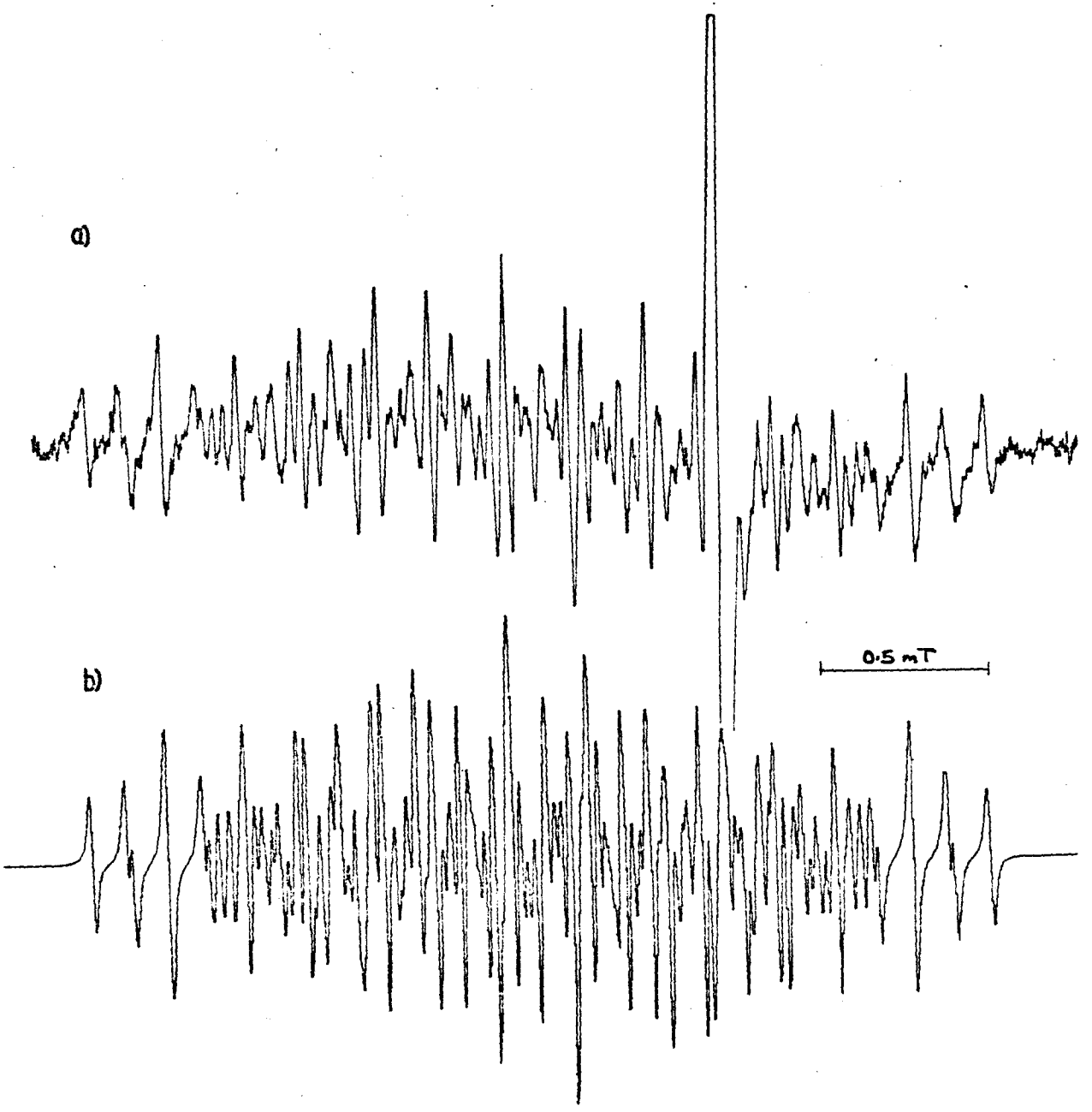
a)
b)
0.5 mT

TABLE 5.1

Experimental and McLachlan Spin Densities for Benzamide

Position	"Experimental" Spin Density Q = -2·75 mT	Simple McLachlan	Calculated Spin Density (McLachlan)		
			α effect $\underline{h}' = -0{\cdot}05$	β effect $\underline{k}' = 0{\cdot}05$	Bond length method
2	0·153	0·131	0·130	0·142	0·150
3	0·033	-0·033	-0·037	-0·040	-0·036
4	0·275	0·267	0·216	0·262	0·267
5	0·023	-0·033	-0·047	-0·027	-0·022
6	0·145	0·131	0·145	0·121	0·098
$\underline{R}$ 2/4	0·556	0·490	0·602	0·542	0·562
$\underline{R}$ 6/4	0·527	0·490	0·671	0·462	0·367
$\underline{R}$ 2/6	1·06	1·00	0·897	1·17	1·53

group, the nitrogen and oxygen Coulomb integrals, $\underline{h}_N$ and $\underline{h}_O$, and the C_1-C_7, C = O and C - N resonance integrals ($\underline{k}_{1-7}$, $\underline{k}_{C=O}$, $\underline{k}_{C-N}$) remain to be determined.

The asymmetric spin density distribution was simulated by application of the so-called α[70,89,142,143] and β[143,144] effects. The α effect corresponds to a change in the Coulomb integral for one of the ortho positions, $\alpha_{\underline{ortho}} = \alpha_C + \underline{h}'\beta_{C-C}$. For terephthaldehyde Reiger and Frankel considered the effect asbeing electrostatic in nature and have justified the use of a negative value of $\underline{h}'$, by saying that the negatively charged oxygen would oppose the charge on the core of C_2. The β effect, which implies the existence of a weak bond between these postions (inset figure), is represented by a small resonance integral $\beta_{X-Z} = \underline{k}'_{X-Z}\beta_{C-C}$ with $0 < \underline{k}' < 0{\cdot}10$. In view of the greater distance over which the α and β effects are considered to operate in benzamides, the upper limits of $\underline{h}'$ and $\underline{k}'$ have been set somewhat lower than those suggested by Johnson and Chang[143]. It is certainly the case that the α effect must involve the more electronegative carbonyl oxygen atom rather than the nitrogen atom and bonding between C_2 and O has been invoked in the β effect.

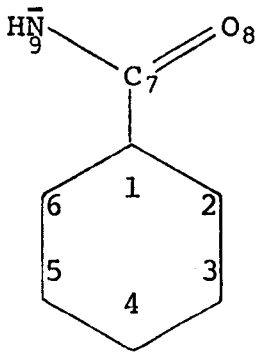

With λ set equal to 1·2, the parameters $\underline{h}_X$, $\underline{k}_{X-Y}$, $\underline{h}'$ and $\underline{k}'$ were varied until the ratios of the spin densities in the 2- and 4-positions ($\underline{R}$ 2/4), the 6- and 4-positions ($\underline{R}$ 6/4) and the 2- and 6-positions ($\underline{R}$ 2/6) were equal to the corresponding ratios of the coupling constants (Table 5.1). The parameters giving the best overall fit with the experi-

TABLE 5.2

Coupling Constants and Spin Densities for Radical-Anions of Benzamide and Related Compounds

Benzamide	Position	Coupling Constant mT	Spin Density			g-factor ± 0·0001
			Experimental[a]	Hückel	McLachlan	
Unsubstituted	2	0·420	0·153	0·117	0·142	
	3	0·092	0·033	0·020	-0·040	
	4	0·757	0·275	0·194	0·262	
	5	0·062	0·023	0·028	-0·027	2·0033
	6	0·399	0·145	0·104	0·121	
	N	0·098	0·100	0·067	0·039	
	N-H	0·337				
2-Methyl-	2	0·400	0·145	0·129	0·161	
	3	0·109	0·040	0·013	-0·050	
	4	0·803	0·292	0·193	0·260	
	5[b]	0·044	0·016	0·040	-0·008	2·0034
	6[b]	0·399	0·143	0·089	0·097	
	N	0·073	0·105	0·065	0·038	
	N-H	0·353				
4-Methyl-	2	0·443	0·161	0·117	0·145	
	3[b]	0·109	0·040	0·014	-0·045	
	4[b]	0·791	0·288	0·183	0·243	
	5	0·087	0·032	0·022	-0·032	2·0033
	6	0·405	0·147	0·103	0·123	
	N	0·109	0·088	0·067	0·038	
	N-H	0·297				

mental data compare favourably with those used by other workers for related carbonyl[70,87,145], amide[132] and imide[145-147] systems, and are as follows:

$\underline{h}_O$	2·00	$\underline{k}_{1-7}$	0·80	$\underline{k}_{7-9}$	0·80
$\underline{h}_N$	0·80	$\underline{k}_{7-8}$	1·60	$\underline{k}_{2-8}$	0·05

(Simple Hückel theory gave only poor correlation.)

Calculations for the C-substituted methyl analogues were carried out using inductive, heteroatom and inductive-plus-heteroatom models and best agreement was obtained using the latter method.

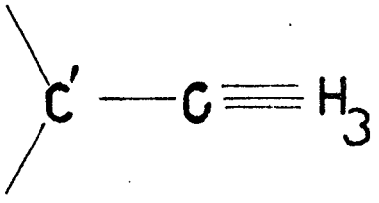

$\underline{h}_{C'} = -0·2$

$\underline{h}_{C} = -0·10$

$\underline{h}_{H_3} = -0·50$

$\underline{k}_{C'-C} = 0·75$

$\underline{k}_{C\equiv H_3} = 2·00$

In the case of the N-substituted methylbenzamides, similar calculations showed the simple heteroatom model to be the most effective.

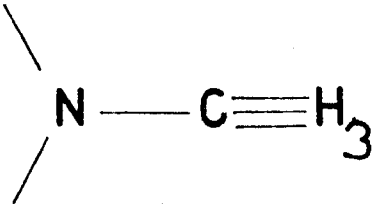

$\underline{h}_{C} = -0·10$

$\underline{h}_{H_3} = -0·50$

$\underline{k}_{N-C} = 0·92$

$\underline{k}_{C\equiv H_3} = 2·00$

With the limited data available, evaluation of really reliable sulphur parameters $\underline{h}_S$, $\underline{k}_{C-S}$ was impossible. By variations of these between the same limits as those used by Lunazzi *et al.*[148] it was possible to obtain reasonably good agreement for thiobenzamide with $\underline{h}_S = 1·2$ and $\underline{k}_{C-S} = 1·0$. However, the N,N-dialkyl analogue gave only poor agreement. The parameters used for fluorine substituents were the same as by Buick *et al.*[87], *i.e.* $\underline{h}_F = 1·60$, $\underline{h}_C = 0·1$ and $\underline{k}_{C-F} = 0·7$.

Table 5.2 (continued)

Benzamide	Position	Coupling Constant mT	Spin Density			g-factor ± 0·0001
			Experimental[a]	Hückel	McLachlan	
2-Fluoro-	2	0·618	0·225	0·132	0·166	
	3	0·119	0·043	0·012	-0·051	
	4	0·867	0·315	0·195	0·263	
	5	0·043	0·015	0·042	-0·005	
	6[c]	0·529	0·088[d]	0·087	0·095	2·0036
	N	0·140	0·030[d]	0·065	0·038	
	N-H_1	0·046				
	N-H_2	0·159				
4-Fluoro-	2	0·479	0·174	0·120	0·149	
	3	0·130	0·047	0·014	-0·046	
	4[c]	1·706	0·284	0·185	0·247	
	5	0·099	0·036	0·021	-0·034	2·0039
	6	0·432	0·157	0·105	0·126	
	N	0·188	0·029	0·067	0·039	
	N-H	0·099				
4-Nitro[e]	2	0·09	0·033	0·021	-0·016	
	3[f]	0·32	0·116	0·085	0·105	
	4[f]	0·914	-	0·059	0·042	
	5	0·32	0·116	0·090	0·112	2·0049
	6	0·09	0·033	0·020	-0·017	
	N	g	-	0·022	0·018	
	N-H	g	-	-	-	

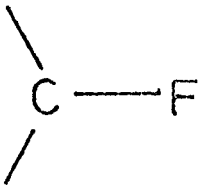

For 4-nitrobenzamide the parameters of Rieger and Fraenkel[149] were employed, namely $\underline{h}_N = 2{\cdot}2$, $\underline{h}_O = 1{\cdot}4$, $\underline{k}_{C-N} = 1{\cdot}2$, $\underline{k}_{N-O} = 1{\cdot}67$.

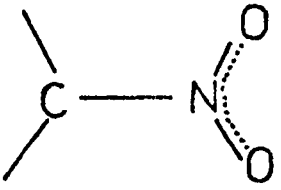

Experimental spin densities for the ring protons were calculated by means of the McConnell equation, the best value of $Q_{CH}^{H} = -2{\cdot}75 \pm 0{\cdot}24$ mT being calculated by the method of least squares using the McLachlan spin densities for the ortho- and para-positions (being rather more reliable than the meta-position), and their corresponding coupling constants. The data for the thiobenzamides were not used in this analysis.

Spin densities for the nitrogen were calculated from $a_{N-H}^{H} = Q_{N-H}^{H}\rho_N$ where $Q_{N-H}^{H} = -3{\cdot}37$ mT[147]. However, correlation was poor, probably because of the variation of charge on the nitrogen atom in this series (Table 5.2). Methyl proton hyperfine coupling constants were related to spin densities by $Q_{CCH_3}^{H} = 2{\cdot}8$ mT. No correlation was made for the N-methyl protons.

Previous estimates have set $Q_{CF}^{F} = -5{\cdot}0 \pm 1{\cdot}0$ mT, but the correlation in this work proved better with a value of $-6{\cdot}0 \pm 1{\cdot}0$ mT.

The α and β effects compare well (Table 5.1) in that they give asymmetries of the correct order of magnitude,

Table 5.2 (continued)

Benzamide	Position	Coupling Constant mT	Spin Density			g-factor ± 0·0001
			Experimental[a]	Hückel	McLachlan	
N-Methyl-	2	0·420	0·153	0·115	0·141	
	3	0·077	0·028	0·019	0·040	
	4	0·572	0·208	0·191	0·258	
	5	0·037	0·013	0·028	-0·027	2·0033
	6	0·398	0·145	0·103	0·120	
	N	0·102	0·064	0·235	0·034	
	N-Me	0·173				
	N-H	0·215				
N,N-Dimethyl-	2,6	0·408	0·148	0·115	0·144	
	3,5	0·089	0·032	0·021	-0·038	
	4	0·702	0·255	0·191	0·261	2·0033
	N	g	-	0·061	0·032	
	N-(Me)$_2$	0·062				
4-Methyl-N,N-dimethyl-	2,6	0·430	0·156	0·111	0·138	
	3,5	0·115	0·042	0·022	-0·033	
	4[a]	0·740	0·269	0·187	0·251	2·0035
	N	g	-	0·059	0·032	
	N-(Me)$_2$	0·056				
4-Fluoro-N,N-dimethyl-	2,6	0·451	0·164	0·119	0·153	
	3,5	0·112	0·041	0·014	-0·047	
	4[b]	1·544	0·257	0·184	0·251	2·0038
	N	g	-	0·062	0·031	
	N-(Me)$_2$	0·056				
4-tert-butyl-N,N-dimethyl-	2,6	0·53[e]	0·193	-	-	2·0034

with the α effect ($\underline{h}' = -0{\cdot}05$) giving marginally better results than the β effect with $\underline{k}' = 0{\cdot}05$, but the two are seriously inconsistent in that they predict changes in opposite directions. Johnson and Chang[143] have commented on the invalidity of the α effect, and in this context it seems even more difficult to justify in that electronic charges are considered as interacting over even larger distances. Accordingly, assignments have been made (Table 5.2) using calculations based on the β effect. It is interesting to note that calculations using non-equivalent resonance integrals for the benzamide ring (derived by assuming a linear relationship between the resonance integral and the x-ray bond length[150], $\underline{k}_{C-C,1{\cdot}47} = 0{\cdot}9$, $\underline{k}_{C=C,1{\cdot}34} = 1{\cdot}1$[124]) lead to the same assignments as the β effect method although the ortho/para ratio is too large. Probably the best method of treating the problem is to use a combination of the two methods. In this situation though the α effect would represent an inductive effect at C_2. Since the oxygen in this situation would be electron-withdrawing a positive value of $\underline{h}'$ would be required.

When an ortho substituent is present, the question arises as to which of the configurations is the more probable.

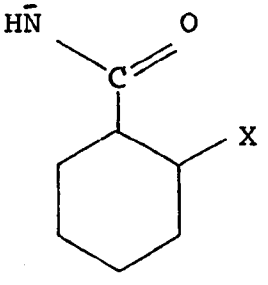

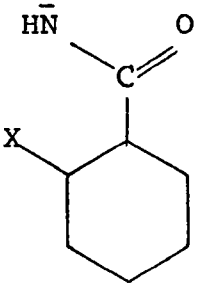

X = Me or F

In both cases calculations point towards configuration (b) although for X = F the situation is not unambiguous, and assignments have been made accordingly. It may well be non-

Table 5.2 (continued)

Benzamide	Position	Coupling Constant mT	Spin Density			g-factor ± 0·0001
			Experimental[a]	Hückel	McLachlan	
Thiobenzamide	2	0·419	0·152	0·105	0·137	
	3	0·126	0·046	0·010	-0·043	
	4	0·643	0·234	0·146	0·200	
	5	0·106	0·039	0·015	-0·035	2·0044
	6	0·388	0·141	0·096	0·122	
	N	0·232	0·167	0·109	0·068	
	N-H	0·562				
N,N-dimethyl-thiobenzamide	2,6	0·377	0·137	0·106	0·141	
	3,5	0·116	0·042	0·011	-0·042	
	4	0·488	0·177	0·148	0·206	2·0058
	N	g	-	0·099	0·056	
	N-(Me)$_2$	0·070				
N-ethyl nicotinamide	N_1	-	-	0·059[i]	0·037[i]	
	2	0·221	0·080	0·034	0·021	
	4	0·702	0·255	0·174	0·204	
	5	-	-	0·008	-0·038	2·0027
	6	0·986	0·359	0·234	0·283	
	N_7	-	-	0·052	0·036	

a Q^H_{CH} = -2·75 ± 0·24 mT

b methyl protons coupling constant

c Fluorine coupling constant

d Calculated from an average of the two nitrogen proton coupling constants

e Large linewidth preventing accurate determination of these couplings

f Nitro group nitrogen coupling

g Coupling unresolved

h MO Parameters used here were for a combination of those used for pyridines and benzamides

g Assignments were made by comparison with calculated spin densities for N-methyl-nicotinamide.

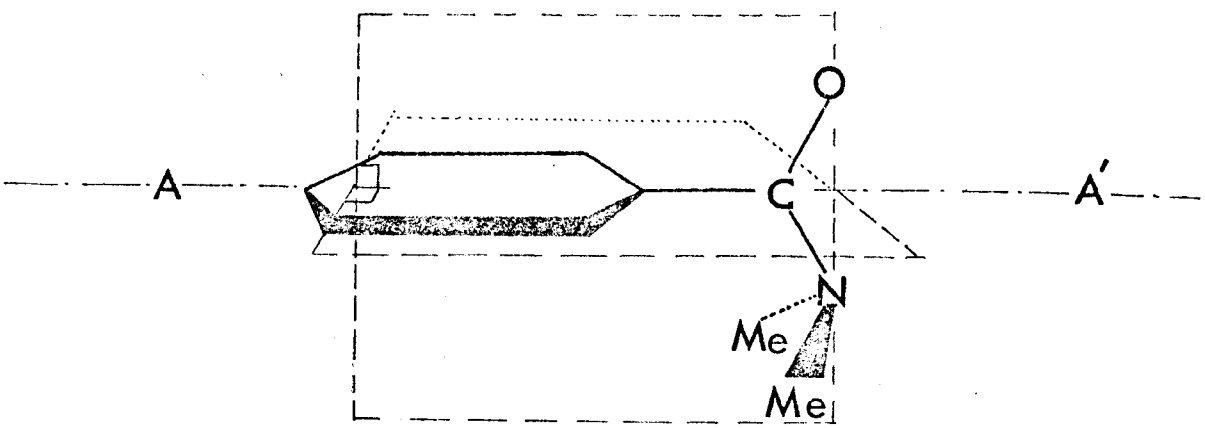

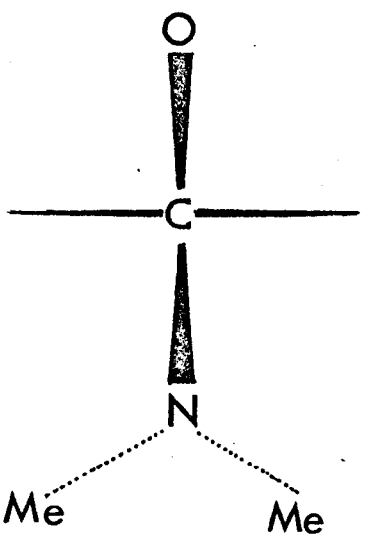

View along
axis A-A'

Fig. 5.5 Fixed symmetric conformation of N,N-dimethyl benzamide

TABLE 5.3

g-factors for Unanalysed Benzamide Radical-Anions

Benzamide	g-factor ± 0·0001
3-Methyl-	2·0033
3-Fluoro-	2·0036
4-Fluoro-N-methyl	2·0049
4-Fluoro-N,N-dimethyl-	2·0038
N-carbmethoxy- (Hippuric acid)	2·0033
Cinnamamide	2·0030

planarity which accounts for the rather high value of Q^{H}_{CH}.

5.4.2 Reduction of Aromatic Amides

As expected, in most cases electron attachment to mono-ionised benzamides takes place to form the corresponding radical-dianion $ArCONH^{2\cdot-}$. Both spectral analysis and assignments of coupling constants to particular nuclei are of unusual difficulty with this set of radicals, both because of the large number of inequivalent positions resulting from restricted rotation about the C_1-C_7 bond in the majority of cases and because of the slight broadening of lines due to small motions of the amide group. The difference between benzamides and N-alkylbenzamides, and N,N-dialkylbenzamides is the symmetry of the unpaired spin density distribution. A separate experiment was devised to find out whether the equivalence in the N,N-dialkylamides was arising through a time averaging effect, from rapid rotation about the C_1-C_7 bond, or though the amide group being in a fixed symmetric confirmation in which the oxygen and nitrogen atoms of the amide group lie on opposite sides of the ring and in the plane perpendicular to it, through the C_1-C_7 axis (Fig. 5.5) The unexpected stability of N,N-dimethylbenzamide radical-anion enable it to be formed with sodium/potassium alloy in 2-methyltetrahydrofuran solution. The lines in the esr spectrum in this instance were much broader, due probably to small coupling with alkali metal counter ions, but such couplings as could be resolved and the g-factor were both consistent with an assignment to the radical-anion. Even at temperatures as low as 170 K, however, no inequivalence of the ortho- or meta-protons was apparent, indicating that no preference exists for a single conformation.

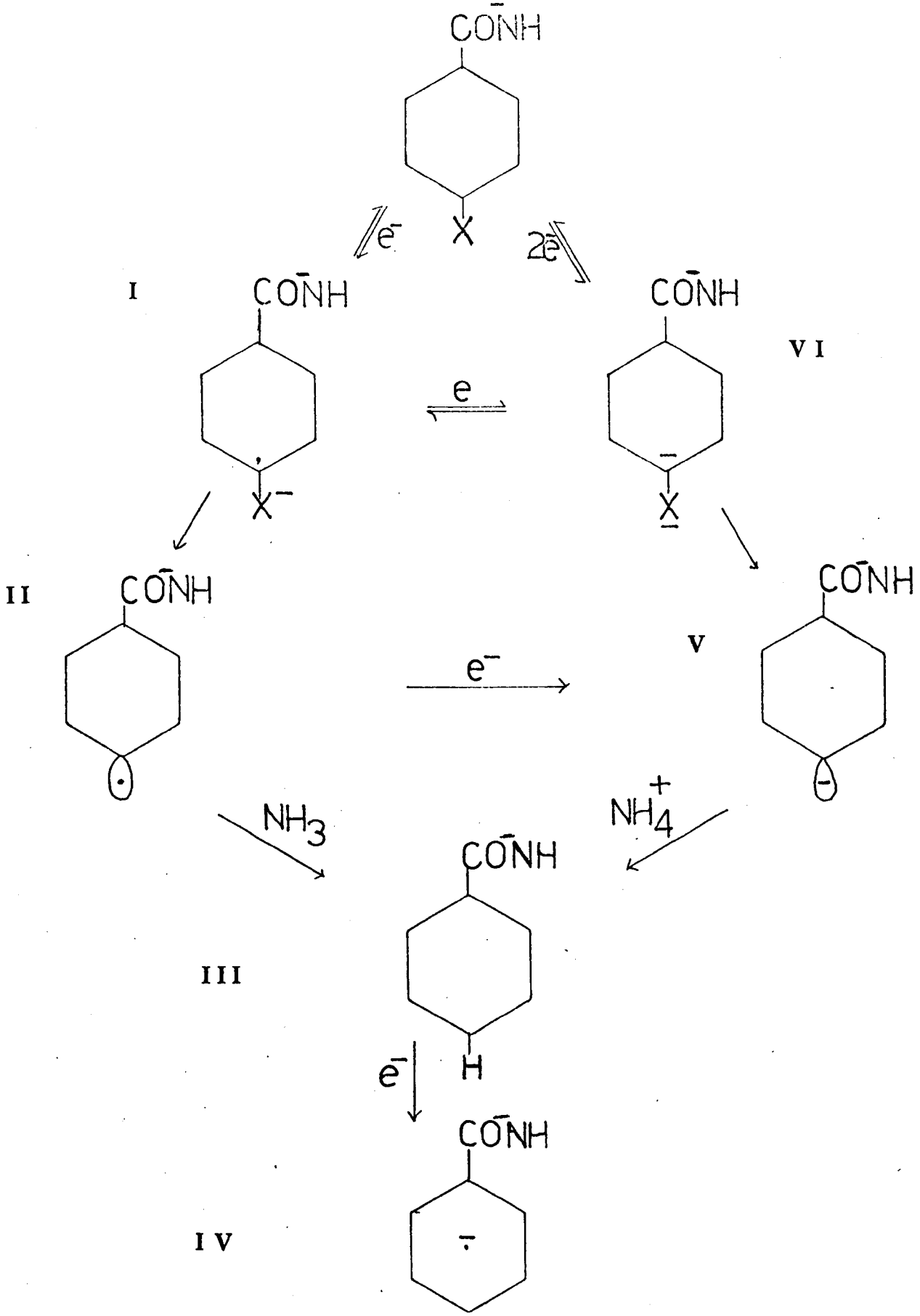

Scheme 5.1 Dehalogenation of 4-fluorobenzamide

5.4.3 Halo-Benzamides

When 4-fluorobenzamide is reduced in the continuous flow system the esr spectrum obtained shows the presence of a poorly resolved, low intensity resonance from a second species, which is undoubtedly the parent radical-anion. Although bond-cleavage by electrons is well known, the exact mechanism by which the benzamide radical-anion arises is still open to controversy, as indicated below.

Second order rate constants for the reaction of e^-_{aq} with various aryl halides have been measured[151] and indicate a rapid initial electron addition, and pr and matrix isolation techniques have shown that reaction of e^-_{solv} with alkyl and aryl halides is one of dissociative electron attachment[100,152,153]

$$RX + e^- \rightarrow R^\cdot + X^-$$

The rate at which fluorine is lost is considerably less than with other halogens, so much so that fluorobenzamide radical-anion is sufficiently long lived to be observed in the flow system. The sequence of reactions giving rise to the parent compound, on the other hand, are extremely rapid and the benzamide radical-anion is observed on the same ms time scale. The sequence of reactions shown in Scheme 5.1 represents the various possible routes by which the reductive dehalogenation may take place. Most evidence points strongly towards the initial step being the formation of the radical-anion I by the reversible addition of an electron. This radical-anion may then characteristically lose halogen as the anion with the formation of the neutral radical II. Abstraction of hydrogen from the solvent or cosolvent by II results in the formation of the neutral species III from which the radical-anion IV is produced by electron attachment.

Although this series of reactions is favoured by Buick et al.[48], Jolly has suggested[29] that the formation of biphenyl from arylhalides is best rationalised by the neutral radical II taking up a second electron to form the diamagnetic anion V which may then form the parent compound III by addition of a proton. (Although the hydrogen ion concentration is normally extremely low in liquid ammonia the ionisation of benzamides does increase this somewhat, but in so doing provides a competitive reaction for e^-_{amm} (equation 1·6).) Clearly V may also arise by the initial formation of the dianion VI. This could be formed by the addition of two electrons either simultaneously or consecutively.

The presence of secondary products could not be detected in 2-fluorobenzamide or in 4-flouro-N,N-dimethylbenzamide. The loss of chlorine from 4-chloro-N,N-dimethylbenzamide occurs at a much greater rate and the sequence of reactions giving rise to the parent radical-anion are completed before observations can be made.

5.4.4 Anomalous Results

The radical-anions of N-methylbenzamide and 2-fluorobenzamide showed anomolous behaviour in that their esr spectra were analysed in terms of a full complement of magnetic nuclei (Table 5.2) rather than the ionised form expected from equation 5·1. Ring substitution by methyl gtoups in benzamide has been shown[154] to reduce the ionisation constant in the ratio meta ($\frac{1}{5}$): ortho ($\frac{1}{10}$): para ($\frac{1}{12}$) and it can be argued that methyl substitution at the site of ionisation would reduce this to the extent that the unionised form is prevalent and accepts the electron. If similar arguments were applied to fluorobenzamides then it would be expected that the para-

substituted species would also show anomolous behaviour. The non-ionisation may arise through electrostatic interaction between the lone pairs on the fluorine and amide protons.

5.5 Conclusions

The radical-anions $ArCONH_2^{\cdot-}$ or radical-dianions $ArCONH^{2\cdot-}$ of a series of ring and N-substituted benzamides, thiobenzamides and nicotinamides have been characterised by esr spectroscopy by use of the continuous liquid ammonia flow system. Most of the radicals are of the dianion type and display restricted rotation about the bond from the ring to the substituent. Assignment of coupling constants have been made by comparison with spin densities calculated by simple MO methods.

CHAPTER 6

REDUCTION OF ACYCLIC AND CYCLIC α,β-UNSATURATED KETONES

6 ACYCLIC AND CYCLIC α,β-UNSATURATED KETONES

6.1 Introduction

Early work on the reduction of α,β-unsaturated ketones by the ammoniated electron was mainly confined to the stereochemistry of the products[155], particularly in reactions involving steroids and triterpenoids. Saturated ketones are normally formed as the end product of the reaction although in the presence of a proton source and excess alkali metal, reduction of the carbonyl group has been observed in several cases.[156] Earlier work[157] on the free radical reduction of simple aliphatic systems, by sodium amalgam for example, had shown that reductive coupling also takes place. More recently reduction and reductive coupling have been studied in detail in a variety of systems[158-162].
Free radical polymerisation frequently occurs during reduction of α,β-unsaturated carbonyl systems.

Conformational equilibria in open chain α,β-unsaturated ketones have been recognised for some time and s-cis and s-trans isomers have been observed spectroscopically in several simple α,β-unsaturated ketones[163-166].

Hitherto, attempts to characterise the one-electron addition products of α,β-unsaturated ketones by esr spectroscopy have only been successful when key positions are substituted with blocking groups. Russell and Stevenson[167] have prepared and characterised the ketyls of several 2-cyclopentenones and 2-cyclohexenones in which all hydrogens α to the Π-system are substituted by methyl groups and have also shown that the reported esr spectrum of Chen and Bersohn[168] for the ketyl of 4,4-dimethyl-2-cyclohexenone is

due to a semidione. House et al.[169] and Harbour and Cuzzo[170] have reported ketyls of a few straight-chain α,β-unsaturated ketones . Unsuccessful attempts at preparing radical-anions of simple enones e.g. MVK, acrolein, crotonaldehyde, by electrolysis in liquid ammonia have been reported by Tolles and Moore[76]. Ray et al.[171] have reported the ketyl of dicyclopropyl ketone but both Russell[167] and the author have been unable to reproduce their results.

In this chapter is described the synthesis of the ketyls of several acyclic and cyclic α,β-unsaturated ketones in the liquid ammonia flow system. In certain of the acyclic systems, equilibria have been observed between s-cis and s-trans conformations and simple MO methods have been applied to them. Alternating linewidth effects have been observed in the esr spectra of the ketyls of 2-cyclohexenone and its 3-methyl homologue and these have been interpreted as arising from slow limit interconversion of protons in axial and equatorial conformations.

The neutral radicals of 3,5,5-trimethyl- and 3,5-dimethyl-2-cyclohexenone have been observed following the addition of a proton source to the reduction medium. In certain cases, static reduction has demonstrated the presence of secondary radicals.

6.2 Experimental

The reduction technique was the same as described in section 4.2. Substrate concentrations were in the range $10^{-3} \rightarrow 10^{-2}$ M and temperatures were maintained near the freezing point of the solvent ≈ 200 K. In cases where higher temperatures were used the temperature of the cryostat was reduced to a few degrees below the desired temperature by the

addition of solid carbon dioxide. The heat capacity of the bath was sufficient to prevent any appreciable change in temperature during the recording of the esr spectra. The temperature was continually monitored during this period and was found to be constant to within ± 2°K.

Samples of 3-methoxy-, 3-ethoxy-, unsubstituted 5,5-dimethyl-2-cyclohexenone and 4,4,6-trimethyl-2-cyclohexenone were prepared by the method of Dauben et al.[172] and 4,4-dimethyl-2-cyclohexenone by the method of Bordwell and Wellman[173]. Samples of the methyl-, ethyl- and t-butyl-esters of 3-methyl-4-carboxy-2-cyclohexenone were kindly provided by Dr. A. Begbie.

6.3 Results

6.3.1 Open chain α,β-unsaturated ketones

Reduction of freshly distilled MVK (10^{-2} M) in the continuous flow system at 233 and 203 K yielded esr spectra which clearly arose from a mixture of two radicals, Fig. 6.1 (a). The major component was analysed in terms of two equivalent protons and three equivalent protons and the other in terms of two inequivalent protons and three equivalent protons, (Table 6.5). These have been assigned to the s-cis (I) and s-trans (II) conformations of the MVK radical-anion respectively (Section 6.4.2). Although both of these species should show coupling from a further proton, this would not be expected to be very large[169] and is probably less than the linewidth (0·03 and 0·05 mT respectively). Relative intensities of the two spectra varied slightly with temperature and the s-cis conformation appeared to predominate nearer the freezing point of the solvent, (s-cis:s-trans = 1·3 @ ≈ 230 K, 1·7 @ ≈ 203 K). The radicals are centred at g = 2·0034 (s-cis)

and g = 2·0038 (s-trans). Fig. 6.1 (c) and (d) show the computer simulations of the esr spectra of s-cis and s-trans forms respectively based on the coupling constants given in Table 6.5, and Fig. 6.1 (b) shows the computer simulation of the mixture at 233 K for a ratio of s-cis : s-trans of 1·3.

The esr spectrum recorded for the ketyl of mesityl oxide (III) (4-methylpent-3-ene-2-one), was of a single species and showed no change with temperature. The spectrum was analysed in terms of six equivalent protons, three equivalent protons and a single proton (Table 6.5), and unequivocal assignment of these couplings could be made to the species $C_6H_{10}O^{\bar{\cdot}}$. Ultrasonic relaxation[174] and dipole moment[175] measurements have indicated the s-cis form of mesityl oxide is predominant and assignments have been made accordingly.

Partial reduction of a freshly distilled commercial sample of 3-methylpent-3-ene-2-one (IV) to its ketyl produced a mixture of radical-anions. The esr spectrum recorded at the lowest temperature (198 K) was the most complex and appeared to arise from more than two species. However, from the spectrum recorded at 203 K it was possible to measure the coupling constants of one of the species i.e. from three inequivalent methyl groups and a single proton (Table 6.5). Reduction of this compound probably yields a mixture of isomeric and conformeric ketyls, and the coupling constants measured have been assigned to the s-trans conformation of the semi-reduced solute (Section 6.4.2).

The rather low solubility of 2,6-dimethylhepta-2,5-diene-4-one (V), phorone, at 203 K prevented any appreciable concentration of the ketyl from being formed, and even

Figure 6.1

a) Esr spectrum of the ketyls of
s-cis and s-trans MVK measured at 230 K

b) Computer simulated mixed spectrum
s-cis : s-trans = 1·3

c) Computer simulation of the ketyl of s-cis MVK

d) Computer simulation of the ketyl of s-trans MVK

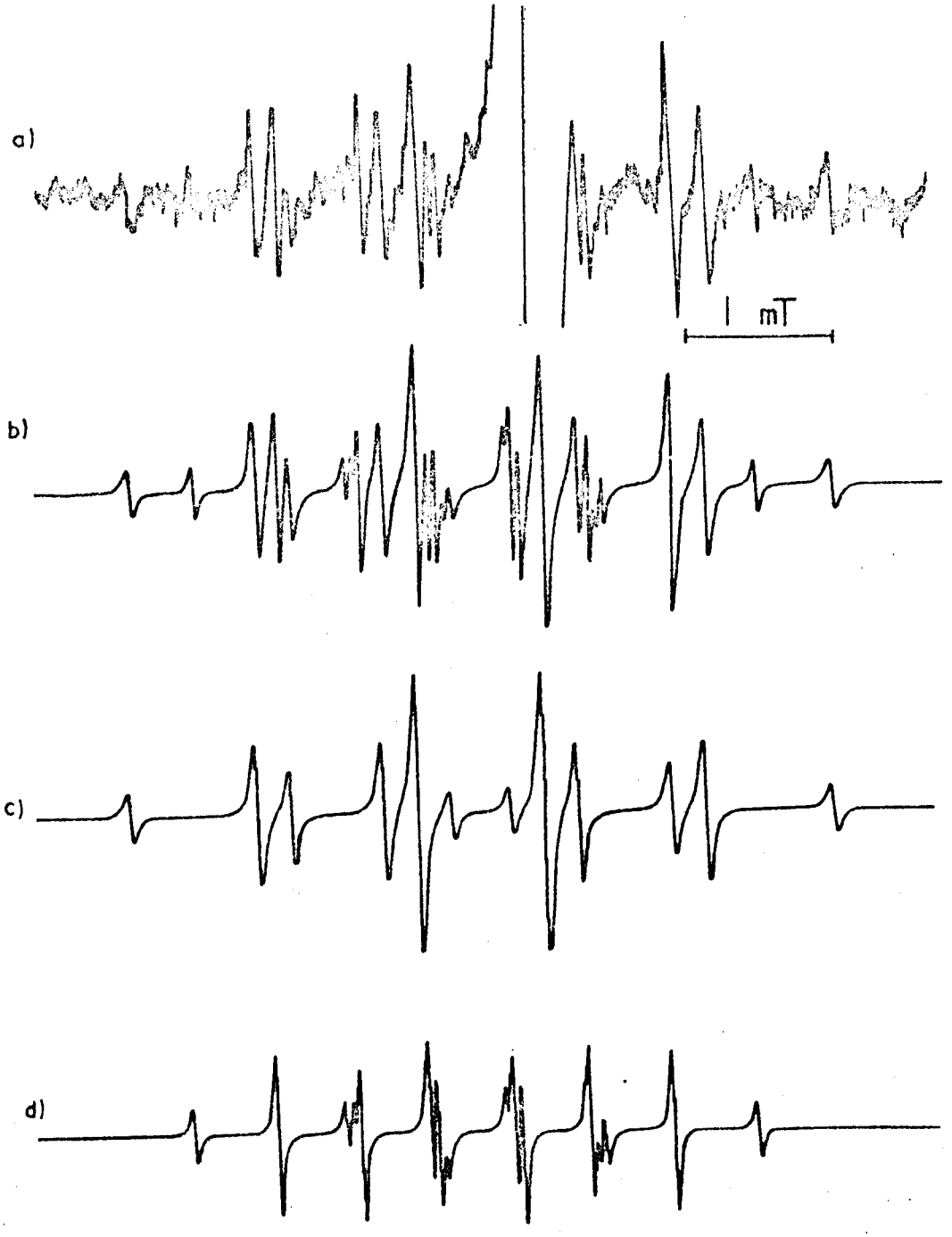
a)
1 mT
b)
c)
d)

at 243 K the signal strength was insufficient to observe groups of lines in the wings of the spectrum. From spectral line intensities, however, it was clear that the unpaired electron was coupling with twelve equivalent protons and two equivalent protons (Table 6.5). There was no evidence of resonance from any other species indicating that only one conformation is present in this radical-anion (Section 6.4.2).

Partial reduction of pent-3-ene-2-one to its ketyl was carried out at several concentrations between 10^{-2} and 2×10^{-2} M and at temperatures as low as 198 K and in all cases the spectra obtained were of low intensity and unanalysable.

Reduction of freshly distilled samples of methylcyclopropyl- and dicyclopropylketones (10^{-2} M) by e^-_{amm} at 200 K was evinced by the rapid rate of decolourisation of the sodium-ammonia solution. In both cases the rather low intensity esr spectra that were recorded had the same deceptively simple appearance, being assymetric about the centre and consisting of less than twenty lines (the signal from e^-_{amm} obscured part of the field and prevented reliable measurement of relative line intensities). The spectra probably arise from a low concentration of common impurities.

The spectrum of the β-ionone ketyl (VI) showed better resolution than that of Harbour and Guzzo[170] and a measurable difference in the couplings for H_C and H_D was observed (Table 6.5). The spectral linewidth (0·083 mT) is probably due to unresolved γ-couplings.

Neither acrolein, nor 2-methacrolein, nor crotonaldehyde gave any resonance in the continuous flow system.

TABLE 6.1

Coupling constants of the esr spectrum of the 2-cyclohexenone ketyl recorded at 230 K and 203 K

Position		Coupling Constant (mT) 230 K	203 K
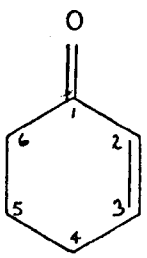	2	0·073	0·077
	3	1·298	1·279
	4a	-	2·326
	4e	-	0·613
	4a + 4e	3·210	2·939
	5a	0·073	0·077
	5e	0·073	0·077
	6a	-	1·315
	6e	-	0·429
	6a + 6e	1·744	1·744

6.3.2 Cyclic α,β-unsaturated ketones

Cyclopentenone (VII) when reduced in the flow system (10^{-2} M) at 220 K, produced a simple, well-resolved spectrum (Fig. 6.2) which could be readily analysed in terms of two pairs of two equivalent protons and one proton (Table 6.6). Although the 2-cyclopentenone ketyl would be expected to show coupling from a further proton at C_2 this is expected to be small[169] and in this case is less than the linewidth.

Reduction of 2-cyclohexenone (VIII) to its ketyl was first effected by Buick[27] at ≃ 230 K and the spectrum obtained shown in part in Fig. 6.3 (a) was analysed in terms of three equivalent protons and three inequivalent protons (Table 6.1). When the reduction was carried out at lower temperatures (≃ 200 K) new groups of low amplitude, broadened lines became apparent (Fig. 6.3 (b)). Re-analysis of this spectrum showed there to be two additional proton couplings (Table 6.1) and that the sum of two particular pairs ($a_{4a} + a_{4e}$ and $a_{6a} + a_{6e}$) were approximately equal to the two largest couplings reported by Buick. Such a phenomenon is characteristic of time dependent modulations of hyperfine coupling constants, in this case arising from conformational interconversions in the 2-cyclohexenone radical-anion.

A well resolved spectrum of the ketyl of 3,5-dimethyl-2-cyclohexenone (IX) was obtained (10^{-2} M) at 203 K and couplings from six inequivalent protons and three equivalent protons, but none from the remote C_5 methyl group (Table 6.6). No temperature dependence of this spectrum was observed indicating that the molecule has a marked preference for one conformation, i.e. the C_5 methyl substituent in an

Figure 6.2

a) Esr spectrum of 2-cyclopentenone ketyl measured at 220 K

b) Computer simulation

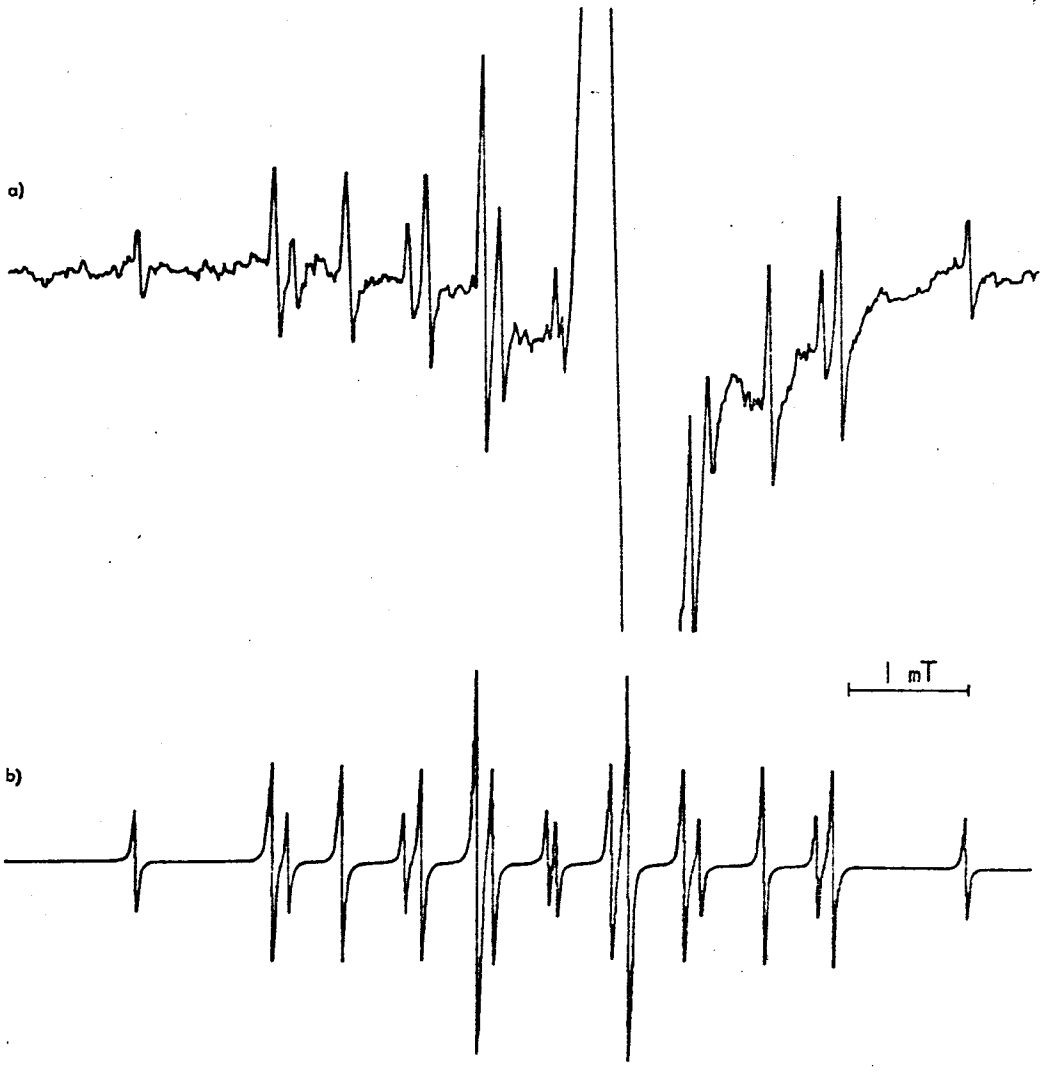
a)
1 mT
b)

Figure 6.3

a) Part of the low-field half of the esr spectrum of 2-cyclohexenone ketyl measured at 230 K

b) Full esr spectrum of 2-cyclohexenone ketyl measured at 200 K

c) Computer simulated spectrum: $\tau = \infty$

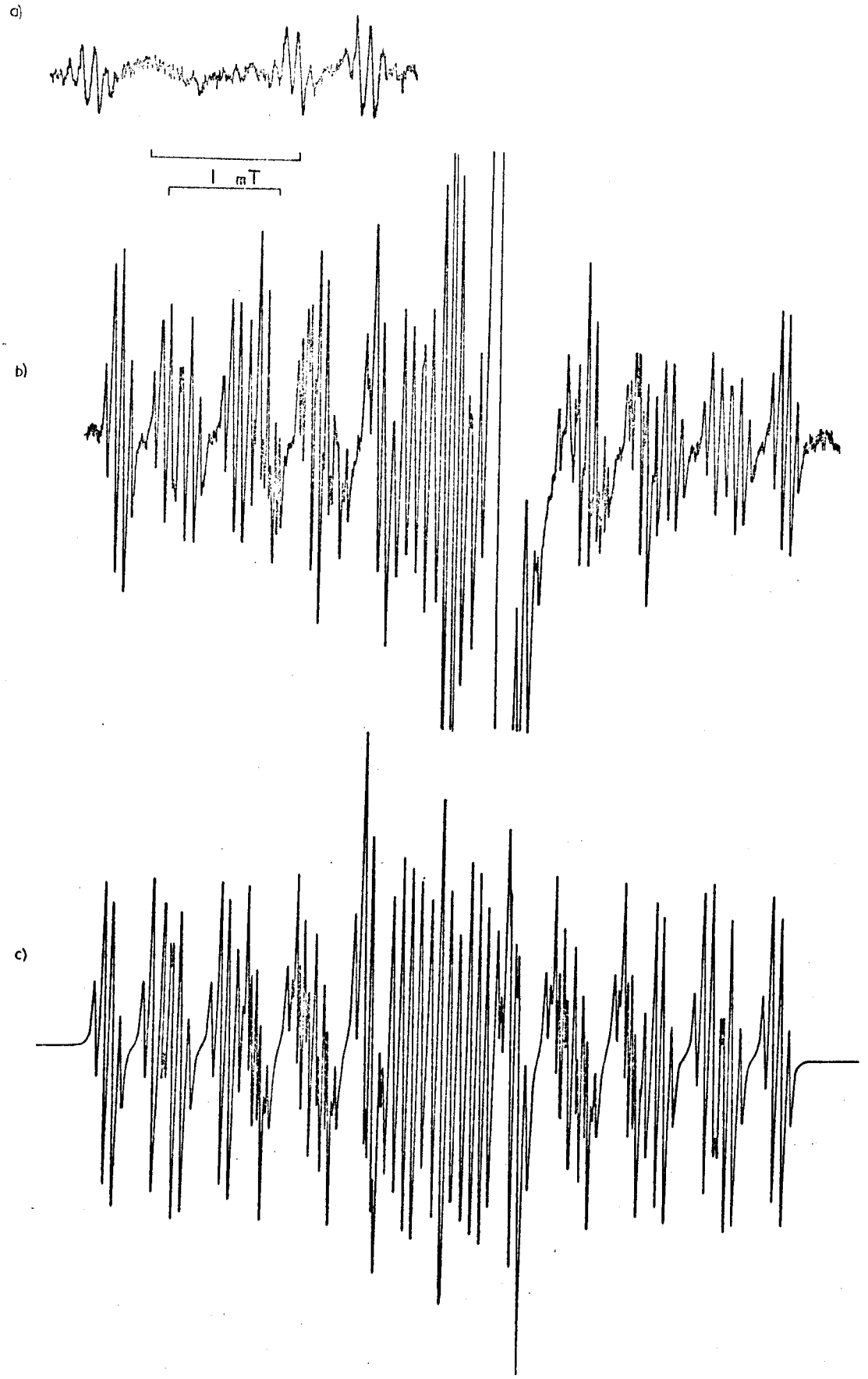
a)
1 mT
b)
c)

equatorial conformation.

Reduction of 10^{-2} M 4,4-dimethyl-2-cyclohexenone (X) at 208 K produced a broad spectrum which showed a large triplet coupling from two equivalent (or almost equivalent) protons split by a smaller doublet (Table 6.6). Under high resolution the lines began to resolve into many overlapping lines arising from small couplings (< 0·1 mT) of the eight γ-protons and the small C_2 proton coupling.

The esr spectrum recorded for the ketyl of 5,5-dimethyl-2-cyclohexenone (XI) at 200 K showed couplings from six inequivalent protons (Table 6.6) and appeared to exhibit line-broadening of certain spectral lines. However, careful re-examination of spectra run at various temperatures showed that this apparent broadening arose from the similarity of two couplings rather than from the time dependent phenomenon as suggested in a preliminary note[176]. Fig. 6.4 (a) shows the low field half of the spectrum obtained at 222 K along with its computer simulation based on the coupling constants given in Table 6.6. This spectrum is typical of those recorded over the whole range. The poor quality of the original spectrum recorded at 200 K is attributed to bubbling in the sodium solution.

Reduction of 10^{-2} M 4,4,6-trimethyl-2-cyclohexenone (XII) at 208 K produced an esr spectrum comprising a large triplet arising from two equivalent or nearly equivalent protons (Table 6.6).

3,5,5-Trimethyl-2-cyclohexenone (XIII) reduced at 230 K produced a well-resolved spectrum which was analysed in terms of five inequivalent protons and three equivalent protons (Table 6.6). The spectral lines showed no broadening

Figure 6.4

a) Low-field half of the esr spectrum of 5,5-dimethyl-2-cyclohexenone ketyl measured at 222 K

b) Computer simulation

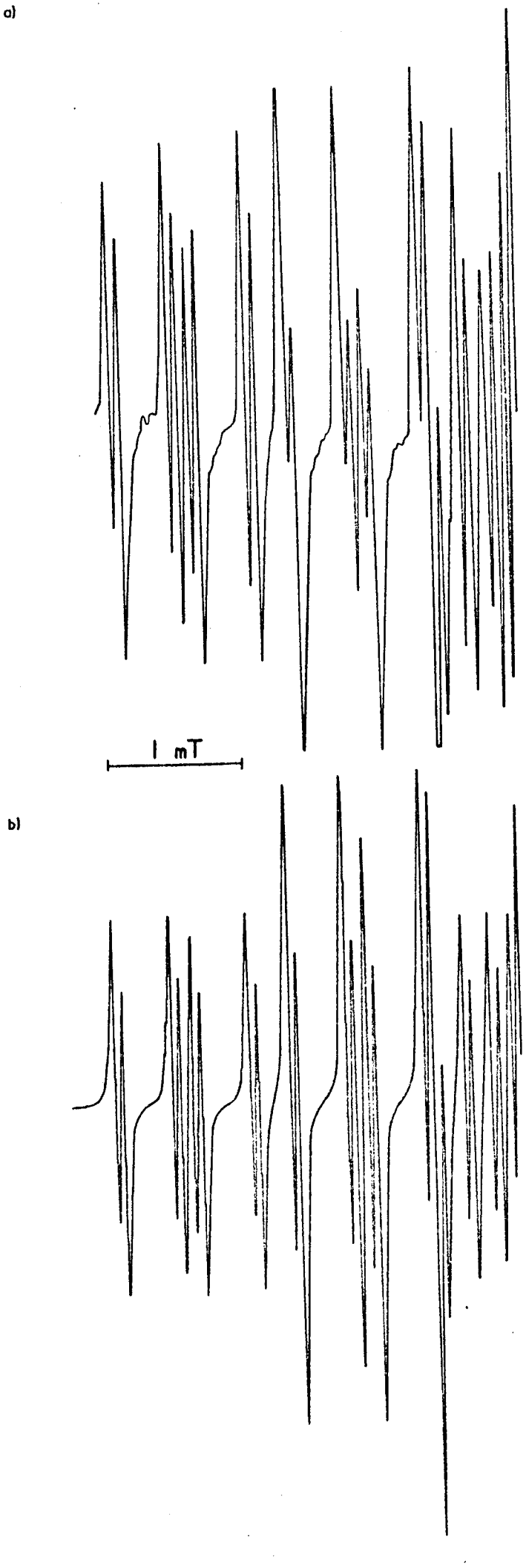
a)
1 mT
b)

Figure 6.5

Plot of methyl group coupling constants for a series of radical-anions produced in liquid ammonia[27,28,48,87-89], versus the calculated McLachlan spin density at the π-centre to which they are attached

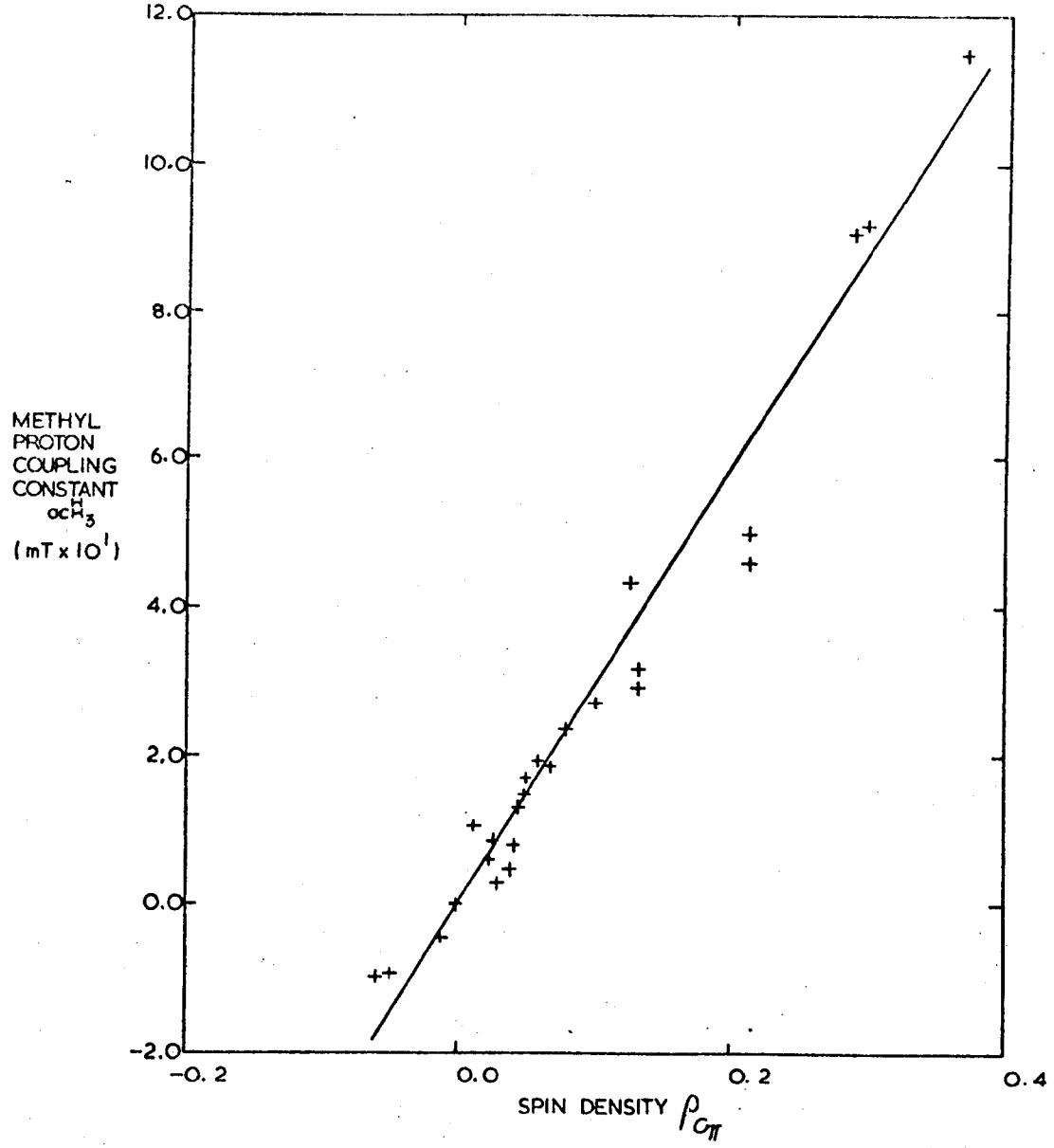
12.0
10.0
8.0
6.0
4.0
2.0
0.0
-2.0
-0.2
0.0
0.2
0.4
METHYL PROTON COUPLING CONSTANT $a^{H}_{CH_3}$ (mT x 10¹)
SPIN DENSITY $\rho_{C\pi}$

even at this temperature.

3-Methoxy-5,5-dimethyl-2-cyclohexenone (XIV) (5×10^{-3} M) was reduced at 203 K and produced a claret coloured eluate which decolourised within a minute. The esr spectrum, which showed no anomalous linewidths, yielded couplings from five inequivalent protons and three equivalent protons (Table 6.6). The corresponding ethoxy derivative (XV) showed similar properties (brown eluate) and esr spectrum, but with a coupling for two ethoxy protons (Table 6.6).

When the methyl-, ethyl- and t-butoxy- esters of 3-methyl- 4-carboxy-2-cyclohexenone (XVI a,b,c) were reduced in the flow system only poorly resolved spectra were obtained. Reducing the concentration ($10^{-2} \rightarrow 10^{-3}$ M), although making some improvement in the resolution, resulted in a decrease in signal strength. Temperatures of 200 K were employed in all cases. Under low resolution it was possible to discern the general features of a large quintet (1:4:6:4:1) split by a single proton (Table 6.6). The spectra of all the esters were generally similar in this respect.

Electron attachment to 2,6-dimethyl-γ-pyrone (XVII) at 204 K (10^{-2} M) produced the corresponding ketyl which gave a well-resolved spectrum and afforded couplings from six equivalent protons and two equivalent protons (Table 6.6), which compare favourably with those found in cyclohexadienones[167,177]

Reduction of 10^{-2} M 3-methyl-2-cyclohexenone (XVIII) at 200 K produced a rather poorly resolved esr spectrum which exhibited extensive line-broadening of certain of the spectral lines. The combination of line-broadening and low resolution has hitherto prevented complete analysis of the

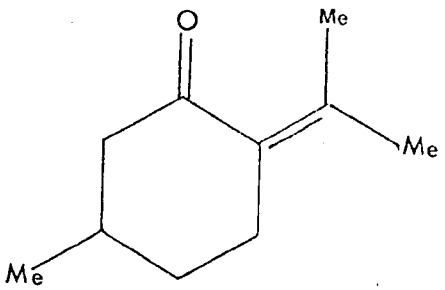

XIX

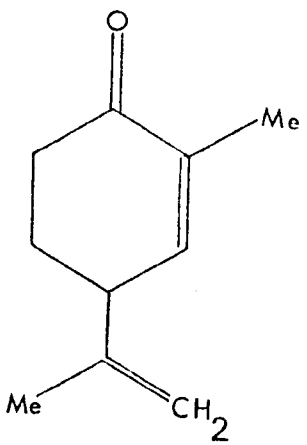

XX

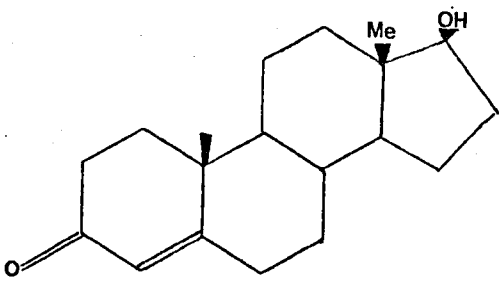

XXI

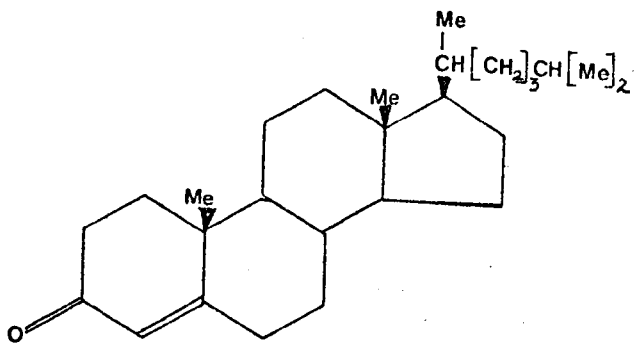

XXII

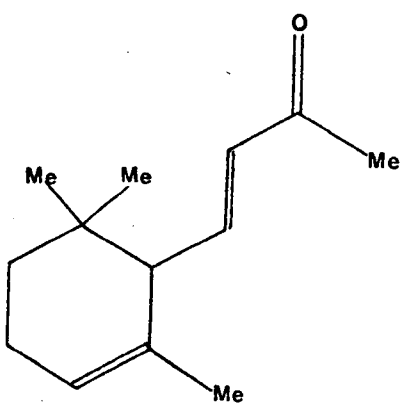

XXIII

spectrum, although coupling from the methyl protons may readily be determined (Table 6.6). From the degree of line-broadening exhibited at this low temperature it is evident that the conformational lifetime is less than that of 2-cyclohexenone.

Although resonance could be observed from the ketyls of pulegone (XIX), carvone (XX) and 3,4,4-trimethyl-2-cyclohexenone, analysis of these spectra could not be effected. Testosterone (XXI), 4-cholesten-3-one (XXII) and 2-benzyl-3-methyl-2-cyclohexenone were too insoluble to produce an observable resonance, despite the addition of up to 10% $^{V}/_{V}$ THF. Reduction of freshly distilled α-ionone (XXIII) produced a spectrum identical to that of β-ionone. Nmr and glc examination showed the presence of ca. 2% impurity of β-ionone which could not be excluded by redistillation.

6.4 Discussion

6.4.1 Reduction of α,β-unsaturated ketones

Ethylene proves resistant to reduction by sodium in liquid ammonia and its radical-anion has not yet been reported. Substitution in this molecule by electronegative groups such as -CN, $-CO_2^-$, $-CO_2R$, -COR results in a dramatic change in the situation and high values of the rate constant for reaction of such compounds with e^-_{aq} have been recorded[31]. This no doubt arises from the electron withdrawing effect of the substituent providing a positive site for electron attachment

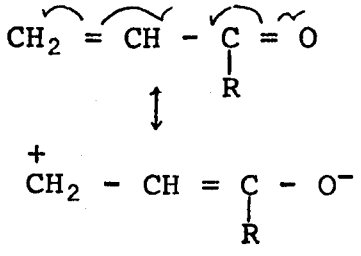

and allowing delocalisation of the unpaired electron in the radical-anion once it is formed.

6.4.2 Assignment of coupling constants and MO calculations

(a) Open chain α,β-unsaturated ketones

The coupling constants for mesityl oxide may be assigned unequivocally without resort to MO calculations. By comparison with this ketyl, it is possible to assign couplings of other ketyls to particular nuclei. However, no indication is given as to the conformation of these radicals. Simple Hückel MO theory is inadequate in this respect in that it cannot distinguish between different conformations of open chain Π-systems. Modifications to the simple theory[70,89,142-144] have been employed to account for asymmetric spin density distribution in benzenoid systems arising from restricted rotation of substituents and these have been discussed in section 5.4.2 of Chapter 5. Still favouring the β-effect method, calculations for s-cis and s-trans MVK have been carried out by representing the interaction between the oxygen and the ethylenic Π-system in the s-cis conformation as a weak bond between atoms C_1 and O_4

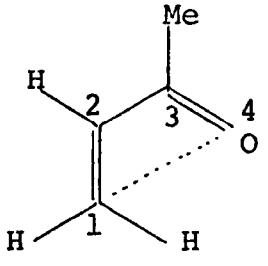

such that

$$\beta_{1-4} = \underline{h}'\beta_0, \left[\underline{h}' = 0{\cdot}05\right] \qquad 6{\cdot}1$$

This model was also used in conjunction with one to represent the non-planarity of the s-cis form[165] which involved variation of the resonance integral of the C_{2-3} bond according to the relationship

$$\beta^{\theta}_{2-3} = \beta^{0}_{2-3} \cdot \cos\ \theta \qquad 6\cdot2$$

where θ is the dihedral angle between the $2p_z$ orbitals of atoms C_2 and C_3, β^{θ}_{2-3} is the resonance integral for the C_{2-3} bond in the absence of twisting, and β^{0}_{2-3} that resonance integral for a dihedral angle of 0^0.

The Hückel parameters $\underline{k}_{C=C}$ and $\underline{k}_{C-C}$ were altered slightly from the values for a single bond and double bond[124] to account for conjugation and were set at 1·05 and 0·95 respectively. The Coulomb integrals, $\underline{h}_C$, were set equal to zero. Parameters for oxygen $\underline{k}_{C=O}$ and $\underline{h}_O$ were both given the value 1·00 (cf. ref. 170 (b)), although higher values have been employed by other workers[70, 87, 145]. Methyl substituents were treated by a mixed heteroatom-inductive model and the parameters were those used in Chapter 5. The McLachlan configuration interaction parameter λ was set equal to 1·2

Experimental spin densities have been related to the experimental coupling constants using the equations 3·5 and 3·6. The value of $Q^{H}_{CCH_3}$, which proves to be constant for a great many systems has been frequently given the value 2·8mT, as has been used in the previous chapter), however, a value of 2·899 ± 0·065 mT is suggested from a least squares analysis of data for a large number of aromatic radical-anions produced in the liquid ammonia flow system (Fig. 6.5), a value which compares favourably with 2·93 mT derived for alkyl radicals[178]. When an sp^2 carbon is both substituted by a methyl group and a proton, the value of Q^{H}_{CH} for α,β-unsaturated carbonyl systems may be calculated from the experimental spin density at that Π-centre, derived from $Q^{H}_{CCH_3}$. This situation arises for 3-methylpent-3-ene-2-one in the present chapter and for trans-crotonic acid and its methyl and ethyl

TABLE 6.2

π-Spin densities for s-cis and s-trans methyl vinyl ketone

Position	Spin Density				
	Experimental		1. McLachlan only	2. McLachlan + β effect	3. McLachlan + β effect + 38° twist
	*s-cis	†s-trans			
1	0·469	0·455	0·588	0·581	0·471
2	<0·020	<0·010	-0·082	-0·080	-0·047
3	0·318	0·209	0·380	0·379	0·457

* Assignments based on model 3.

† Assignments based on model 1.

esters (Chapter 7). Although the data is limited, the value of Q^{H}_{CH} is fairly constant for the radical-anions of the acid and its esters (2·49 ± 0·008 mT) but is somewhat higher than the value calculated for the ketone viz., 2·337 mT. An average of these four values has been employed i.e. 2·45 ± 0·04 mT.

Inclusion of the β-effect results in a decrease in spin density at both C_1 and C_2 Table 6.2. The magnitude of these changes is of the correct order of magnitude for the position C_1 but is only about 1% of the observed difference at position C_3. The β-effect would lead to the assignment of the group of couplings with $a^{H}_{CH_3}$ = 0·922 mT to the s-trans form. Calculations for the non-planar model, ($\theta = 38^{o}$ [165]) predict changes of the correct order of magnitude for ρ_3, in the opposite direction to the β-effect, but fail to predict that both ρ_1 and ρ_3 change in the same direction.

On the basis of these models it appears that the large difference between the conformers arises mainly from the non-planarity of the s-cis conformer, and that this effect overwhelms any from the interaction of the ethylenic and carbonyl π-systems. Hückel spin densities for the combined model predict that the ρ_3 would now be larger than ρ_1, (Table 6.5). Assignments have been made on the basis that the twisted s-cis model gives rise to the methyl coupling of 0·922 mT. These assignments are consistent with those given for mesityl oxide and also compare favourably with Russell's unambiguous assignments[98(a)] for the s-cis and s-trans conformers of diacetyl ($a^{H}_{CH_3}$ = 0·70 mT_{expt} cf. 0·97 mT_{calc} and s-trans $a^{H}_{CH_3}$ = 0·56 mT_{expt} cf. 0·85 mT_{calc}). The magnitude of the experimental spin density at C_3 in 3-methylpent-3-ene-2-one indicates that

TABLE 6.3

Spin densities for the phorone ketyl

Position	π-Spin Densities				
	Experimental	s-cis/s-cis	s-cis/s-trans	s-trans/s-trans planar	s-trans/s-trans twisted
1	0·275	0·270	0·237	0·326	0·266
2	0·067	-0·092	-0·081	-0·098	-0·091
3	0·067	-0·092	-0·108	-0·098	-0·091
4	0·275	0·270	0·366	0·326	0·266

this is in an s-trans conformation, and suggests that in this particular isomer, the β-methyl group is trans to the carbonyl group. Raman and ir spectroscopy[163] have indicated that if the olefinic methyl groups were trans to each other then the twisted s-cis conformation would be favoured.

The results for mesityl oxide (III) are disappointing. For a dihedral angle of 38° the calculated spin density at C_3 is greater than that for C_1. Calculations indicate that θ should not exceed ≈ 20°, and the best results are obtained are for θ = 10° (Table 6.5). In the phorone ketyl (V) three conformational arrangements are possible i.e. a) s-cis/s-cis , b) s-trans/s-cis , and c) s-trans/s-trans. Calculations for each of these have been carried out (Table 6.3) using θ = 38°. The fact that conformation a) gives the best agreement is encouraging, since b) would be expected to give rise to an asymmetric spin density distribution (as the calculations show) and c), because of the steric interaction of the methyl groups, would be unfavourable in the planar form at least. When this twisting is taken into account in c), even using θ = 38° so that the only difference between the two conformers s-cis/s-cis and twisted s-trans/s-trans is given by the β effect, the calculations still favour the s-cis/s-cis arrangement and coupling constants have been assigned accordingly.

Harbour and Guzzo[170] have carried out extensive studies on α- and β-ionones and have applied MO calculations to aid in the assignment of coupling constants. Physical measurements, such as molecular polarisability[179] have indicated that the conjugated Π-system is non-planar and that the plane of the double bond in the ring is inclined to that of

TABLE 6.4

Spin densities for the β-ionone ketyl

Position	π-Spin Densities		
	Experimental	McLachlan 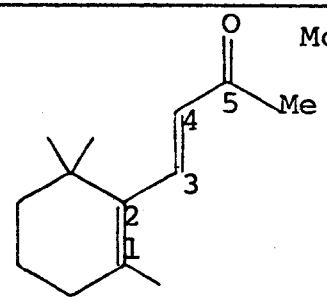	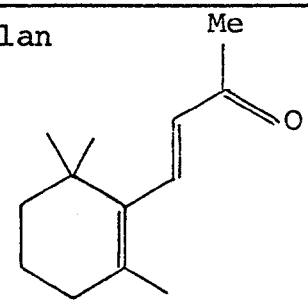
5	0·224	0·307	0·372
4	<0·019	-0·045	-0·016
3	0·678	0·443	0·365
2	-	-0·084	-0·073
1	0·224	0·230	0·204

the adjacent ethylenic bond ($\theta = 34^{\circ}$). Assuming these to be in an s-trans conformation the non-planarity has been accounted for using the equation 6.2 for the C_{3-4} resonance integral. In the present work calculations have also been carried out for the enone system of the side chain in both s-cis and s-trans conformations (Table 6.4). Better correlation is obtained for the planar s-trans conformation. Agreement is good overall except for the spin density at position C_3 which is very much lower than that which is observed experimentally. Gerson et al.[180] and Harbour and Guzzo[170(b)] have suggested that the additional coupling from this position may arise from a hyperconjugative type mechanism in which the C_3-H_3 σ bond, now twisted out of the nodal plane, overlaps with the $2p_z$ orbital at C_2. The negative spin density at this position leading to an enhancement of the coupling constant at C_3. This effect is formulated by the equation

$$a_{H_3} = Q^{H}_{CH}\rho_{C_3} + Q'\rho_{C_2} \cdot \cos^2(90 - \theta)$$

where Q' is estimated as being 13·5 ± 5 mT, and Q^{H}_{CH} is the McConnell constant (ca. - 2·5 mT). If this equation is applied to calculating the α-proton coupling in s-cis MVK then a value is predicted which is far in excess of that which is observed (ca. 2·4 cf. < 0·05 mT). This suggests that either the effect does not operate (or at least not to the extent that is suggested by the value of Q'), or the radical-anions of the s-cis ketones, unlike the neutral molecules, are planar.

Table 6.5 summarises the coupling constants and calculated spin densities for these radical-anions.

TABLE 6.5

Experimental and Calculated Spin Densities for α,β-unsaturated ketones (acyclic)

Compound		Position	Coupling (mT)	π-spin density			g-factor ± 0·0001
				Experimental	Hückel	McLachlan	
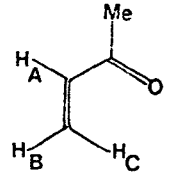	I	Me_e	0·922	0·318	0·379	0·457	2·0034
		H_A	< 0·05	< 0·020	0·083	- 0·047	
		H_B	1·169	0·477	0·330	0·471	
		H_C	1·169				
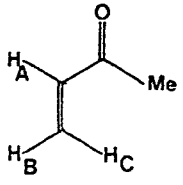	II	Me_e	0·606	0·209	0·326	0·380	2·0038
		H_A	< 0·03	< 0·010	0·073	-0·082	
		H_B (a)	1·103	0·462 (b)	0·399	0·588	
	-	H_C (a)	1·162				
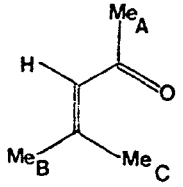	III	Me_A	0·955	0·329	0·346	0·425	2·0037
		H	0·136	0·056	0·017	- 0·114	
		Me_B	1·324	0·457	0·359	0·490	
		Me_C	1·324				

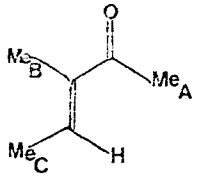	IV	Me_A	0·669	0·231	0·367	0·445	
		Me_B	0·052	0·018	0·003	- 0·115	2·0039
		Me_C	1·421	0·490 (c)	0·340	0·490	
		H	1·145	0·467 (d)			
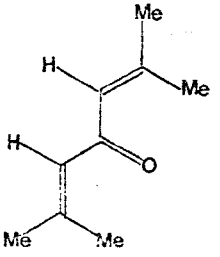	V						
		Me	0·797	0·275	0·199	0·270	2·0036
		H	0·165	0·067	0·003	- 0·092	
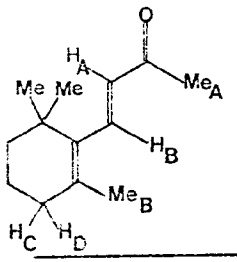	VI	Me_A	0·648	0·224	0·256	0·307	
		H_A	< 0·083	< 0·034	0·060	- 0·045	
		H_B	1·623	0·662	0·315	0·443	2·0036
		Me_B	0·648	0·224	0·164	0·230	
		H_C	0·841	-	-	-	
		H_D	0·979	-	-	-	

(a) Uncertainty in the assignment of these couplings.

(b) Calculated from an average of the two proton couplings.

(c) Calculated from the methyl coupling constant.

(d) Calculated from the proton coupling constant.

TABLE 6.6

Coupling constants for ketyls of cyclic α,β-unsaturated ketones

Reference	Ketyl	Coupling Constants (mT) (i)								g-factor (ii)
		2	3	4a	4e	5a	5e	6a	6e	
VII		<0·029	1·265	1·724	1·724	1·126	1·126	-	-	2·0035
VIII	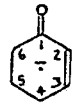	0·077	1·279	2·326	0·613	0·077	0·077	1·315	0·429	2·0037
IX	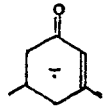	0·125	(iii) 1·481	2·319	0·746	0·074	-	1·381	0·462	2·0037
X	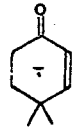	<0·1	≈1·30	(iii) <0·1	(iii) <0·1	<0·1	<0·1	1·30	0·48	2·0036
XI	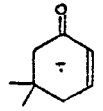	0·062	1·301	2·363	0·577	-	-	1·301	0·423	2·0038
XII	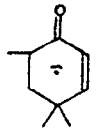	<0·1	≈1·29	(iii) <0·1	(iii) <0·1	<0·1	<0·1	≈1·29	(iii) <0·1	2·0040

XIII	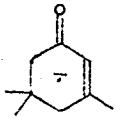	0·121	(iii) 1·429	2·255	0·689	-	-	1·366	0·435	2·0036
XIV	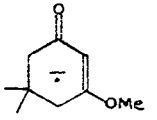	0·198	(iv) 0·088	2·261	0·763	-	-	1·410	0·446	2·0039
XV	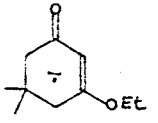	0·206	(v) 0·093	2·314	0·782	-	-	1·440	0·463	2·0038
XVI a) R=Me b) R=Et c) R=t-Bu^t	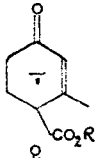	-	(iii) ≈1·3	-	≈0·7	-	-	≈1·3		-
XVII	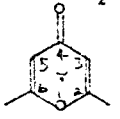	(iii)(vi) 0·807	(vii) 0·165	-	-	-	-	-	-	2·0040
XVIII	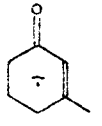		(iii) 1·48	-	-	-	-	-	-	-

(i) ± 0·005 mT except for X and XII which are ± 0·02 mT and XVI a), b) and c), which are ± 0·2 mT.

(ii) ± 0·0001

(iii) Methyl coupling.

(iv) Methoxy coupling.

(v) Methylene coupling from ethoxy group.

(vi) $a_2 = a_6$

(vii) $a_3 = a_5$

(b) Cyclic α,β-unsaturated ketones

The assignment of coupling constants in 3,5,5-trimethyl-2-cyclohexenone (XIII) may be made as follows. The methyl coupling (1·429 mT) clearly arises from the C_3 methyl group. Assuming the 2-cyclohexenone ketyl ring to be planar except for C_5, as it is in the neutral molecule[181] then the methylene protons at C_4 and C_6 will be, to a first approximation, in pure axial and equatorial conformations and the ratio $\frac{a_a}{a_e}$ will be given by

$$\frac{\text{Cos}^2\text{O}}{\text{Cos}^2 60} = 4 \qquad 6\cdot3$$

The two pairs of couplings which give closest agreement with this value are 2·255 : 0·689 = 3·27 and 1·366 : 0·435 = 3·14. Since MO calculations for the fragment A show that $\rho_3 > \rho_1$ (Table 6.8), then the former pair of couplings must arise from

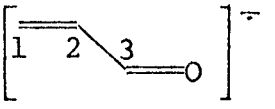

A

the methylene protons attached to C_4. The remaining coupling (0·121 mT) must arise from the C_2 proton. These assignments are confirmed by examining the coupling constants from X and XII, i.e. the gem-dimethyl substituents at C_4 in X result in the disappearance of couplings of ca. 2·3 and 0·6 mT and further substitution by methyl at C_{6e} in XII, results in the disappearance of a coupling of ca. 0·5 mT. Assignment of coupling constants in the other ketyls is now straightforward, except for 2-cyclohexenone and the 5,5-dimethyl-derivative (VIII, XI), where two proton couplings of the same magnitude (ca. 1·3 mT) are found. In VIII, one of these proton couplings is being modulated by conformational interchange and a correct computer simulation of the alternating linewidths (Section 6.4.5) can only be made by assigning the

TABLE 6.7

Dihedral angles for cyclic α,β-unsaturated ketones

Ketyl	Ratio of methylene proton coupling constants, a_{a/a_e} (± 0·05)		Calculated dihedral angle, θ[a] (± 12')	
	C_4	C_6	C_4	C_6
VII	1·00	1·00	30° 0'	30° 0'[b]
VIII	3·79	3·07	0° 54'	5° 6'
IX	3·11	2·98	4° 24'	5° 12'
XI	4·10	3·08	- 0° 21'	5° 6'
XIII	3·27	3·14	3° 30'	4° 15'
XIV	2·96	3·16	5° 0'	4° 15'
XV	2·96	3·11	5° 0'	4° 16'

(a) $a_{a/a_e} = \frac{\cos^2\theta}{\cos^2 60 - \theta}$

(b) C_5 in this ketyl

1·315 mT coupling to the C_{6a} position, leaving that of 1·279 mT to be assigned to C_3. The two corresponding couplings in XI are assigned by comparison with VIII, i.e. the larger one, (1·301 mT) to the C_{6a} proton. The assignments summarised in Table 6.6 compare favourably with coupling constants calculated by the INDO method for these systems[182].

6.4.3 Conformation of the cyclic ketyls

In the previous section it was assumed that the methylene protons at C_4 and C_6 in the cyclic ketyls occupied pure axial and equatorial positions. This, however, is not the case since the coupling constant ratios are not exactly equal to four ‡ (Table 6.7).

In general the 2-cyclohexenone ring in ketyls VIII, IX, XI, XIII, XIV and XV is very close to the structure that was assumed for assigning coupling constants, although θ_6 (Fig. 6.6) tends to be about 4° to 5° and is usually slightly larger than θ_4 (except in the alkoxy derivatives where it is ca. 1° smaller). The fact that the coupling constant ratio in XI is greater than four is readily explained in terms of θ_4 becoming slightly negative ($\simeq -12'$), possibly through the oxygen lying slightly below the plane defined by C_2, H_2, C_3 and H_3, and on the same side as C_5 (Fig. 6.7). The values of θ_4 and θ_5 of 30° for VII must arise thrcugh all heavy atoms lying in the same plane.

6.4.4 Spin density distribution

From these values of θ_4 for IX and XIII it is possible

‡ In the ketyls where axial and equatorial couplings can be determined, the accuracy of the measurements, 0·005 mT, corresponds to an error in the coupling constant ratio of 0·05, and so the observed differences are significant.

Figure 6.6

2-cyclohexenone ring showing dihedral angles θ_4 and θ_6 when all the heavy atoms are planar except C_5

Figure 6.7

2-cyclohexenone ring showing dihedral angles θ_4 and θ_6 when the oxygen atom lies below the plane defined by C_2, H_2, C_3 and H_3, and on the same side at C_5

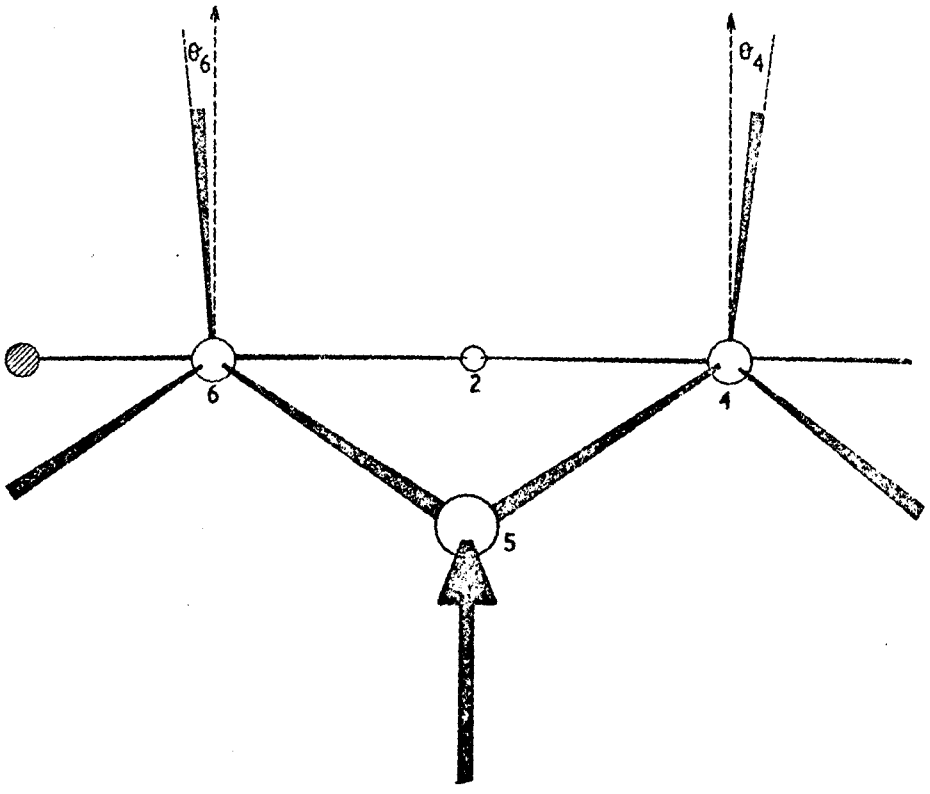
θ6
θ4
6
2
4
5

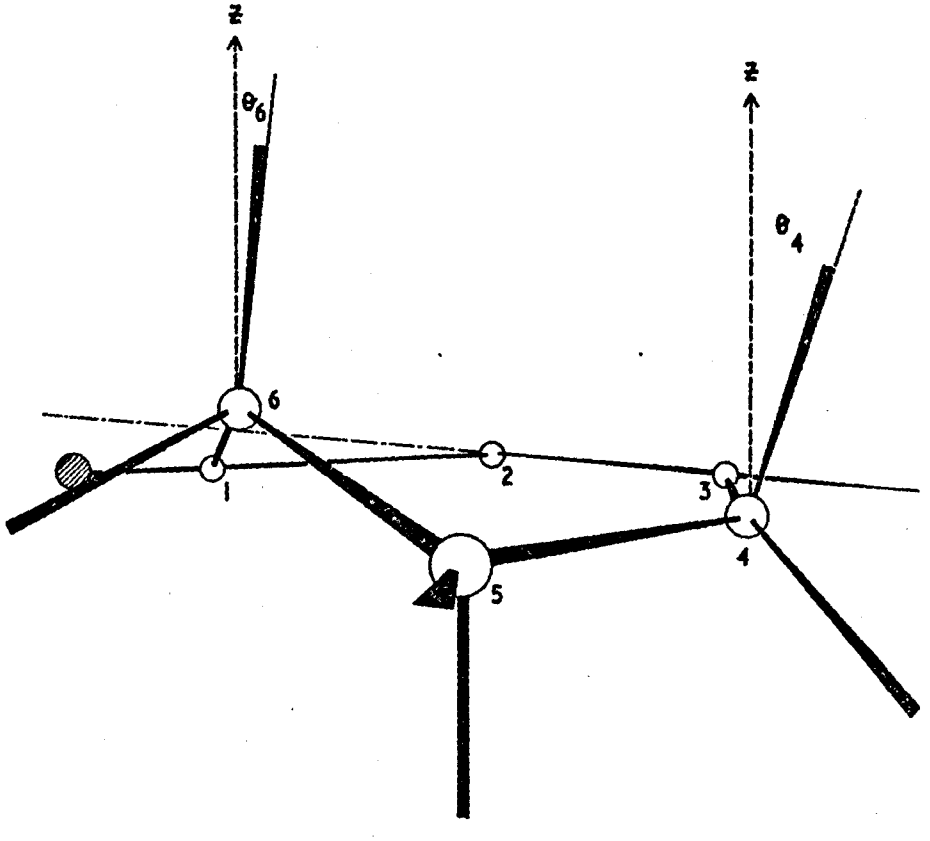
z
θ6
z
θ4
6
1
2
3
4
5

TABLE 6.8

Summary of Spin densities for cyclic α,β-unsaturated ketones

Ketyl	π-Spin Densities		
	1 (a)	2 (b)	3
Hückel	0·365	0·050	0·392
McLachlan	0·376	-0·023	0·423
VII	0·339	<0·01	0·508 (b)
VIII	0·289	0·031	0·510 (b)
IX	0·306	0·050	0·511 (c)
X	≃0·286	<0·04	≃0·520 (b)
XI	≃0·285	0·029	0·519 (b)
XII	0·284	<0·04	≃0·516 (b)
XIII	0·302	0·049	0·493 (c)
XIV	0·312	0·080	0·501 (a)
XV	0·318	0·083	0·513 (a)

(a) Calculated from $Q^{H}_{C'CH'}\rho_{C'} \cdot \cos^2\theta$

(b) Calculated from $Q^{H}_{CH}\rho_{C}$

(c) Calculated from $Q^{H}_{C'CH'_3}\rho_{C'}$

to estimate the value of Q^{H}_{CCH} in equation 3·7 since the spin density at C_3 may be calculated from the methyl group coupling constant. For these two ketyls the average value, 4·55 mT (4·54 and 4·57 mT respectively) lies well within the expected range. Russell has employed a value of 4·0 mT[183] although values of 5·0 mT are generally accepted. The spin density at C_3 in ketyls VIII and XI, calculated from 3·7, give an average value of Q^{H}_{CH} of 2·49 ± 0·02 mT (cf. 2·45 ± 0·04 mT for the open chain α,β-unsaturated carbonyl compounds). Experimental spin densities for positions C_1, C_2 and C_3 for these ketyls are given in Table 6.8 and may be compared with values calculated for the fragment A ($\underline{k}_{C=C}$ = 1·05, $\underline{k}_{C-C}$ = 0·95, $\underline{k}_{C=O}$ = 1·0, $\underline{h}_{O}$ = 1·00).

6.4.5 Time-dependent effects

The esr experiment is only capable of detecting time dependent physical or chemical changes in paramagnetic species if the change is taking place with a frequency lying in the range $10^6 \rightarrow 10^8$ s^{-1}**. Thus in the case of ring flipping if the rate falls below about 10^6 s^{-1} then as far as the resonating electron is concerned the molecule is stationary and appears to exist in only one form and at rates > 10^8 s^{-1} it can only see an average of the two forms. Intermediate rates result in the appearance of anomalous linewidths. In the group of 2-cyclohexenone ketyls studied

** If, as in the present situation, there are two equivalent forms having the same lifetime, τ, then $\tau \approx \frac{1}{\gamma_e(a^A_x - a^B_x)}$ where $(a^A_x - a^B_x)$ is the difference between the coupling constant of nucleus X in forms A and B, this difference for organic radicals is usually 0·01 → 1·0 mT hence τ = $10^{-6} \rightarrow 10^{-8}$ s.

TABLE 6.9

Rate constants at T K for

ring flipping process in 2-cyclohexenone

Temperature ^{o}K	Rate constant $\times 10^{5}$ s^{-1}
229	10·10
224	5·88
219	4·76
208	2·50
206	1·92
202	1·66
202	2·00

in this work both that 2-cyclohexenone and 3-methyl-2-cyclohexenone show anomalous linewidths, whereas the other ketyls show couplings from apparently stationary axial and equatorial protons and therefore must have conformational lifetimes greater than 10^{-6} s. In ketyls IX and XII where a methylene group has only one methyl substituent, one conformation is favoured, i.e. the methyl group in an equatorial position. The esr spectrum of the 2-cyclohexenone ketyl is described by the slow limit condition, where those lines subject to broadening may be determined by equation 3·13 and the lifetimes by equation 3·10.

By recording esr specta of the 2-cyclohexenone ketyl at different temperatures (200 → 230 K), see figure 6.8, and determining the corresponding rate constants, $\frac{1}{\tau}$, by computer simulation (Appendix V), it has been possible to find the energy of activation for the ring flipping process. Table 6.9 gives the values of the rate constants and corresponding temperatures, and a plot of log $\left(\frac{1}{\tau}\right)$ vs $\frac{1}{T}$ is shown in figure 6.9.

The Arrhenius plot gives an energy of activation ΔE_a of 23·59 ± 1·9 kJ $mole^{-1}$ from which may be determined the enthalpy of activation, $\Delta H^{\ddagger}$ = 21·08 ± 1·9 kJ $mole^{-1}$ @ 298 K and the entropy of activation, $\Delta S^{\ddagger}$ = -36·55 ± 8·99 J K^{-1} mol^{-1} @ 298 K**. These parameters compare well with those derived for substituted cyclohexanesemidione radical-anions[184].

6.5 Continuous flow reduction in the presence of a proton source

By incorporating ethanol (1M) into the reaction medium, reduction of 3,5,5-trimethyl-2-cyclohexenone yielded a paramagnetic species affording a spectrum which could be analysed

** The Arrhenius parameters were determined using the program ACTPAR, Appendix IV.

Figure 6.8

The first twelve low-field lines in the esr spectrum of 2-cyclohexenone ketyl.

a), b) and c) are experimental spectra measured at 202 K, 206 K and 224 K respectively:

d), e) and f) are computer simulated spectra based on ring inversion frequencies of $1{\cdot}66 \times 10^5\ s^{-1}$, $1{\cdot}92 \times 10^5\ s^{-1}$ and $5{\cdot}88 \times 10^5\ s^{-1}$ respectively

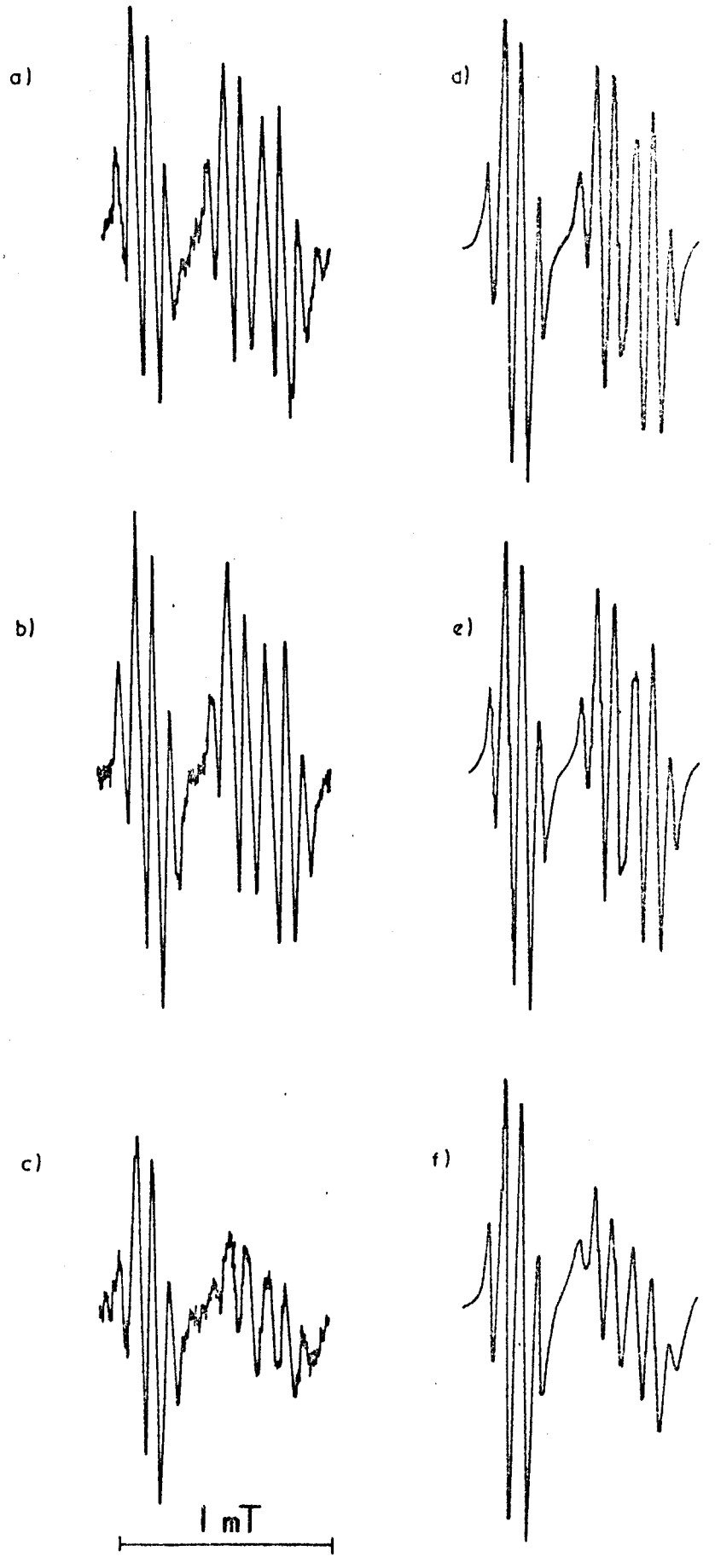
a)
b)
c)
d)
e)
f)
1 mT

Figure 6.9

Plot of log ($^{1}/_{\tau}$) versus $^{1}/_{T}$ for the ring inversion process in the ketyl of 2-cyclohexenone

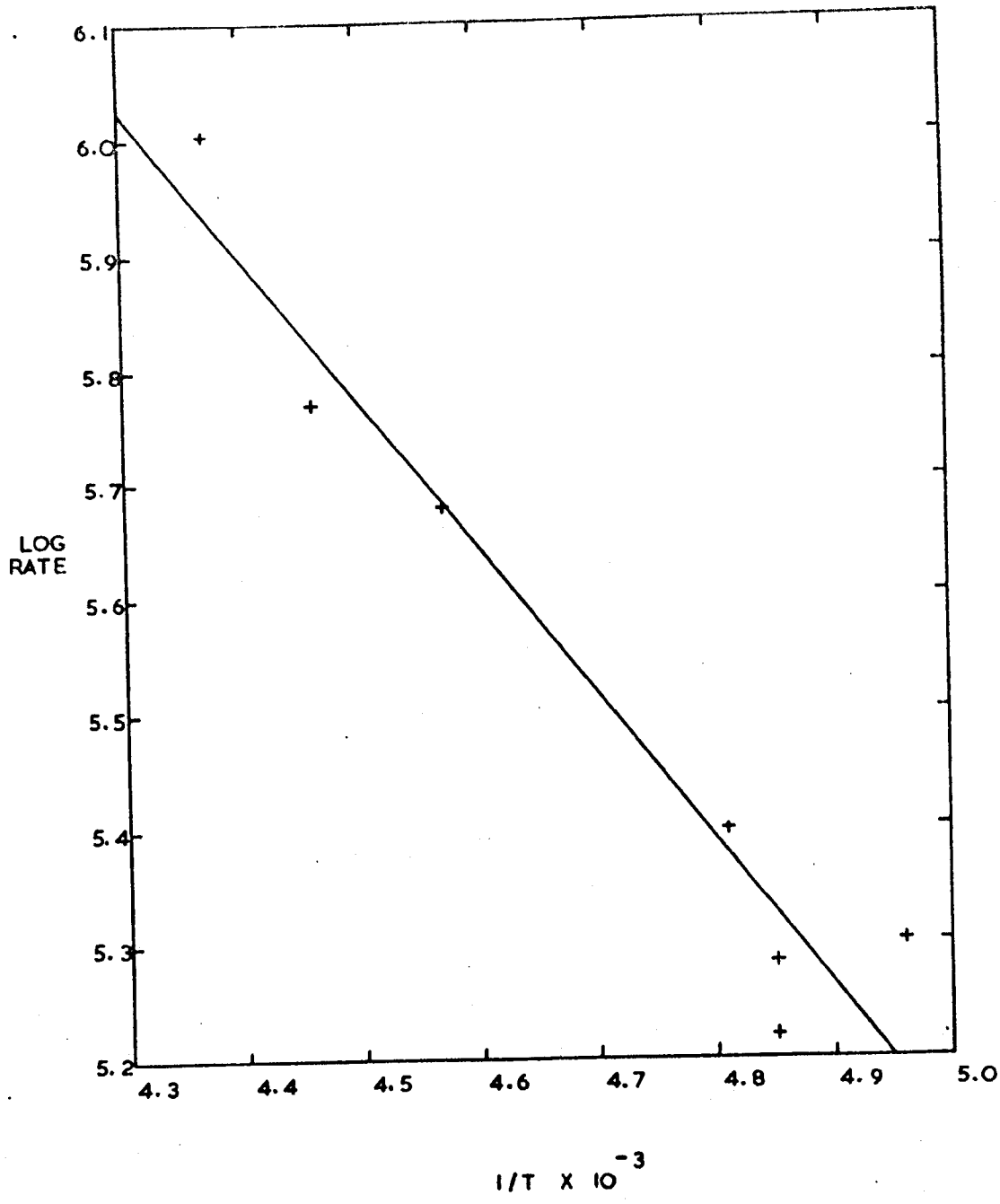
6.1
6.0
5.9
5.8
5.7
5.6
5.5
5.4
5.3
5.2
LOG
RATE
4.3
4.4
4.5
4.6
4.7
4.8
4.9
5.0
1/T X 10^-3

in terms of five equivalent protons and three equivalent protons. The magnitudes of the couplings compare well with those for radicals of the following type (B)[185]

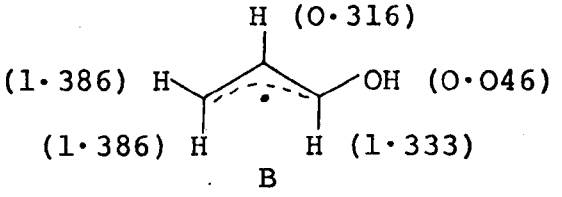

B

and the couplings have been assigned to the neutral radical (XXIV).

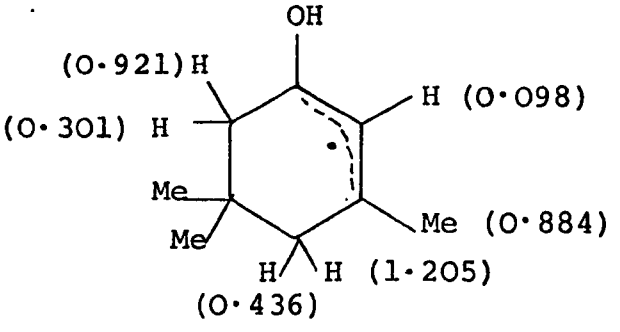

XXIV

The coupling constants of the C_4 and C_6 methylene protons reveal that they are in axial and equatorial conformations with dihedral angles of 6° 30' and 5° respectively. By calculating the spin density at C_3 from the methyl proton coupling constant, it is possible to estimate the magnitudes of the C_4 methylene couplings, and the calculated values (a_{axial} = 1·35 and $a_{equatorial}$ = 0·48 mT) are in excellent agreement with those observed experimentally. Assignment of the coupling of 0·098 mT is ambiguous, but by comparison with B it has been assigned to C_2. The hydroxyl proton coupling is less than the linewidth (0·027 mT).

Similar experiments were carried out with 3,5-dimethyl- and 2-cyclohexenone. Reduction of the latter in this manner failed to produce any resonance at all, but the former gave a fairly large signal which at the time of writing is not analysed. It is thought probable that this is also due to

the neutral radical.

6.6 Static Reduction of α,β-unsaturated ketones

Static reductions of α,β-unsaturated ketones were carried out in an attempt to reproduce the spectra reported by Chen and Bersohn[168] for comparison with those obtained in the flow system. Since the time that the present work was undertaken, Russell has shown[167] that Chen and Bersohn's radicals were either semidiones or semiquinones formed by oxidation of the enolate radicals or anions.

6.6.1 Open chain α,β-unsaturated ketones

Several attempts were made to repeat the results of Ray *et al.*[171] in the reduction of dicyclopropylketone, but no resonance whatsoever could be observed. The colour of the sodium-ammonia solution disappeared instantaneously, and a white solid was precipitated. Similar experiments with methylcyclopropylketone were equally unsuccessful.

Reduction of 3-methylpent-3-ene-2-one produced a well-resolved esr spectrum (Fig. 6.10) which showed couplings from two methyl groups and two inequivalent protons.

Although care had been taken to exclude oxygen from the system it is thought that spectrum was that of the semidione (XXV) arising from oxidation of the ketyl,

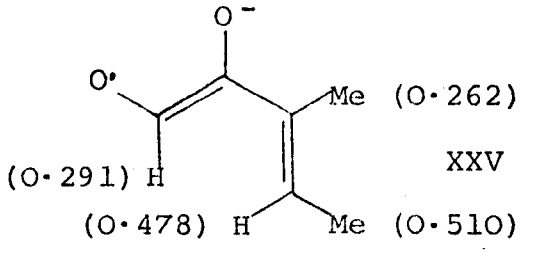

and the assignment or couplings for similar cyclic semidiones reported by Russell[167] support this view.

Under static reduction conditions, mesityl oxide initially produced a rather complex spectrum arising from

Figure 6.10

a) Esr spectrum of the semidione produced in the static reduction of 3-methylpent-3-ene-2-one

b) Computer simulation

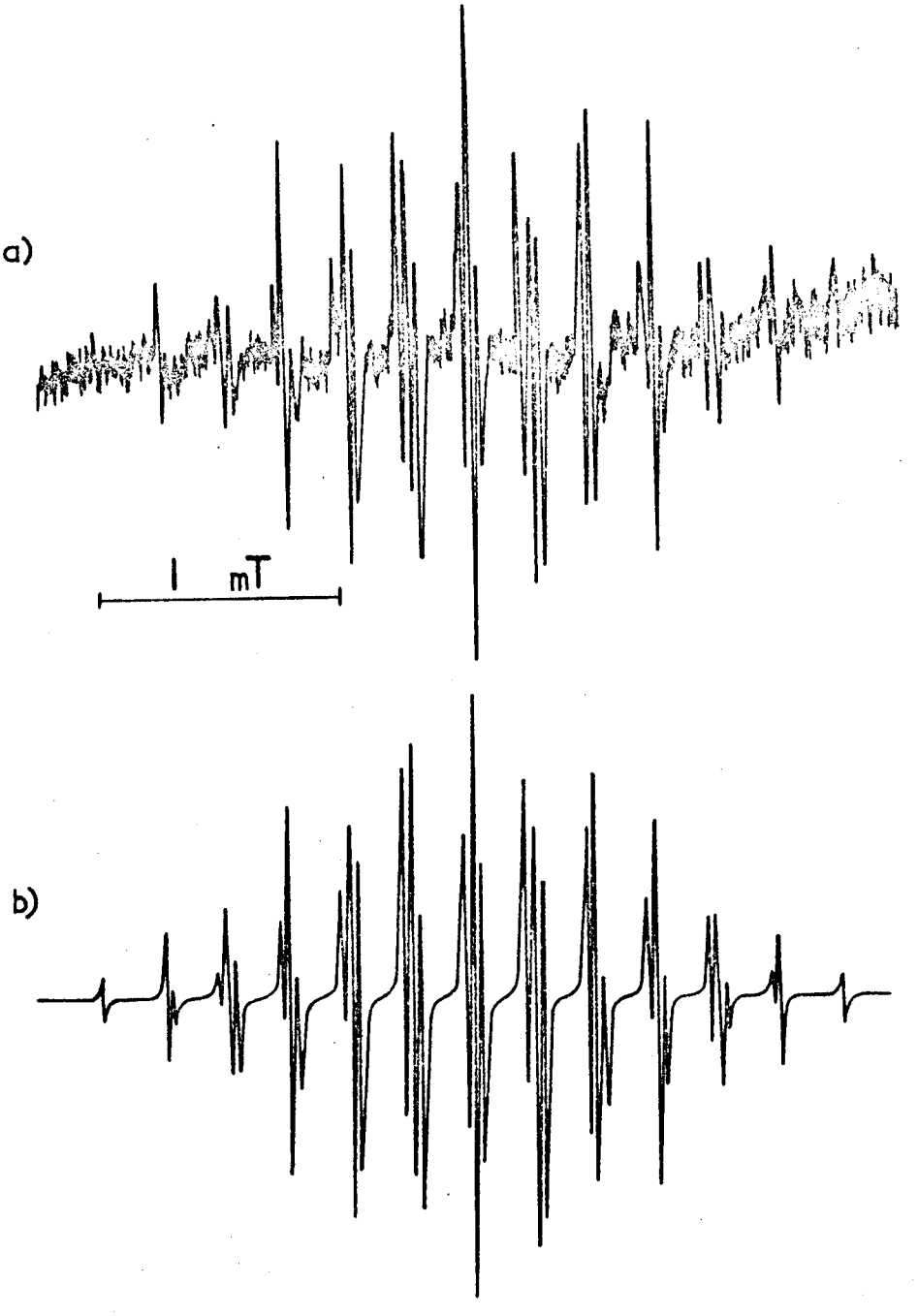
a)
1 mT
b)

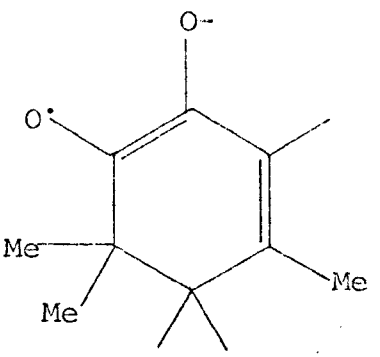

XXVI

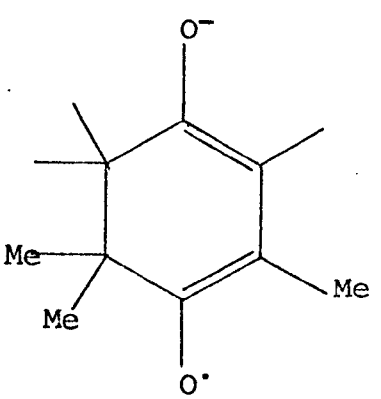

XXVII

more than one species, which after a few minutes gave way to a 1:3:3:1 quartet, ($a^{H}_{CH_3}$ = 0·68 mT). The rather broad nature of the spectral lines (0·16 mT) suggest that this may have arisen from the radical 'tail' of the polymeric material precipitated during the reduction.

6.6.2 Cyclic α,β-unsaturated ketones

Reduction of 3,5,5-trimethyl-2-cyclohexenone under static condtions produces a deep purple paramagnetic solution, the esr spectrum of which affords couplings from a methyl group (0·549 mT) a methylene group (0·199 mT) and a single proton (0·484 mT). The methylene protons couplings were time-averaged at 273 K and gave rise to a 1:2:1 triplet. At lower temperatures the central line of these triplets became broadened. This time dependent effect suggests that the methylene group is in a ring and is being subjected to conformation interchanges.

Two semidione structures may be drawn for this species both of which could arise from oxidation of the ketyl IX . If the esr spectrum arose from XXVI, then by comparison with Russell's couplings for the corresponding 4,4-dimethyl- compound[167] the C_2 proton coupling would be expected to be small. Furthermore calculations show that the spin density at C_3 would give rise to a methylene coupling of ca. 0·65 mT. Assignment to XXVII is more favourable since position C_2 and C_3 would be expected to have similar spin densities, somewhat higher than that for C_1 and C_4. Table 6.10 compares the experimental spin densities for these two species with theoretical values calculated for the fragments C and D.

TABLE 6.10

Calculated spin densities for the fragments C and D

Position	Π-spin densities			
	Experimental**	Calculated (McLachlan)		Experimental†
		C	D	
1	-	0·202	0·148	-
2	-	0·212	0·173	0·198
3	0·198	-0·082	0·173	0·189
4	0·189	0·219	0·148	-

** Based on the assignment of coupling constants to the semidione XXVI

† Based on the assignment of coupling constants to XXVII

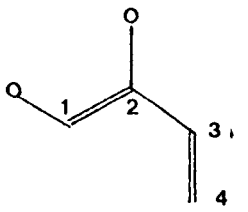

C

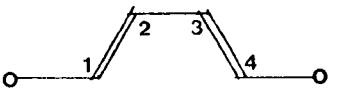

D

Reduction of 3,5-dimethyl- and 4,4-dimethyl-2-cyclohexenone both yielded two paramagnetic species, neither of which could be attributed to a semidione of semiquinone. It is thought that these may either be due to products of reductive coupling or impurities.

6.7 Conclusions

The radical-anions of a series of acyclic and cyclic α,β-unsaturated ketones have been prepared by electron attachment in the continuous liquid ammonia flow system and characterised by esr spectroscopy. The open chain ketyls can exist in either s-cis or s-trans conformations and in certain cases electron attachment to both forms has been observed. Assignment of groups of coupling constants to paraticular conformations has been made by comparison with spin densities calculated by simple MO methods.

The coupling constants of the cyclic ketyls show that the heavy atoms in these molecules with the exception of C_5, lie almost in a plane and that the C_4 and C_6 methylene protons are in almost pure axial and equatorial positions. Activation parameters have been determined for the ring flipping process observed in the 2-cyclohexenone ketyl. The neutral radical of 3,5,5-trimethyl-2-cyclohexenone has been observed by incorporating a proton source in the reduction medium.

CHAPTER 7

REDUCTION OF ACYCLIC α,β-UNSATURATED CARBOXYLIC ACIDS, ESTERS AND NITRILES

7 REDUCTION OF α,β-UNSATURATED CARBOXYLIC ACIDS, ESTERS AND NITRILES

7.1 Introduction

In view of the success of the liquid ammonia flow technique over electrolytic methods for preparing and characterising α,β-unsaturated ketyls and since the rate constants for the reaction of the hydrated electron with α,β-unsaturated acids and esters is of the order of 10^9 to 10^{10} l mol^{-1} s^{-1} [31], it seemed probable that the continuous flow technique would provide a means of characterising the radical-anions of these compounds, and as a result the following study was undertaken.

As with α,β-unsaturated ketones, the earliest work on the reduction of α,β-unsaturated acids was concerned with the stereochemistry of the hydrogenation of the double bond[186], whereas for the esters only alkylation was investigated[187]. More recently esr studies have been made of γ-irradiated, polycrystalline, saturated and unsaturated acids and esters[63,64]. In solution, Nelsen[188] has studied the radical-anions of maleic, fumaric and phthalic esters by electrolysis in DMSO and Neta and Fessenden[189] have studied the reaction of hydrated electrons with unsaturated acids, finding that the radical-anions of acrylic and acetylenedicarboxylic acids react rapidly with water to give the radicals $CH_3\dot{C}HCO_2^-$ and $^-O_2C\text{-}CH = \dot{C}\text{-}CO_2^-$ respectively. They also characterised radical-anions of muconic, chelidonic, maleic and dihydroxy-fumaric acids.

Conformational studies of the neutral molecules have been made by George and coworkers[190,191].

In this chapter are described the radical-anions of several α,β-unsaturated and mono- and di-acids and esters produced in the continuous flow system at ca. 200 K. In certain cases s-cis/s-trans conformations have been observed in the radical-anions of the esters. The radical-anion of trans-crotonitrile has also been characterised. Reduction of acetylenic to ethylenic bonds has been observed on the ms timescale for phenylpropiolic acid and ethyl propiolate and anomalous spectral line intensities noted in the esr spectrum of the latter. Spin-densities calculated by the Hückel and McLachlan methods have been used to aid in the assignment of coupling constants.

7.2 Experimental

The compounds used were commercial samples and were distilled immediately prior to use. The continuous flow reduction was carried out as described in Chapter 4. Substrate concentrations were usually between 10^{-2} and 5×10^{-3} M and where low solubility was experienced the minimum amount of THF was added as co-solvent.

7.3 Results

7.3.1 α,β-Unsaturated Acids

Reduction of acrylic acid (10^{-2} M) at 223 K produced a simple esr spectrum which consisted of a large 1:2:1 triplet split by a small doublet (Fig. 7.1 (a), Table 7.1) with linewidths of 0·044 mT. Since acrylic acid would be expected to be in its ionised form in liquid ammonia, assignment has been made to the species $CH_2 = CH\ CO_2^{2-}$. Even by varying the concentration of the substrate and reducing the temperature to ca. 200 K no improvement in this spectrum could be made.

At 203 K trans-crotonic acid (10^{-2} M) gave rise to an esr spectrum (Fig. 7.2) which was analysed in terms of a large methyl

Figure 7.1

a) Esr spectrum of acrylic acid radical-anion measured at 223 K

b) Computer simulation

Figure 7.2

a) Esr spectrum of trans-crotonic acid radical-anion measured at 203 K

b) Computer simulation

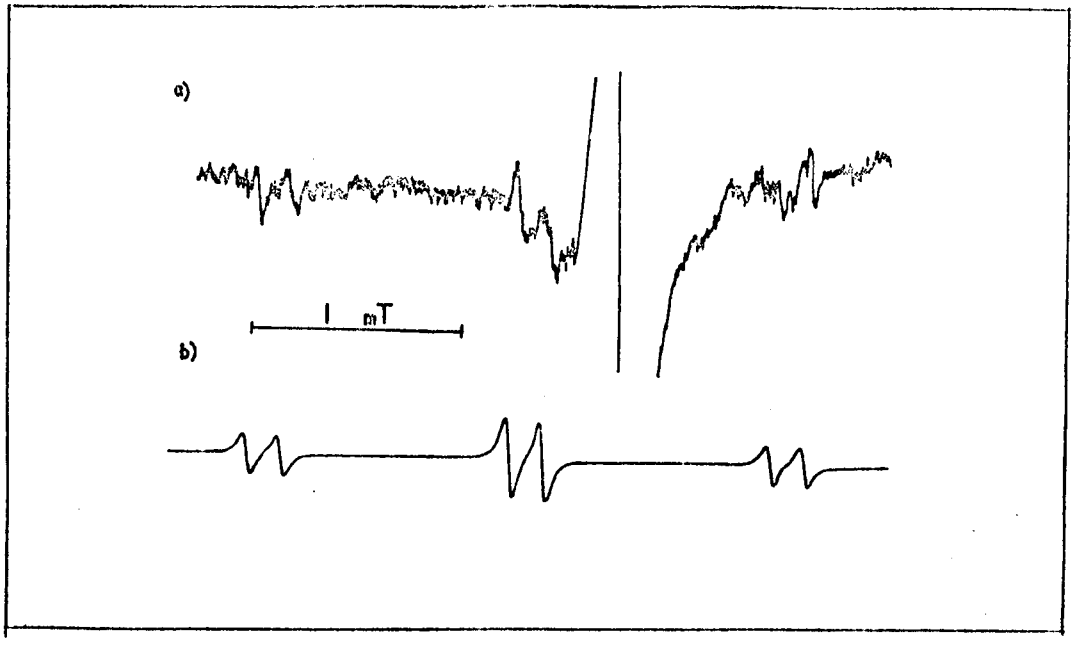
a)
1 mT
b)

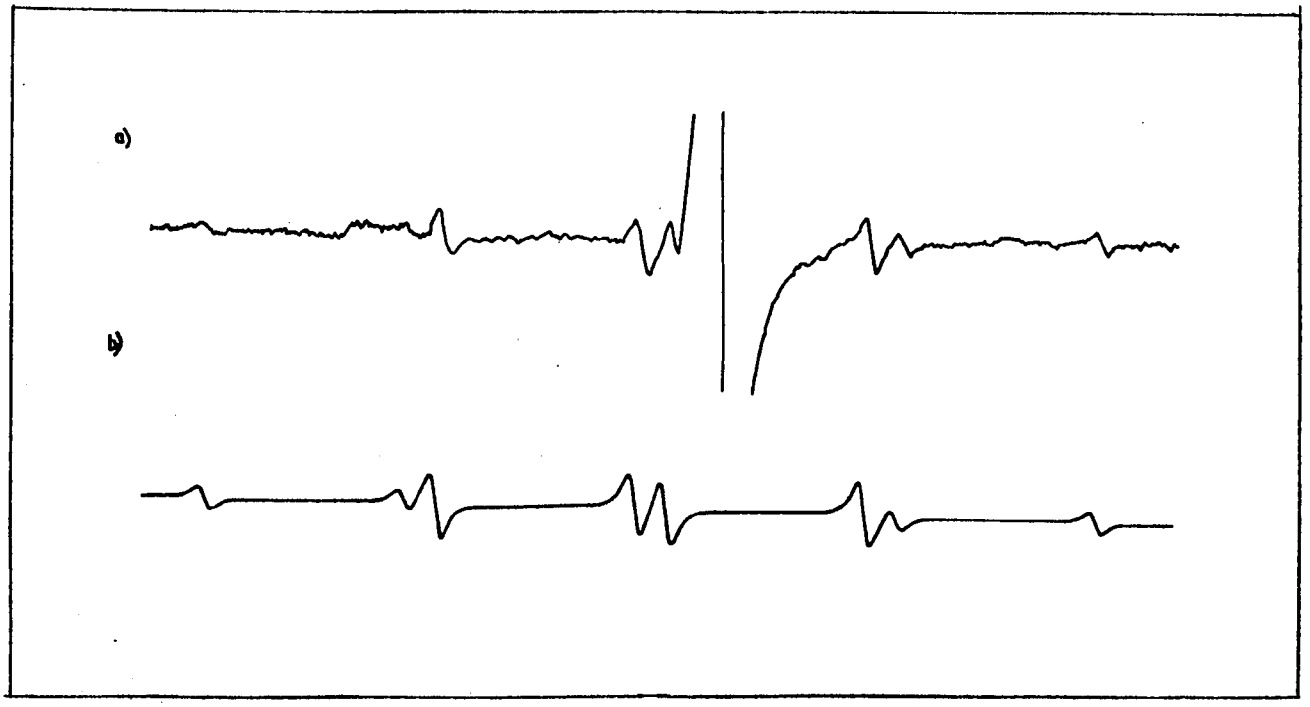
a)
b)

TABLE 7.1

Coupling constants of α,β-unsaturated acids, esters and nitriles

Radical-Anion	g-factor ± 0·0001		Pos'n	Coupling constant mT
Acrylic acid	2·0033	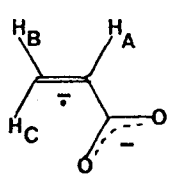	H_A	0·162
			H_B	1·245
			H_C	1·245
Trans-crotonic acid	2·0031	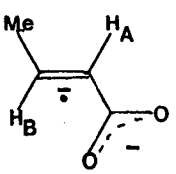	H_A	<0·10
			H_B	1·348
			Me	1·563
3,3-Dimethyl-acrylic acid	2·0034	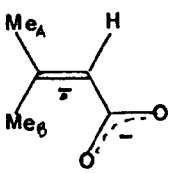	H	0·074
			Me_A	1·289
			Me_B	1·289
Fumaric acid	2·0035	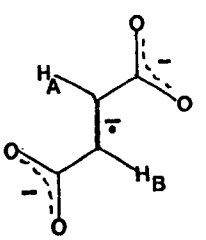	$H_A=H_B$	0·681
Butadiene-1-carboxylic acid	2·0032	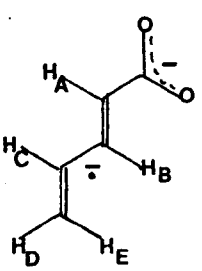	H_A	0·273
			H_B	0·809
			H_C	0·158
			H_D(a)	0·998
			H_E(a)	0·935
Cinnamic acid	2·0032	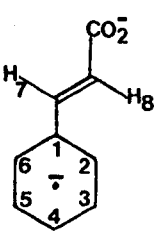	H_2	0·387
			H_3	0·118
			H_4	0·491
			H_5	0·081
			H_6	0·320
			H_7	0·808
			H_8	0·302

coupling and a large proton coupling (Table 7.1). Although the radical-anion would be expected to show a further small proton coupling, the large linewidth (0·09 mT) probably obscures this and assignment has been made to the species $CH_3CH = CHCO_2^{2-}$.

The esr spectrum obtained by reducing 10^{-2} M 3,3-dimethylacrylic acid in the continuous flow system at 210 K yielded an esr spectrum of rather low intensity, arising from six equivalent protons and having a linewidth of ca. 0·08 mT. Re-running at the same concentration, but at a slightly lower temperature (203 K) produced a better resolved spectrum which afforded the coupling from a further proton (Table 7.1). The linewidth in this case was 0·042 mT. Assignment has been made to the radical-anion.

Even though butadiene-1-carboxylic acid showed very low solubility in liquid ammonia, reduction of a saturated solution (< 10^{-3} M) at 212 K produced the esr spectrum of its radical-anion which was analysed in terms of five inequivalent proton couplings (Table 7.1).

Reduction of 10^{-2} M phenylpropiolic acid (233 K)** produced resonance from a single species which showed couplings from seven inequivalent protons. Comparison of this spectrum with that of cinnamic acid[87], showed it to be identical, and assignments have been made to the species $PhCH = CHCO_2^{2-}$ (Table 7.1).

Both maleic and fumaric acids were almost completely insoluble in liquid ammonia and even addition of up to 20% ($^{V}/_{V}$) THF failed to produce a strong enough solution to observe resonance. However, by reducing acetylenedicarboxylic acid it has been possible to record the esr spectrum of a single species possessing two equivalent protons. By analogy

** This work was carried out in conjunction with Dr. A. R. Buick.

Table 7.1 continued

Radical-Anion	g-factor ± 0·0001		Pos'n	Coupling constant mT
Ethyl acrylate	2·0035	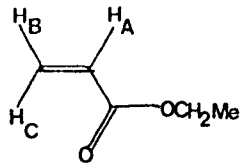	H_A	0·157
			H_B	1·218
			H_C	1·218
			CH_2	0·214
Methyl methacrylate	2·0034	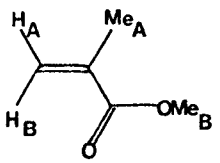	Me_A	0·101
			Me_B	0·101
			H_A	1·152
			H_B	1·152
Methyl crotonate	2·0034	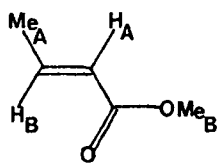	H_A	0·053
			Me_A	1·534
			H_B	1·315
			Me_B	0·094
Ethyl crotonate	2·0034	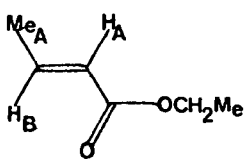	H_A	0·041
			Me_A	1·564
			H_B	1·336
			CH_2	0·102
Diethyl maleate/ fumarate				
major components	2·0039	A or B (b)	H	0·683
			CH_2	0·139
	2·0040		H	0·662
			CH_2	0·139
minor components	2·0042	A or B (b)	H	0·673
			CH_2	0·135
	2·0045		H	0·673
			CH_2	0·135

with other acetylenic compounds rapid reduction of the triple bond to the corresponding olefin would be expected, even in the absence of a proton source. Since only one species is observed it is probably the case that the rate of reduction to the olefin is sufficiently slow to allow the more electrostatically favoured isomer to be formed (i.e. trans arrangement of the carboxylic groups) and accordingly the couplings have been assigned to the radical-anion of fumaric acid (Table 7.1) (see also Section 7.4.1).

Propiolic and methacrylic acids reacted with the ammoniated electron to produce only very faint resonances. (Trans, trans- butadiene-1,4-dicarboxylic, mesaconic and itaconic acids were too insoluble even with THF as cosolvent.)

7.3.2 Esters of α,β-unsaturated mono-acids

The esr spectrum (Fig. 7.3) obtained at 203 K on reduction of 10^{-2} M ethyl acrylate, when examined under high resolution, was shown to arise from two species, one considerably more intense than the other. It has only been possible to determine the couplings for the major component in this spectrum, i.e. from two pairs of two equivalent protons and one proton (Table 7.1). In all probability the two radical-anions arise from electron attachment to the s-cis and s-trans conformations of this ester.

The methyl ester of trans-crotonic acid (2×10^{-2} M) when reduced to its radical-anion at 210 K gave an esr spectrum which showed couplings from two inequivalent methyl groups and two inequivalent protons. Under similar conditions the ethyl ester produced an esr spectrum in which the smaller methyl coupling had been replaced by a 1:2:1 triplet, (Fig. 7.4, Table 7.1). Close examination of these spectra

Table 7.3

a) Esr spectrum of s-cis and s-trans ethyl acrylate radical-anions measured at 203 K

b) Computer simulated spectrum of s-cis ethyl acrylate radical-anion

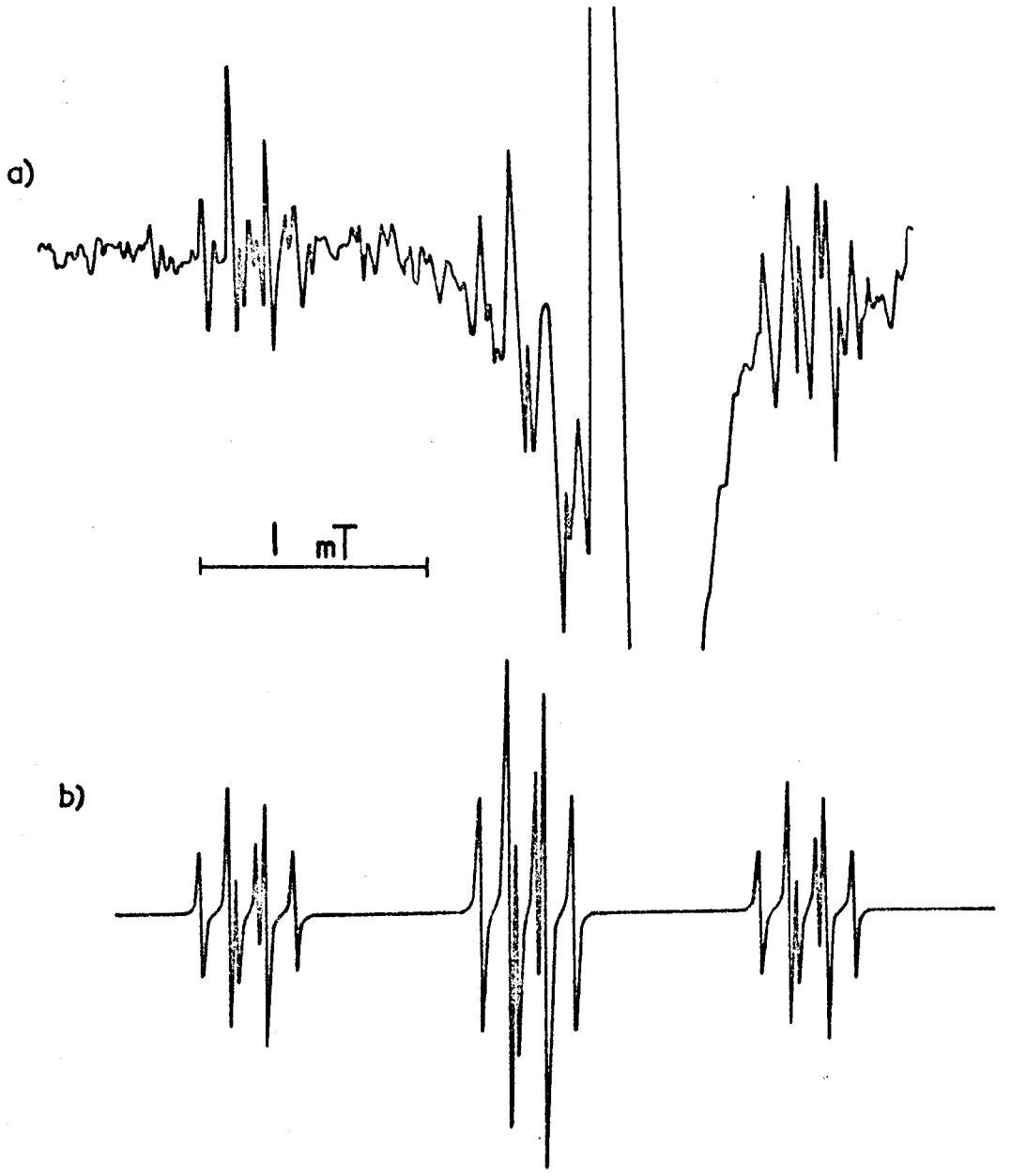
a)
1 mT
b)

Figure 7.4

a) Esr spectrum of ethyl crotonate radical-anion measured at 210 K:
INSET: group under high resolution

b) Computer simulation of low resolution spectrum

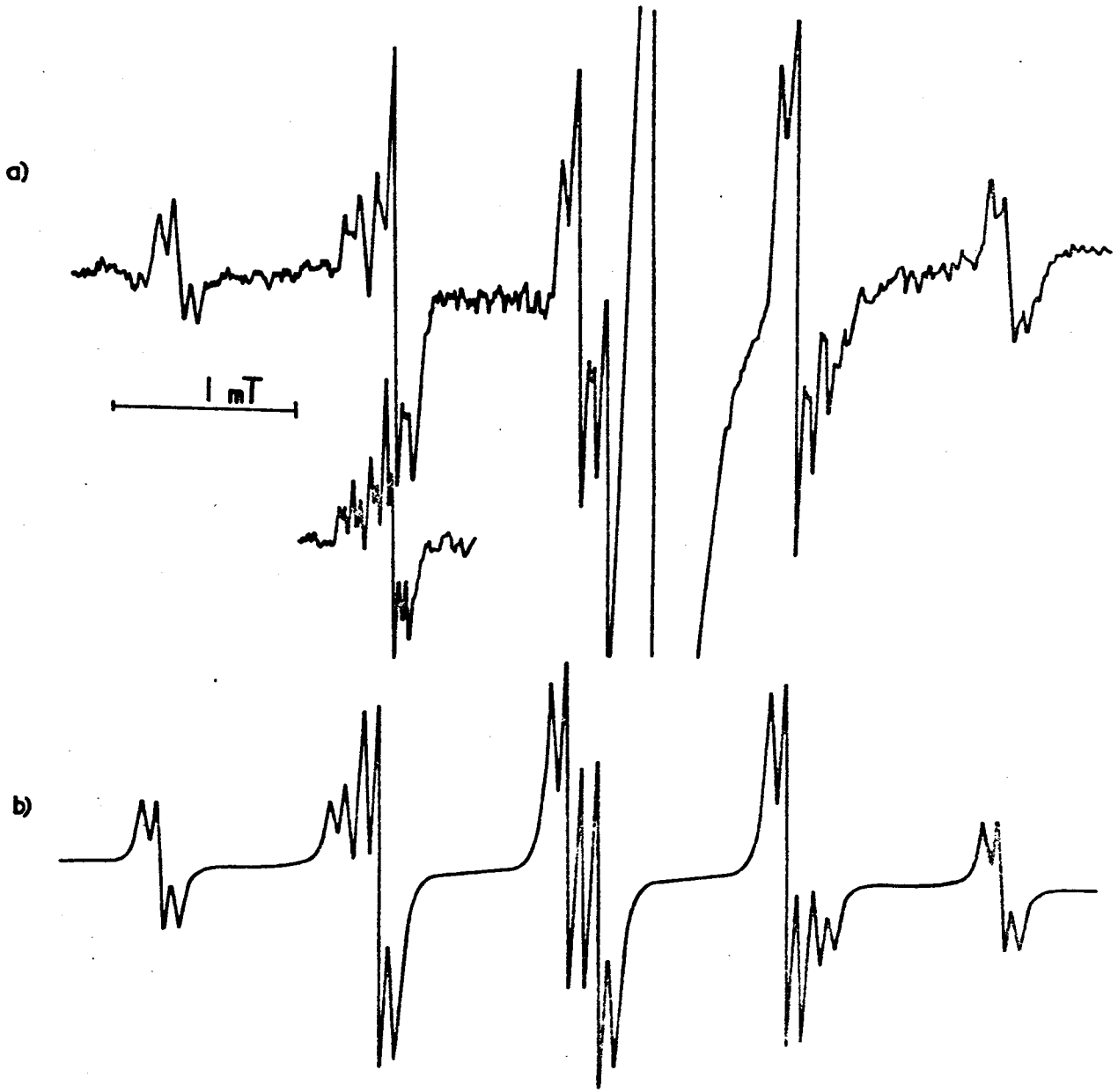
a)
1 mT
b)

Radical-Anion	g-factor ± 0·0001		Pos'n	Coupling constant mT
Dimethyl maleate/ fumarate				
major components	2·0036	C or D (b)	H	0·673
			Me	0·124
	2·0039		H	0·673
			Me	0·124
minor component	2·0044	A or B (b)	H	0·662
			Me	0·135
ethyl propiolate	2·0032	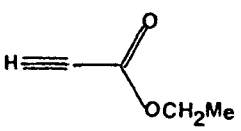	H	2·997
			CH_2	0·075
crotonitrile	2·0026	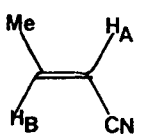	H_A	0·308
			Me	1·513
			H_B	1·156
			N	0·226

(a) Assignments of these couplings are ambiguous

(b) See Fig. 7.7

failed to reveal contributions from any other species although they may have been hidden by overlapping lines.

Methyl methacrylate (10^{-2} M) when reduced at 210 K gave an esr spectrum which yielded coupling constants for two (accidently) equivalent methyl groups and two equivalent protons (Table 7.1). The spectral lines were rather broad (0·05 mT) and slightly distorted, suggesting that a second species was contributing to the linewidth: however the spectrum is assigned to $[CH_2 = C(CH_3)CO_2CH_3]^{\bar{\cdot}}$.

By reducing ethyl propiolate in the flow system at 210 K it was possible to observe electron attachment to both the parent compound and the dihydro-product to give $[HC \equiv CCO_2Et]^{\bar{\cdot}}$ and $[CH_2 = CHCO_2Et]^{\bar{\cdot}}$ respectively. The esr spectrum of the propiolate radical-anion showed a large coupling from a single proton, split by a 1:2:1 triplet (Table 7.1) from the methylene protons of the ethyl group, but rather surprisingly, the low field lines were about half as intense as those at high field (Fig. 7.5). In order to ascertain whether or not this was an artefact of the flow system, the spectrum was run again and the same effect was noted. The fact that no similar effect was observed in the spectrum of the underlying secondary radical, supports the possibility that this is a genuine effect arising from Chemically Induced Dynamic Electron Polarisation (CIDEP)[192].

7.3.3 Esters of α,ß-unsaturated di-acids

Reduction of diethyl maleate and diethyl fumarate (both 10^{-2} M) at 210 K produced esr spectra which arose from a mixture of radicals. The spectrum obtained from the former compound was not as well resolved as that from the latter but it was clear that in both cases the same radicals were

Figure 7.5

a) Mixed spectrum of ethyl propiolate and ethyl acrylate radical-anions

b) Computer simulated mixed spectrum

c) Computer simulated spectrum of ethyl propiolate radical-anion

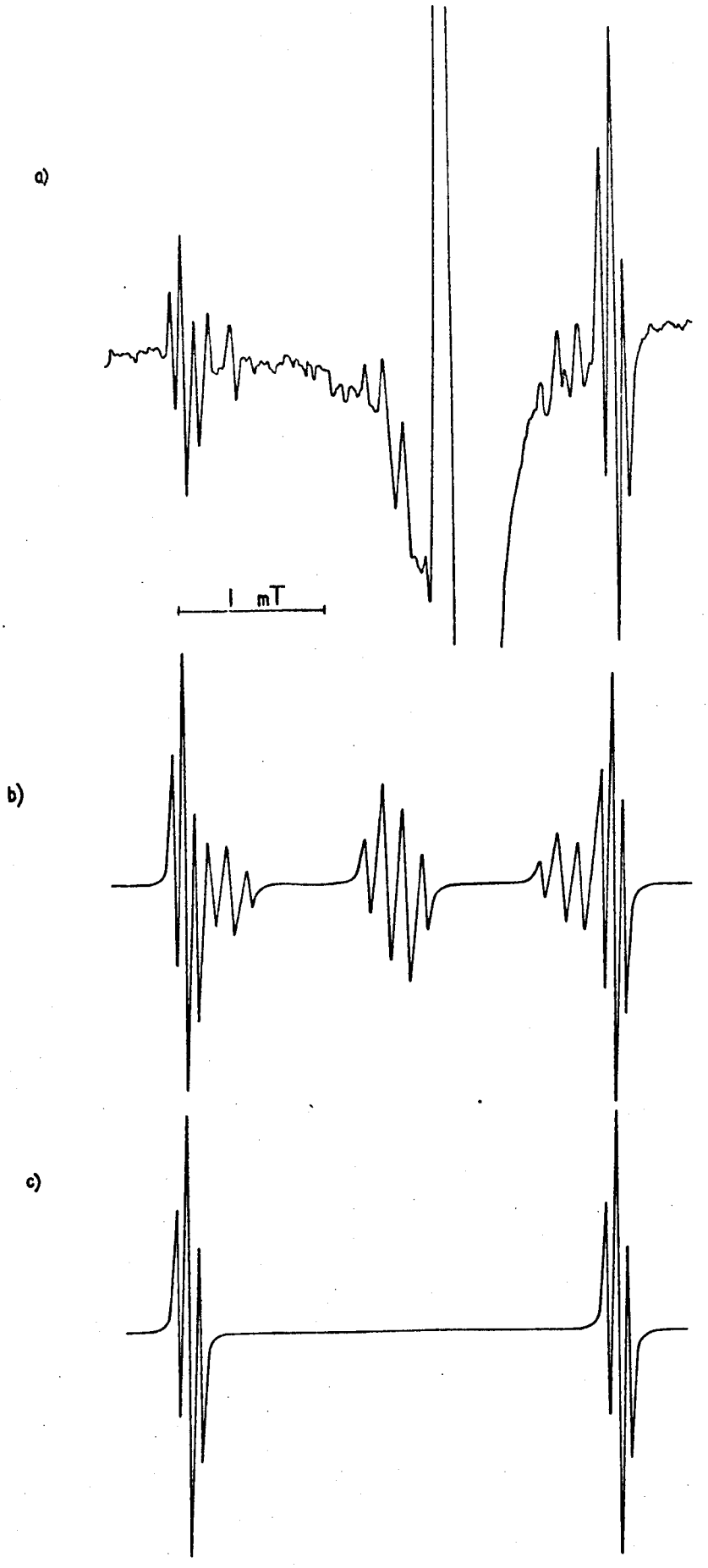
a)
1 mT
b)
c)

present. Examination of the spectrum from the better-resolved fumarate ester (Fig. 7.6) shows the presence of two major components ($\underline{g}$ = 2·0040 and $\underline{g}$ = 2·0039) and two smaller ones ($\underline{g}$ = 2·0045 and $\underline{g}$ = 2·0042), (Fig. 7.6 (b) shows the misleading spectral line intensities arising from the superposition of many of the low field lines): each component showed couplings from four equivalent protons and two equivalent protons (Table 7.1). Analysis of the mixed spectrum in this way accounts for all the lines that can be observed. Nevertheless the intensity of lines (marked in Fig. 7.6 with an asterisk) suggests the presence of other species that are completely obscured.

Reduction of dimethyl acetylenedicarboxylate and dimethyl maleate (both 10^{-2} M) at 208 K again produced a mixture of spectra. (No spectrum could be recorded for dimethyl fumarate since it was insoluble.) It was possible to measure the coupling constants from six equivalent protons and two equivalent protons for two major components in both spectra, ($\underline{g}$ = 2·0036 and $\underline{g}$ = 2·0040), and in the better-resolved spectrum obtained for the maleate system similar couplings from a minor component centred at $\underline{g}$ = 2·0044 (Table 7.1). The rather distorted line shapes in some instances suggest the presence of other species.

Reduction of monoethyl and monomethyl fumarates produced complex spectra arising from two or three similar species, but at the time of writing these have not been completely analysed.

7.3.4 α,β-Unsaturated Nitriles

Reduction of a commercial sample of crotonitrile produced as esr spectrum for which couplings from one methyl group,

Figure 7.6

a) High resolution spectrum of the radical-anions produced in the reduction of diethyl fumarate

b) Low resolution spectrum of (a) showing misleading spectral line intensities arising through superposition of many low-field lines

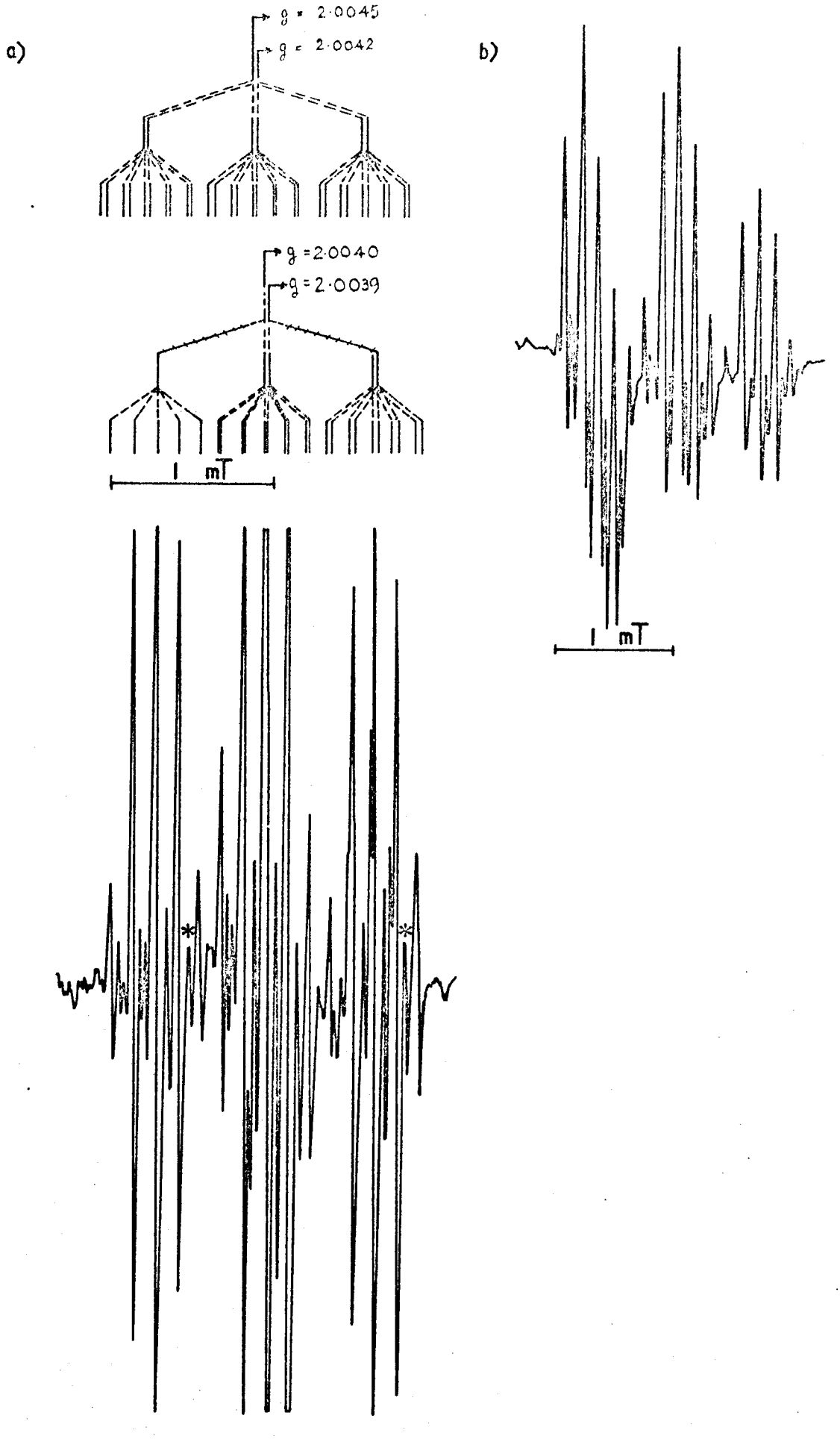
a)
g = 2·0045
g = 2·0042
g = 2·0040
g = 2·0039
1 mT
b)
1 mT

two inequivalent protons and one nitrogen nucleus, were determined. An additional, weaker resonance was observed. Glc and nmr examination showed that the commercial sample was a mixture of cis and trans isomers (≈ 1:10). The spectrum recorded has been assigned to the trans isomer.

Allyl cyanide and methacrylonitrile gave esr spectra identical to that of crotonitrile. The latter was found to be present as a trace impurity in both instances. Acrylonitrile gave no resonance. Although the esr spectrum of acrylamide radical-anion has been recorded in the solid state[193], it was not possible to observe it in liquid ammonia.

7.4 Discussion

7.4.1 Reduction of α,β-Unsaturated Acids, Esters and Nitriles

The situation here is similar to that described earlier for α,β-unsaturated ketones. The radical-anions once formed may be stabilised by delocalisation of the unpaired electron over the carboxyl or carbalkoxy group. The alkyl substituent of the alkoxy group in the esters gives additional stability (cf. the acids) through providing another centre for delocalisation and because of the lower charge reducing the rate of proton attachment. The behaviour of the radical-anions of acrylic and acetylenedicarboxylic acids in the two solvents, liquid ammonia and water, contrasts. In water, Neta and Fessenden[189] were not able to observe these species but only those corresponding to more stable monoprotonated forms, whereas in liquid ammonia the former is fairly readily observed and the latter is rapidly converted to the radical-anion of the dihydro derivative.

In aqueous solution the radical-anion of hexadienoic acid ($CH_3CH = CH - CH = CH\ CO_2^{2-}$) appears to be very

unstable whereas in liquid ammonia that of butadiene-1-carboxylic acid is quite long lived.

Triple bonds in both mono- and di-substituted acetylenes undergo reduction with metals in liquid ammonia to form the corresponding olefins even in the absence of proton donors. Howton and Davies[194] have shown that in the absence of such, 5-octynoic acid is reduced in high yield to the trans-5-octenoic acid. The mechanism can be understood in terms of a stepwise two electron addition to the triple bond to produce the dianion. If this has sufficient time to assume the most stable configuration which is the trans arrangement of the two newly-created negatively charged sp^2 orbitals, then the trans olefin will be produced.

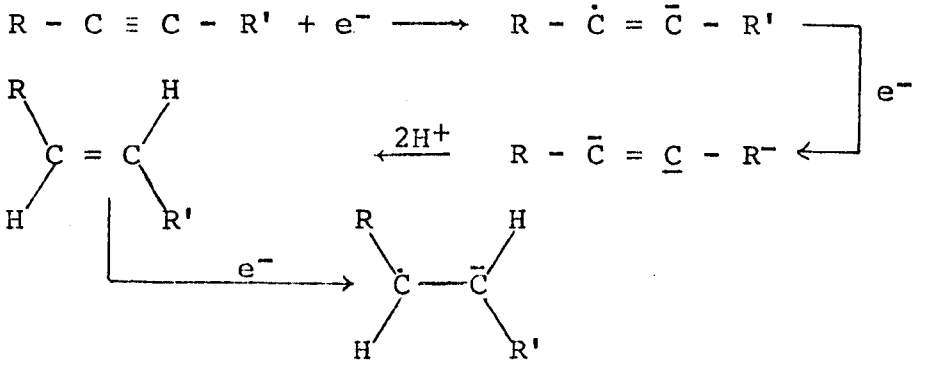

Addition of an electron to the olefin produces its radical-anion. It is by such a mechanism that the ethyl acrylate radical-anions appears during the reduction of ethyl-propiolate.

Trans-addition to phenylpropiolic acid will result in the formation of trans-cinnamic acid. In acetylenedicarboxylic acid trans addition would lead to the formation of fumaric acid, but further addition of an electron to form the radical-anion would result in an ability for the molecule to isomerise

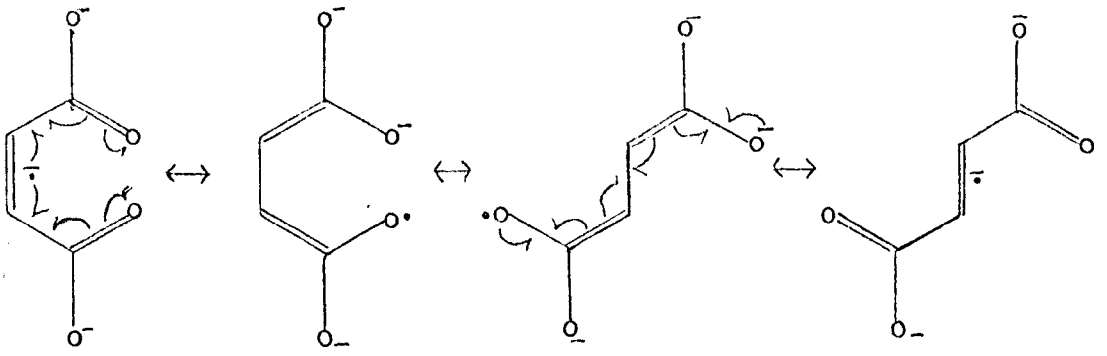

However this would not be favourable in view of the charge on the carboxyl groups. This is not true of the dialkyl esters of this acid and therefore isomerisation would be expected (Section 7.4.2).

Neta[195] has recorded the esr spectrum of the radical-anion of fumaric acid in aqueous solution and found the coupling for the two protons to be 0·66 mT. This value is slightly lower than that obtained in the present work (0·68 mT). The difference probably arises through solvent effects. The g-factors are however in close agreement

$g_{aq} = 2{\cdot}00357 \pm 0{\cdot}00005 \quad g_{NH_3} = 2{\cdot}0035 \pm 0{\cdot}0001.$

The fate of these radical-anions in liquid ammonia may either be protonation to form the saturated acids, or formation of dimers by reaction of two radical-anions or a radical-anion and a neutral molecule followed by anionic polymerisation. Electrolytic studies[196] of the reduction of crotonitrile and methacrylonitrile have shown that dimeric products, arising through coupling of positions of high spin density, predominate.

7.4.2 Dialkyl Maleates and Fumarates

Reduction to the radical-anion of diethyl maleate and diethyl fumarate led to identical mixed spectra from which can be determined the couplings from four distinct species. Nelsen[188] was only able to observe two species which he

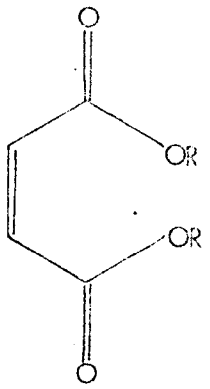

(A)

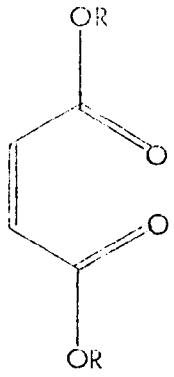

(B)

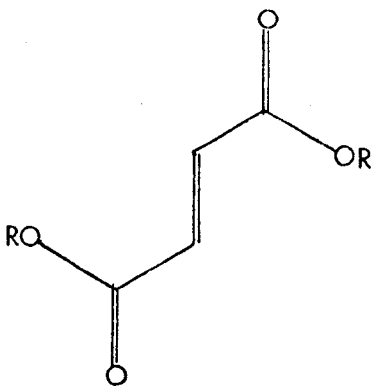

(C)

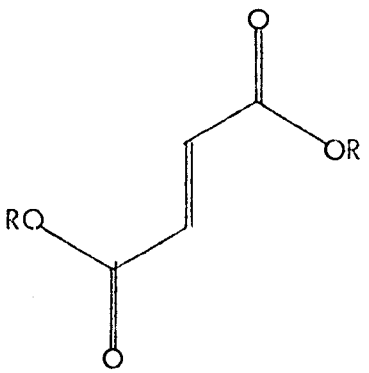

(D)

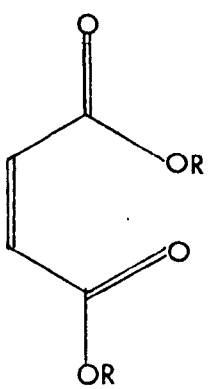

(E)

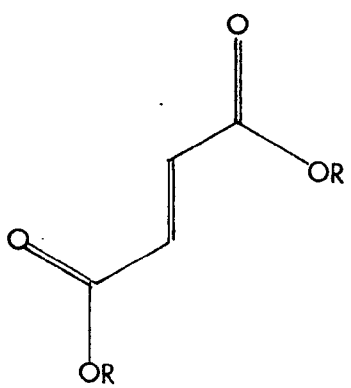

(F)

attributed to the radical-anions of diethyl maleate and diethyl fumarate, without specifying the conformation of the alkoxy groups relative to the double bond: this suggests isomerisation is occurring in these radical-anions (Section 7.4.1). If this is the case then trans-crotonic acid would be expected to behave in a similar manner and it is of interest to note that this radical-anion shows a larger line-width than either acrylic acid or 3,3-dimethylacrylic acid, possibly due to the presence of both isomeric radical-anions. Clearly if s-cis and s-trans conformations are taken into account then there are six possible radical-anions that can arise in the reduction of alkyl maleates or fumarates (Fig. 7.7). Calculations for mixed conformations (e.g. s-cis/s-trans) indicate that the spin density distribution would be sufficiently different to be reflected in the coupling constants (cf. calculations for the phorone ketyl, Section 6.4.2) and so out of the six conformations, four would be expected to give highly symmetric spectra. The esr spectra obtained from the four species observed in the reduction of diethyl maleate and fumarate have this property and are most likely the radical-anions of A, B, C and D. Examination of the g-factors of these species show that they may be grouped in pairs. The pair at high field (g = 2·0039, g = 2·0040) have been assigned to the less sterically hindered structures of C and D, since these are the more intense resonances, and the others at g = 2·0042, g = 2·0045 to structures A and B. Any more definitive assignment is not possible. MO methods are insufficiently accurate to predict the subtle differences observed between the coupling constants of these four radical-anions. The unresolved resonances also observed probably

TABLE 7.2

Experimental and calculated π-spin densities

for α,β-unsaturated acids and esters

Radical-anion	Pos'n	π-Spin density		
		Experimental	Hückel	McLachlan
Acrylic acid	1	0·508	0·418	0·616
$\overset{(1)}{=}\overset{(2)}{=}-CO_2^-$	2	0·066	0·069	-0·097
trans-crotonic acid	1	0·539(a) 0·550(b)	0·403	0·570
	2	0·040	0·035	-0·117
3,3-dimethyl-	1	0·445	0·377	0·509
acrylic acid	2	0·030	0·015	-0·123
Fumaric acid $^-O_2C\ C = C\ CO_2^-$ (1) (2)	1=2	0·278	0·186	0·193
Butadiene-1-carboxylic acid	1	0·394(c)	0·270	0·427
	2	0·064	0·024	-0·096
$=-=-CO_2^-$ (1) (2) (3) (4)	3	0·330	0·274	0·372
	4	0·111	0·087	-0·019
	1	0·497	0·336 *0·404*	0·483(d) *0·597*(e)
	2	0·064	0·088 *0·077*	-0·043 *-0·079*
ethyl acrylate	3(f)	0·689	0·375 *0·323*	0·462 *0·384*
$=-\overset{\alpha}{C}=O$ (1) (2) (3)	OR	-	0·042 *0·038*	0·012 *0·010*
	H_3	-	0·0084 *0·0080*	0·0040 *0·0036*

arise from structures E and F. By applying similar arguments to the partial reduction of dimethyl esters, the two more intense spectra ($\underline{g}$ = 2·0036, $\underline{g}$ = 2·0039) have been assigned to structures C and D and the third one ($\underline{g}$ = 2·0044) to either structure A or structure B.

7.4.3 Molecular Orbital Calculations

MO calculations have been performed using the HMO method in conjunction with the McLachlan procedure to aid in the assignment of coupling constants. The values of $\underline{k}_{C=C'}$ $\underline{k}_{C-C}$ and $\underline{h}_C$ were those used for the α,β-unsaturated ketones. Since the carboxyl group is ionised in liquid ammonia the two oxygen atoms may be considered as being equivalent. Accordingly averaged values of the parameters for $\rangle C=O$ and $\rangle C-O^-$ were employed viz.,

$$\underline{k}_{C=O} = \tfrac{1}{2}\{\underline{k}_{C=O} + \underline{k}_{C-O}\} = 0{\cdot}9$$

and $$\underline{h}_O = \tfrac{1}{2}\{\underline{h}_O + \underline{h}_O\} = 1{\cdot}5$$

The McLachlan adjustable parameter was set equal to 1·2.

Since no parameterisation has been proposed for ethyl substituents assignment of coupling constants was effected by comparison of 'experimental' spin densities with theoretical values derived for methyl esters only. The values of $\underline{k}_{C=C'}$ $\underline{k}_{C-C}$ and $\underline{h}_C$ were those used for the α,β-unsaturated ketones and acids. The $\underline{k}$ value for the carbonyl bond integral was the same as that used for α,β-unsaturated ketones. The parameters for the methoxy group, using the notation C' - O - C ≡ H_3 were as follows

$$\underline{k}_{C'-O} = 0{\cdot}70,\ \underline{k}_{O-C} = 0{\cdot}90,\ \underline{k}_{C\equiv H_3} = 2{\cdot}00,\ \underline{h}_{C'} = 0,\ \underline{h}_O = 1{\cdot}6,$$

$$\underline{h}_C = -0{\cdot}10 \text{ and } \underline{h}_{H_3} = -0{\cdot}50$$

s-Cis and s-trans conformations were distinguished in the same manner as described for α,β-unsaturated ketones.

Table 7.2 continued

Radical-anion	Pos'n	π-Spin density		
		Experimental	Hückel	McLachlan
methyl methacrylate	1	0·470	0·293 *0·363*	0·424 *0·548*
	2	0·035	0·082 *0·074*	-0·025 *-0·061*
	3(f)	0·561	0·401 *0·346*	0·497 *0·413*
	OR	-	0·044 *0·040*	0·013 *0·011*
	H_3	-	0·0089 *0·0080*	0·0043 *0·0036*
methyl crotonate	1	0·529(a) 0·537(b)	0·321 *0·391*	0·453 *0·559*
	2	0·022	0·049 *0·042*	-0·080 *-0·104*
	3(d)	0·522	0·391 *0·330*	0·487 *0·400*
	OR	-	0·040 *0·035*	0·013 *0·012*
	H_3	-	0·0082 *0·0071*	0·0044 *0·0037*
ethyl crotonate	1	0·539(a) 0·545(b)	see methyl crotonate	
	2	0·016		
	3(f)	0·567		

(a) Calculated from the methyl group coupling constant

(b) Calculated from the proton coupling constant

(c) Calculated from the average proton coupling constant

(d) Values for the s-cis conformation

(e) Values for the s-trans conformation

(f) Calculated from $a_{OR}^{H} = Q_{COR}^{H} \cdot \rho_C$, Q_{COR}^{H} = 0·18 mT (see section 7.4.3)

Experimental spin densities were calculated using $Q^{H}_{CH_3}$ = 2·899 mT, Q^{H}_{CH} = -2·45 mT.

Coupling constants for the methoxy protons of s-cis and s-trans conformations of the esters were calculated from the spin density in the heteroatom H_3 using $Q^{H}_{H_3}$ 16·9 mT. Calculations for the radical-anions of the unsaturated acids predict spin densities which (Table 7.2) confirm the assignments of coupling constants given in Table 7.1. Overall, neither the Hückel nor the McLachlan spin densities give exceptional agreement. The Hückel values tend to be too low at position C_1 but quite close for C_2 (ignoring the sign), whereas the McLachlan procedure tends to overestimate spin density at C_1 and although predicting negative spin density at C_2, predicts rather high values there as well. No attempt has been made to alter λ in these calculations, and improved agreement may result by doing so. Better results were obtained for fumaric acid when values of $k_{C\cdots O}$ = 1·6 were used. This value has been favoured by Neal[28] and other workers[70,145] but gives rather poor results for these systems, predicting not only high values for ρ_1 and ρ_2 (≃ 0·64 and 0·16 respectively) but also a positive sign for the latter. For consistency $k_{C\cdots O}$ = 0·9 has been used in all cases.

For the esters correlation was better overall, being marginally better for the McLachlan values.

The values of the methoxy couplings calculated from the McLachlan spin densities for the two conformations of the esters are given in Table 7.3. Calculated coupling constants for both conformations are lower than those observed experimentally. Better agreement is found for the s-cis confor-

TABLE 7.3

Experimental and calculated alkoxy coupling constants

Radical-anion	Alkoxy coupling constant (mT)				
	Experimental	Calculated			
		$a^{H}_{OR} = Q^{H}_{H_3} \cdot \rho_H$ (a)		$a^{H}_{OR} = Q_{COR}{}^{H} \cdot \rho_C$ (b)	
		s-cis	s-trans	s-cis	s-trans
Ethyl acrylate	0·124	0·068	0·054	0·083	0·069
Methyl methacrylate	0·101	0·073	0·061	0·089	0·074
Methyl crotonate	0·094	0·074	0·063	0·088	0·072
Ethyl crotonate	0·102				

(a) $Q^{H}_{H_3} = 16{\cdot}9$ mT

(b) $Q_{COR}{}^{H} = 0{\cdot}18$ mT

mations. These coupling constants were also calculated from the theoretical spin density at C_3. This involved a proportionality constant Q^{H}_{COR} (which would imply that the alkoxy group is treated in the calculations as a heteroatom). An estimate of the value of this constant (0·18 mT) was obtained from the ketyls XIV and XV (Table 6.6), since in these ketyls the spin density at C_3 can be calculated directly from the C_4 methylene coupling constants. Using this method calculated alkoxy couplings are still low for both conformations, but are slightly higher than those calculated by the first method, and again favour the s-cis conformation. The calculated McLachlan spin density at the oxygen of the alkoxy group would indicate that $Q^{H}_{OCH_3}$ was of order of 8 mT. The Hückel value suggests a lower figure of 2·5 mT which compares more favourably with other estimates which lie in the range 0·56 to 3·0 mT[197-199].

Since no coupling constants could be determined for the second conformation it is difficult to be definitive about the structure of the radical-anions observed. Calculations favour the s-cis conformation (cf. MKV) and tentative assignments are made to this structure for all the esters. Observations[190-192] made for the neutral molecule which suggest that the s-trans form is more stable need not necessarily hold for the radical-anion.

7.5 Conclusion

Reaction of α,β-unsaturated acids, esters and nitriles with e^-_{amm} results in the formation of the corresponding radical-anions, the stability of the esters being greater than that of the acids and nitriles. In situations where s-cis and s-trans conformations can arise, electron attach-

ment has been seen to take place to both forms. The radical-anions of the esters of maleic and fumaric acids have been shown to interconvert. Reduction of acetylenic acids and esters to the olefinic compounds is observed on the ms timescale.

Application of MO methods to these radical-anions give only moderate agreement, and distinction between s-cis and s-trans conformations remain ambiguous.

APPENDICES

APPENDIX I

The input and output procedures are written essentially for the procedure EIGENSOLVE. The McLachlan calculation is performed after solution of the secular equations. The amount of input data is minimised by initially assigning the value zero to all Coulomb and resonance integrals, and either zero or one to all overlap integrals. The only bond and atom data then required are those values different from zero.

Input of data for the program is as follows:

INSTRING Title of the molecule under investigation

LAMBDA The adjustable McLachlan parameter λ

ENO The number of electrons contributing to the pi-electron framework in the neutral molecule

ATOM NO The number of atoms in the pi-electron framework

BOND NO The number of bonds in the pi-electron framework

For each bond, the corresponding atom labels and the value of the resonance integral parameter are input. This is followed by any Coulomb integral parameter different from zero, preceded by the atom label. Finally, 0 or -1 are input: 0 if another set of data is to follow or -1 if the current set of data is the last.

All the input data are printed out, and are followed by a listing of the energy of each molecular orbital with the atom coefficients for the orbital. Finally, the Hückel and McLachlan spin densities are given for each atom position in the lowest lying antibonding molecular orbital.

The program, in Algol, is presented below.

```
HUCKEL;
 "BEGIN"
"COMMENT"        MAIN PROGRAM
      THIS PROGRAM CALCULATES HUCKEL MOLECULAR ORBITALS FOR AROMATIC
HYDROCARBONS.  ENERGIES,BOND ORDERS,CHARGE DENSITIES AND FREE VALENCE
ARE CALCULATED;
"INTEGER"ATOM NO,BOND NO,I,J,K,P,M,S,T,MM;"INTEGER""ARRAY"HEAD[1:15];
"INTEGER" ENO, X;
"REAL"B,C,D;"BOOLEAN"ODD,NEW MOLECULE;
"REAL" LAMBA, CHANGE;
"LIBRARY" EIGENSOLVE;
START: "PRINT" ´´L2S25`HUCKEL MOLECULAR ORBITALS FOR `;
MM:=1;
INSTRING(HEAD,MM);
MM:=1;
OUTSTRING(HEAD,MM);
"READ" LAMBA, ENO;
"READ" ATOM NO, BOND NO;
"PRINT" ´´L6S26`NO OF ELECTRONS`, SAMELINE, ENO;
"PRINT" ´´L2S30`NO OF ATOMS`, SAMELINE, ATOM NO;
"PRINT" ´´L2S30`NO OF BONDS`, SAMELINE, BOND NO;
"PRINT" ´´L2S30`LAMBDA`, SAMELINE, ´´S11``, LAMBA;
"PRINT" ´´L2S13`BOND´S10`K-VALUES`;
"COMMENT" ATOM NO IS TOTAL NUMBER OF CARBON PI CENTRES AND BOND NO IS
THE NUMBER OF BONDS;
"BEGIN" "ARRAY" COEFF[1:ATOM NO,1:ATOM NO], ENERGY[1:ATOM NO],
BOND ORDER[1:BOND NO], H, SS, CC[1:ATOM NO,1:ATOM NO];
      "INTEGER""ARRAY"BONDS[1:2,1:BOND NO];
"PROCEDURE"PRINT ENERGY AND COEFF(A,W,N);
"VALUE"N;"INTEGER"N;"ARRAY"A,W;
"BEGIN""COMMENT" PRINTS ENERGIES AND COEFFICIENTS IN 10 COLUMNS WITH
HEADINGS;
"INTEGER"I,J,T,Q;
"FOR"Q:=1"STEP"10"UNTIL"N"DO"
"BEGIN"T:="IF"N-Q<10"THEN"N"ELSE"Q+9;
      "PRINT"´´L5S30`ENERGIES IN ASCENDING ORDER´L2``;
      "FOR"I:=Q"STEP"1"UNTIL"T"DO""PRINT"PREFIX(´´S2``),W[I];
      "PRINT"´´L3S32`COEFFICIENTS IN COLUMNS´L2``;
      "FOR"I:=1"STEP"1"UNTIL"N"DO"
      "BEGIN""FOR"J:=Q"STEP"1"UNTIL"T"DO""PRINT"PREFIX(´´S2``),A[J,I];
      "PRINT"´´L``;
      "END"
"END"
"END"OF PRINT ENERGY AND COEFF;
"PROCEDURE" MCLACHLAN(AN, H, L, C, E);
"VALUE" AN, H, L;   "INTEGER" AN, H;   "REAL" L;   "ARRAY" C, E;
"COMMENT" CALCULATES AND PRINTS HUCKEL AND MCLACHLAN SPIN
DENSITIES FOR ANION RADICALS WITH ANY NUMBER OF DEGENERATE
LOWEST ANTIBONDING ORBITALS;
"BEGIN" "INTEGER" X, Y, I, J, S, T;
"REAL" D;
"REAL" "ARRAY" SUMPI, SPI, PI[1:AN,1:AN], SD, SUMRHO, RHO[1:AN];
"FOR" X:=1 "STEP" 1 "UNTIL" AN "DO"
"FOR" Y:=1 "STEP" 1 "UNTIL" AN "DO" "BEGIN"
SPI[X,Y]:=0.0;
"FOR" J:=H+1 "STEP" 1 "UNTIL" AN "DO" "BEGIN"
SUMPI[X,Y]:=0.0;
"FOR" I:=1 "STEP" 1 "UNTIL" H "DO"
SUMPI[X,Y]:=SUMPI[X,Y]+((C[I,X]*C[I,Y])/(E[J]-E[I]));
SPI[X,Y]:=SPI[X,Y]+SUMPI[X,Y]*(C[J,X]*C[J,Y]);   "END";
```

```
PI[X,Y]:=-(4*SPI[X,Y]);   "END";
"FOR" X:=1 "STEP" 1 "UNTIL" AN "DO" "BEGIN"
S:=1;   T:=H+1;
D:=C[T,X]↑2;
SDIN:   T:=T+1;
"IF" ABS(E[T]-E[T-1])<10-3 "THEN" "GOTO" DENIN "ELSE" "GOTO" SPIND;
DENIN:   D:=D+C[T,X]↑2;   S:=S+1;   "GOTO" SDIN;
SPIND:   D:=D/S;   SD[X]:=D;   "END";
"FOR" X:=1 "STEP" 1 "UNTIL" AN "DO" "BEGIN"
SUMRHO[X]:=0.0;
"FOR" Y:=1 "STEP" 1 "UNTIL" AN "DO"
SUMRHO[X]:=SUMRHO[X]+(PI[X,Y]*SD[Y]);
RHO[X]:=SD[X]+(L*SUMRHO[X]);   "END";
"PRINT" ´´L2S20`ATOM´S14`SPIN DENSITIES´L1``;
"PRINT" ´´S35`HUCKEL´S9`MCLACHLAN´L2``;
"FOR" X:=1 "STEP" 1 "UNTIL" AN "DO"
"PRINT" ´´S14``, SAMELINE, X, ´´S6``, PREFIX(´´S2``), SD[X],
´´S6``, PREFIX(´´S2``), RHO[X], ´´L1``;
"END" OF MCLACHLAN;
      "FOR"I:=1"STEP"1"UNTIL"ATOM NO"DO"
          "FOR"J:=1"STEP"1"UNTIL"ATOM NO"DO"
"BEGIN"
"IF" J=I "THEN" SS[I,J]:=1.0 "ELSE" SS[I,J]:=0.0;
H[I,J]:=0.0;
"END";
      "COMMENT"WE INITIALLY SET ALL ELEMENTS OF BETA MATRIX TO ZERO;
      "FOR"I:=1"STEP"1"UNTIL"BOND NO"DO"
      "BEGIN""READ"K,P;
      BONDS[1,I]:=K;BONDS[2,I]:=P;
      "READ" H[K,P];
H[P,K]:=H[K,P];
      "PRINT"´´L``,PREFIX(´´S2``),K,P;
"PRINT" PREFIX(´´S4``), H[K,P];
      "END";
COEFF[I,J]:=CC[J,I];
PRINT ENERGY AND COEFF(COEFF, ENERGY, ATOM NO);
      "COMMENT"TABULATES THE ENERGIES AND COEFFICIENTS;
"COMMENT"NOW TO CALCULATE BOND ORDERS,PRINT THEM AND STORE THEM FOR
THE FREE VALENCE CALCULATIONS;
"PRINT" ´´L6S40`BOND ORDERS´L2S38`BOND`;
"IF" ODD "THEN" "PRINT" ´´S11`POSITIVE´S6`NEUTRAL´S7`NEGATIVE`
"ELSE" "PRINT" ´´S11`NEUTRAL`;
"PRINT"´´L2``;
"FOR"I:=1"STEP"1"UNTIL"BOND NO"DO"
"BEGIN""PRINT"´´S25``;K:=BONDS[1,I];P:=BONDS[2,I];
      "PRINT"PREFIX(´´S2``),K,P;B:=0;J:=0;
      "FOR"J:=J+1"WHILE"ABS(ENERGY[J]-ENERGY[M])>10-3"DO"
"BEGIN"B:=2*COEFF[J,P]*COEFF[J,K]+B;T:=J"END";
      S:=0;C:=0;J:=T;
      "FOR"J:=J+1"WHILE"ABS(ENERGY[J]-ENERGY[M])<10-3"DO"
      "BEGIN"C:=COEFF[J,P]*COEFF[J,K]+C;S:=S+1"END";
      C:=C/S;B:=2*C*(M-T)+B;
      "PRINT"PREFIX(´´S4``),B;
      "COMMENT"BOND ORDER OF NEUTRAL MOLECULE IF EVEN AND OF
      POSITIVE ION IF ODD;
      "IF"ODD"THEN"
      "BEGIN""IF"ABS(ENERGY[M+1]-ENERGY[M])>10-3"THEN"
        "BEGIN"S:=0;C:=0;
         "FOR"J:=M+1,J+1"WHILE"ABS(ENERGY[J]-ENERGY[M+1])<10-3"DO"
         "BEGIN"C:=C+COEFF[J,P]*COEFF[J,K];
         S:=S+1
```

```
          "END";
          C:=C/S
        "END";
        "PRINT"PREFIX(``S4``),(B+C),(B+2*C)
      "END"OF CALCULATION OF BOND ORDERS OF NEUTRAL MOLECULE AND
      NEGATIVE ION;
      "PRINT"``L``;
      BOND ORDER[I]:="IF"ODD"THEN"B+C"ELSE"B
"END" OF I LOOP OVER BONDS;
"COMMENT" NOW TO CALCULATE PI DENSITIES,SPIN DENSITIES AND FREE
VALENCE;
"PRINT" ``L6S27`PI DENSITY, SPIN DENSITY AND FREE VALENCE`L2S6`ATOM`;
"IF" ODD "THEN" "PRINT" ``S19`DENSITY`S18`SPIN DENSITY`S6`FREE VALENCE`
"ELSE"
"PRINT" ``S5`DENSITY`S12`SPIN DENSITY`S8`FREE VALENCE`; "PRINT" ``L1``;
"IF" ODD "THEN" "PRINT" ``S15`POSITIVE`S6`NEUTRAL`S7`NEGATIVE` "ELSE"
"PRINT" ``S29`POSITIVE`S6`NEGATIVE`; "PRINT" ``L2``;
"FOR"I:=1"STEP"1"UNTIL"ATOM NO"DO"
"BEGIN" B:=0; "PRINT" I; J:=0;
      "FOR"J:=J+1"WHILE"ABS(ENERGY[J]-ENERGY[M])>10-3"DO"
      "BEGIN"B:=2*COEFF[J,I]↑2+B;T:=J"END";
      S:=0;C:=0;J:=T;
      "FOR"J:=J+1"WHILE"ABS(ENERGY[J]-ENERGY[M])<10-3"DO"
      "BEGIN"S:=S+1;C:=C+COEFF[J,I]↑2"END";
      "PRINT"``L2``;
"COMMENT" INPUT OF BOND DATA;
"PRINT" ``S13`ATOM`S10`H-VALUES`L1``;
NEW:"READ"K;
      "IF"K"LE"0"THEN""GOTO"END DATA;
"PRINT" PREFIX(``S2``), K;
      "READ"P;"PRINT"PREFIX(``S2``),P;
      "IF"K"NE"P"THEN""GOTO"FAIL;
"READ" H[K,K]; "PRINT" PREFIX(``S4``), H[K,K];
"PRINT" ``L1``; "GOTO" NEW;
      END DATA:NEW MOLECULE:=K=0;
      "COMMENT"INPUT OF ATOM DATA FOR HETEROATOMS. NEW MOLECULE IF TRUE
      MEANS A NEW SET OF DATA FOLLOWS THIS SET, IF FALSE THAT THIS IS
      THE LAST SET OF DATA FOR THIS RUN;
      M:=ENO"DIV"2;ODD:=2*M"NE"ENO;
      "COMMENT" M GIVES THE NUMBER OF DOUBLY ACCUPIED ORBITALS.
      ODD TAKES THE VALUE TRUE IF THE TOTAL NUMBER OF PI ELECTRONSIS
      ODD;
EIGENSOLVE(H, SS, COEFF, ATOM NO, FAILED);
"GOTO" MHTN;
FAILED:  "PRINT" ``L2S10`AND YET THEIR REWARD APPEARETH NOT,`;
"PRINT" ``L2S10`AND THEIR LABOUR HATH NO FRUITE....`;
"GOTO" FINISH;
MHTN:
"FOR" I:=1 "STEP" 1 "UNTIL" ATOM NO "DO" ENERGY[I]:=H[I,I];
"COMMENT" NOW SORT OUT THE EIGENVALUES IN DECREASING ORDER,
IE. INCREASING ENERGY, AND CORRESPONDINGLY CHANGE THE
EIGENVECTORS;
"FOR" X:=ATOM NO "STEP" -1 "UNTIL" 2 "DO"
"FOR" I:=2 "STEP" 1 "UNTIL" X "DO"
"IF" ENERGY[I-1]<ENERGY[I] "THEN" "BEGIN"
CHANGE:=ENERGY[I-1];   ENERGY[I-1]:=ENERGY[I];   ENERGY[I]:=CHANGE;
"FOR" J:=1 "STEP" 1 "UNTIL" ATOM NO "DO" "BEGIN"
CHANGE:=COEFF[J,I-1];   COEFF[J,I-1]:=COEFF[J,I];
COEFF[J,I]:=CHANGE;   "END";   "END";
"COMMENT" NOW EFFECTIVELY TRANSPOSE THE COEFF MATRIX SO THE
PRINT ENERGY AND MCLACHLAN PROCEDURES WORK;
"FOR" I:=1 "STEP" 1 "UNTIL" ATOM NO "DO"
```

```
"FOR" J:=1 "STEP" 1 "UNTIL" ATOM NO "DO"
CC[I,J]:=COEFF[I,J];
"FOR" I:=1 "STEP" 1 "UNTIL" ATOM NO "DO"
"FOR" J:=1 "STEP" 1 "UNTIL" ATOM NO "DO"
      C:=C/S;B:=B+2*C*(M-T);
      "COMMENT"B IS CHARGE OF NEUTRAL EVEN MOLECULE;
      "IF"ABS(ENERGY[M+1]-ENERGY[M])>10-3"THEN"
      "BEGIN"S:=0;D:=0;
        "FOR"J:=M+1,J+1"WHILE"ABS(ENERGY[J]-ENERGY[M+1])<10-3"DO"
        "BEGIN"D:=COEFF[J,I]↑2+D;S:=S+1"END";
        D:=D/S
      "END""ELSE"D:=C;
      "IF"ODD"THEN""BEGIN""PRINT"PREFIX(´´S4``),B;B:=B+D;C:=D"END";
      "COMMENT" EXTRA TERM FOR ODD ELECTRON;
      "PRINT"PREFIX(´´S4``),B;
      "IF"ODD"THEN""PRINT"PREFIX(´´S4``),(B+D);
      "PRINT"PREFIX(´´S4``),C;
      "IF"ODD"THEN""PRINT"´´S4``"ELSE""PRINT"PREFIX(´´S4``),D;
      "COMMENT" NOW TO CALCULATE THE FREE VALENCE FOR THIS ATOM;
      D:=0;
      "FOR"J:=1"STEP"1"UNTIL"BOND NO"DO"
      "IF"BONDS[1,J]=I"OR"BONDS[2,J]=I"THEN"
      D:=D+BOND ORDER[J];
      "PRINT"PREFIX(´´S4``),(SQRT(3)-D),´´L``;
"END" OF I LOOP OVER ATOMS;
"IF" ODD "THEN" "PRINT" ´´L6`ODD NO OF ELECTRONS IN NEUTRAL MOLECULE`;
"COMMENT"TOTAL PI ENERGY;
B:=0;
"FOR"I:=1"STEP"1"UNTIL"M"DO"B:=B+ENERGY[I];
B:=2*B;
"IF"ODD"THEN"B:=B+ENERGY[M+1];
"PRINT" ´´L6S30`TOTAL PI ENERGY´S4``, SAMELINE, B, ´´L6``;
"COMMENT"RESONANCE ENERGY FOR EVEN SYSTEMS, +VE AND -VE ION ENERGIES
FOR ODD SYSTEMS;
"IF""NOT"ODD"THEN"
"BEGIN"C:=B-ATOM NO;
"PRINT" ´´S30`RESONANCE ENERGY`;
"PRINT" ´´S4``, SAMELINE, C;
"PRINT" ´´L2S10`N.B. RESONANCE ENERGIES FOR HETEROATOM SYSTEMS WILL
´S10`BE INCORRECT AS THEY ARE BASED ON C-C BOND ENERGIES`;
"END""ELSE"
"BEGIN" "PRINT" ´´L6S20`TOTAL PI ENERGY OF IONS RELATED TO RADICAL`;
"PRINT" ´´L2S30`POSITIVE ION´S5``, SAMELINE, (B-ENERGY[M+1]);
"PRINT" ´´L2S30`NEGATIVE ION´S5``, SAMELINE, (B+ENERGY[M+1]);
      "END";
MCLACHLAN(ATOM NO, M, LAMBA, COEFF, ENERGY);
"END";
"IF"NEW MOLECULE"THEN"
"BEGIN""PRINT"´´F``;
"GOTO"START"END""ELSE""GOTO"FINISH;
FAIL:"PRINT"´FAILURE EXIT FROM DATA´L``;"GOTO"FINISH;
FINISH:
"END";
```

APPENDIX II

The program ESRTEST enables the computation and simulation of an experimental esr spectrum. Having been fed with the coupling constants, together with the spin and number of atoms comprising each magnetically equivalent group, calculation of the line positions and relative intensities ensues with subsequent sorting of the lines into their correct positions. A further procedure, based on a Lorentzian line-shape function enables graphical simulation of the spectrum, hence giving a direct check of the interpretation of the experimental spectrum.

The input data are as follows

CHOICE — 0 if only tabular output is required and 1 for graphical presentation

CONFAC — Conversion factor in oersted per centimetre, which allows all measured data to be input in centimetres while output is oersteds is obtained

CWID — Peak-to-peak line width

HITE — Peak-to-peak height of the largest line. This factor allows scaling of the simulated spectrum to the experimental one

N — The number of magnetically non-equivalent groups in the molecule in question

For each group of magnetic nuclei the following data are input

NO[M] — The number of equivalent nuclei

SP[M] — Twice the spin for the nucleus

CA[M] — The coupling constant for the group

The tabulated output gives the line width and, for each

group of equivalent nuclei, the number of nuclei, their spin and the coupling constant. This is followed by the position of each line, relative to the centre of the spectrum, and for each line, its degeneracy or relative intensity and the group spin quantum numbers by which its position is determined.

The program, in Algol, is presented below.

```
EDITEST;
"BEGIN" "INTEGER" N, X, MOVE, CHOICE, FINAL;
"REAL" Y, YP, YY, BK, WIDTH, CWID, CONFAC, HMAX,
T, DIM, NUMBL, IGNORE, HITE;
"READ" CHOICE, CONFAC, CWID, HITE;
"IF" CHOICE=0 "THEN" "GOTO" OK;  "IF" CHOICE=1 "THEN" "GOTO" OK;
"PRINT" `YOU FORGOT THE VARIABLE THAT DIRECTS WHETHER OR NOT YOU USE
THE GRAPH PLOTTER`; "GOTO" ERROR; OK:
"PRINT" ``37`ATOM`34`NO IN GROUP`37`SPIN`,
SAMELINE, ``37`SPLITTING CONSTANT`38`LINE WIDTH`;
"PRINT" ``L1S45`CHE`38`GAUSS`37`CHE`37`GAUSS`;
WIDTH:=CWID/1.27;
"PRINT" ``L2S67``, SAMELINE, ALIGNED(1,3), CWID,
``34``, ALIGNED(1,3), CWID*CONFAC;
"READ" N;
"BEGIN" "INTEGER" "ARRAY" BLIM, NO, SP, LIMIT[1:N];
"REAL" "ARRAY" A[1:N], CA[1:N];
"INTEGER" M, L, BLIMAX, LIMAX, J, I, Z, P, K, X, CH, ML;
"REAL" CHANGE;
LIMAX:=BLIMAX:=0; ML:=1;
"PRINT" ``L2``;  "FOR" M:=1 "STEP" 1 "UNTIL" N "DO"
"BEGIN" "READ" NO[M], SP[M], CA[M];
A[M]:=CA[M]/2.54;
"PRINT" ``L1``, M, SAMELINE, ``34``, NO[M],
``S11``, ALIGNED(1,1), SP[M]/2, ``35``, ALIGNED(3,3), CA[M],
``34``, ALIGNED(3,3), CA[M]*CONFAC;
BLIM[M]:=(SP[M]+1)↑NO[M];
"IF" BLIM[M]> BLIMAX "THEN" BLIMAX:= BLIM[M];
LIMIT[M]:= SP[M]* NO[M] +1;
"IF" LIMIT[M] > LIMAX "THEN" LIMAX:= LIMIT[M];
ML:=ML* LIMIT[M]; "END";
"BEGIN" "INTEGER" "ARRAY"AA[1:N,1:BLIMAX] , IL, M[1:N,1:LIMAX],
MT,QQ[0:N,1:ML];
"REAL" "ARRAY" PL[0:N,1:ML];
"INTEGER" Q, MAX, LIMIT, TEST, SCOPE, P, F, D, E, MAXI, SPIN;
"FOR" M:=1 "STEP" 1 "UNTIL" N "DO" "BEGIN" "COMMENT" WE FIND ALL POSS-
-IBLE NUCLEAR SPIN CONFIGURATIONS FOR EACH GROUP;

"INTEGER" "ARRAY"  B[0:NO[M],1:BLIM[M]];
B[0,1]:= 0;  F:= D:= E:= MAXI:=1;
NEWDEE: SPIN:= -SP[M];
ADD: "IF" SPIN=SP[M]+ 2 "THEN" "BEGIN" F:=F+1;
SPIN:= -SP[M]; "END";
"IF" F> MAXI "THEN" "GOTO" NEWDEE;
B[D,E]:= B[D-1,F] + SPIN;
E:= E+1; SPIN:= SPIN + 2; "GOTO" ADD;
```

```
NEWORD: "IF" D= NO[M] "THEN" "GOTO" CONDENSE;
MAXI:= MAXI * (SP[M] + 1); D:= D+1;  Z:= Z:= 1; "GOTO" NEWROW;
CONDENSE: "FOR" Z:=1 "STEP"1 "UNTIL" ELIM[M] "DO"AA[M,Z]:=Z[NO[M],Z];
J:= I:= Z:=0; NEXT: J:= J+1; NEW: Z:= Z+1;
"IF" Z> ELIM[M] "THEN" "GOTO" MORE;
I:= Z;  P:=AA[M,I];
"IF" I =1 "THEN" "GOTO" START;
"FOR" K:=1 "STEP" 1 "UNTIL" Z-1 "DO" "IF"AA[M,K]=AA[M,I] "THEN"
"GOTO" NEW;  START: LL[M,J]:= P;  H[M,J]:= 1;
"IF"  Z= ELIM[M] "THEN" "GOTO" MORE;
"FOR" I:=1+Z "STEP" 1 "UNTIL" ELIM[M] "DO"
"IF"AA[M,I] = P "THEN" H[M,J]:= H[M,J] + 1;
"GOTO" NEXT; MORE: "END";
"COMMENT"  NOW WE PUT THE GROUP QUANTUM NUMBERS TOGETHER TO GET
LINE POSITIONS AND DEGENERACIES; L:= J:= 0;  M:= Q:= MAX:= 1;
PL[0,1] := 0;  HT[0,1] := 1;
CYCLE: LIMIT:= SP[M] * NO[M] + 1; R:=0;  TEST:=0 ;
       SCOPE:=M / (MAX * LIMIT );
INC: "IF" J = LIMIT "THEN" "BEGIN" J:=0; Q:= Q+1;
"END";  "IF" Q > MAX "THEN" "GOTO" LEAP ;
TEST:= TEST + SCOPE;
L:=L+1; J:=J+1;
PL[M,L]:=PL[M-1,Q]+LL[M,J]*A[M];
HT[M,L]:= HT[M-1,Q] * H[M,J];
LABEL: "IF" D= TEST "THEN" "GOTO" INC;
R:= R+1; QQ[M,R]:= LL[M,J];  "GOTO" LABEL ;
LEAP: M:= M+1;  MAX:= LIMIT * MAX;  L:= J:= 0;  Q:=1;
"IF" M>N "THEN" "GOTO" FURTHER; "GOTO" CYCLE;
       "COMMENT" NOW WE SORT THE LINES BY POSITION;
FURTHER:
"FOR"K:=M "STEP" -1 "UNTIL" 2 "DO" "FOR" J:=2 "STEP" 1 "UNTIL" K "DO"
"IF"PL[N,J-1] >PL[N,J] "THEN" "BEGIN"
CHANGE:=PL[N,J-1]; PL[N,J-1]:=PL[N,J]; PL[N,J]:= CHANGE;
CH     := HT[N,J-1];  HT[N,J-1]:= HT[N,J];  HT[N,J]:= CH     ;
"FOR"M:=1 "STEP" 1 "UNTIL" N "DO" "BEGIN"
CH     :=QQ[M,J-1]; QQ[M,J-1]:=QQ[M,J]; QQ[M,J]:= CH     ; "END"; "END";
"PRINT" ``L4S6`LINE NO`39`LINE POSITION`S10`DEGENERACY``,
SAMELINE, ``36`GROUP SPIN QUANTUM NOS``; "PRINT" ``L16S21`CMS`39`GAUSS``;
"PRINT" ``L2S55``;
SAMELINE; "FOR" M:=1 "STEP" 1 "UNTIL" N "DO"
"PRINT" SAMELINE, ``S1``, M;  "PRINT" ``L2``;
"FOR" J:=1 "STEP" 1 "UNTIL" M "DO" "BEGIN"
"PRINT" ``L1S1``, J, SAMELINE, ``S7``, ALIGNED(4,3), PL[N,J]*1.27,
``S4``, ALIGNED(4,3), PL[N,J]*CONFAC*1.27, ``S3``, HT[N,J], ``S5``;
"FOR" M:=1 "STEP" 1 "UNTIL" N "DO"
"PRINT" ``S4``, ALIGNED(3,1), QQ[M,J]/2;  "END";
"IF" CHOICE=0 "THEN" "GOTO" FINIS;  PUNCH(5);
HMAX:=0;  "FOR" J:=1 "STEP" 1 "UNTIL" M "DO" "IF" HT[N,J] > HMAX
"THEN" HMAX:=HT[N,J]; HMAX:=(HMAX*14.72)/HITE; SETORIGIN(1300,1);
MOVEPEN(-4,0);
  IGNORE:=WIDTH*1500.0; FINAL:=PL[N,M]*100.0+200.0;
"FOR" XX:=0 "STEP" 2 "UNTIL" 2*FINAL "DO" "BEGIN" RX:=XX-FINAL;
Y:=0.0;  "FOR" J:=1 "STEP" 1 "UNTIL" M "DO" "BEGIN"
NEWPL:= PL[N,J] * 100.0;
"IF" ABS(RX-NEWPL) > IGNORE "THEN" "GOTO" CUT;
T:= (0.011547 * (RX-NEWPL)) / WIDTH;  DEN:= 1+T*T;
Y:= Y + (T * HT[N,J]) / (DEN *DEN); CUT: "END";
YP:=(1800.0*Y)/HMAX; YY:=-YP; DRAWLINE(XX,YY);
"END"; FINIS: "END"
```

APPENDIX III

The program ESRTT2 enables the computation and simulation of any number of superimposed spectra, although for convenience it has been modified from its general form to simulate two spectra only. The method of solution is as in ESRTEST and the output is similar, the data being presented separately for each component and also for the mixed spectrum where the lines from both species are sorted by position and the graphical simulation is based upon the final line positions.

The input of data is similar to that for ESRTEST, but some additional parameters are required, the order being given below

CHOICE — 0 for tabular presentation alone and 1 for tabular presentation and graphical simulation

MOLNO — The number of component species present; in this work always two

CONFAC — Conversion factor

CENSEP — Separation of the centres of the two component spectra

For each component the input is then

INSTRING — The title of the species

CWID — The peak-to-peak line width

HITE — The peak-to-peak height of the largest line

N — The number of magnetically non-equivalent groups

Again, for each component the input of data for the separate groups of nuclei is

NO[M] — The number of equivalent nuclei

SP[M] — Twice the spin for the nucleus

CA[M] The coupling constant for the group

The program, in Algol, is presented below.

```
ESRTT2;
"BEGIN" "INTEGER" CHOICE, MOLNO, XX, MOVE, FINAL, NML, TN, C, O, J,
M, MM, CHA, NMAX, S, B, BS, GMAX, BMAX, LMAX, MLMAX;
"REAL" RK, CONFAC, CENSEP, CHAN, T, DEN, NEWPL, Y, YY, OO;
"READ" CHOICE, MOLNO, CONFAC, CENSEP;
"IF" CHOICE=0 "THEN" "GOTO" OK; "IF" CHOICE=1 "THEN" "GOTO" OK;
"PRINT" `YOU FORGOT THE VARIABLE THAT SELECTS WHETHER OR NOT
YOU USE THE GRAPH PLOTTER`; "GOTO" ERROR;
OK:
NML:=0;
"BEGIN" "INTEGER" "ARRAY" N, HMAX[1:MOLNO], HEAD[1:20];
"REAL" "ARRAY" WIDTH, CWID, GWID, HITE, IGNORE, HHMAX[1:MOLNO];
GMAX:=0;
MM:=1;
"FOR" B:=1 "STEP" 1 "UNTIL" MOLNO "DO" "BEGIN"
INSTRING(HEAD,MM);
"READ" CWID[B], HITE[B], N[B];
GWID[B]:=CWID[B]*CONFAC; WIDTH[B]:=CWID[B]/1.27;
"IF" N[B]>GMAX "THEN" GMAX:=N[B];   "END";
"BEGIN" "INTEGER" "ARRAY" BLIM, LIMIT, NO, SP[1:MOLNO,1:GMAX],
ML, BLIMAX, LIMAX[1:MOLNO];
"REAL" "ARRAY" A, GA, CA[1:MOLNO,1:GMAX];
"INTEGER" L, I, Z, P, K, X, CH;
"REAL" CHANGE;
LMAX:=BMAX:=MLMAX:=0;
"FOR" B:=1 "STEP" 1 "UNTIL" MOLNO "DO" "BEGIN"
LIMAX[B]:=BLIMAX[B]:=0;  ML[B]:=1;
"FOR" M:=1 "STEP" 1 "UNTIL" N[B] "DO"
"BEGIN" "READ" NO[B,M], SP[B,M], CA[B,M];
GA[B,M]:=CA[B,M]*CONFAC; A[B,M]:=CA[B,M]/2.54;
BLIM[B,M]:=(SP[B,M]+1)↑NO[B,M];
"IF" BLIM[B,M]>BLIMAX[B] "THEN" BLIMAX[B]:=BLIM[B,M];
"IF" BLIMAX[B]>BMAX "THEN" BMAX:=BLIMAX[B];
LIMIT[B,M]:=SP[B,M]*NO[B,M]+1;
"IF" LIMIT[B,M]>LIMAX[B] "THEN" LIMAX[B]:=LIMIT[B,M];
"IF" LIMAX[B]>LMAX "THEN" LMAX:=LIMAX[B];
ML[B]:=ML[B]*LIMIT[B,M];
"IF" ML[B]>MLMAX "THEN" MLMAX:=ML[B];
"END";   "END";
C:=ML[1];
NML:=NML+ML[1]+ML[2];
OO:=ABS(CENSEP);
"PRINT" ``L2S10`SPECTRA SEPARATION`S1``, SAMELINE, ALIGNED(1,3), OO,
``S1`CMS`S3``, ALIGNED(1,3), OO*CONFAC, ``S1`GAUSS`;
"PRINT" ``L2S10`RELATIVE INTENSITIES`S1``;
"IF" HITE[1]"GE" HITE[2] "THEN" "BEGIN"
OO:=HITE[1]/HITE[2];
"PRINT" SAMELINE, ALIGNED(3,3), OO, ``S1`1:2`; "END" "ELSE" "BEGIN"
OO:=HITE[2]/HITE[1];
"PRINT" SAMELINE, ALIGNED(3,3), OO, ``S1`2:1`; "END";
"BEGIN" "INTEGER" "ARRAY" AA[1:GMAX,1:BMAX], LL,
H[1:GMAX,1:LMAX], HT, QQ[1:MOLNO,0:GMAX,1:MLMAX], LIMIT[1:MOLNO],
DT, SS[1:NML], DQ, TQ[0:GMAX, 1:NML];
"REAL" "ARRAY" PL[1:MOLNO,0:GMAX,1:MLMAX],
DL[1:NML];
```

```
"INTEGER" Q, MAX, TEST, SCOPE, R, F, D, E, MAXI, SPIN;
"FOR" B:=1 "STEP" 1 "UNTIL" MOLNO "DO" "BEGIN"
"FOR"M:=1 "STEP" 1 "UNTIL" N[B] "DO" "BEGIN"
"COMMENT" WE FIND ALL POSSIBLE NUCLEAR SPIN CONFIGURATIONS
FOR EACH GROUP;
"INTEGER" "ARRAY" BB[0:NO[B,M], 1:BLIM[B,M]];
BB[0,1]:=0; F:=D:=E:=MAXI:=1;
NEWROW: SPIN:=-SP[B,M];
ADD: "IF" SPIN=SP[B,M]+2 "THEN" "BEGIN" F:=F+1; SPIN:=-SP[B,M]; "END";
"IF" F>MAXI "THEN" "GOTO" NEWDEE;
BB[D,E]:=BB[D-1, F]+SPIN;
E:=E+1; SPIN:=SPIN+2; "GOTO" ADD;
NEWDEE: "IF" D=NO[B,M] "THEN" "GOTO" CONDENSE;
MAXI:=MAXI*(SP[B,M]+1); D:=D+1; E:=F:=1; "GOTO" NEWROW;
CONDENSE: "FOR" E:=1 "STEP" 1 "UNTIL" BLIM[B,M] "DO"
AA[M,E]:=BB[NO[B,M], E];
J:=I:=Z:=0;
NEXT: J:=J+1;
NEW: Z:=Z+1;
"IF" Z>BLIM[B,M] "THEN" "GOTO" MORE;
I:=Z; P:=AA[M,I];
"IF" I=1 "THEN" "GOTO" START;
"FOR" K:=1 "STEP" 1 "UNTIL" Z-1 "DO"
"IF" AA[M,K]=AA[M,I] "THEN" "GOTO" NEW;
START: LL[M,J]:=P; H[M,J]:=1;
"IF" Z=BLIM[B,M] "THEN" "GOTO" MORE;
"FOR" I:=1+Z "STEP" 1 "UNTIL" BLIM[B,M] "DO"
"IF" AA[M,I]=P "THEN" H[M,J]:=H[M,J]+1;
"GOTO" NEXT; MORE: "END";
"COMMENT" NOW WE PUT THE GROUP QUANTUM NUMBERS TOGETHER
TO GET THE LINE POSITIONS AND DEGENERACIES;
L:=J:=0; M:=Q:=MAX:=1;
PL[B,0,1]:=0; HT[B,0,1]:=1;
CYCLE: LIMIT[B]:=SP[B,M]*NO[B,M]+1; R:=0; TEST:=0;
SCOPE:=0;
SCOPE:=ML[B]/(MAX*LIMIT[B]);
INC: "IF" J=LIMIT[B] "THEN" "BEGIN" J:=0; Q:=Q+1; "END";
"IF" Q>MAX "THEN" "GOTO" LEAP;
TEST:=TEST+SCOPE;
L:=L+1; J:=J+1;
PL[B,M,L]:=PL[B,M-1,Q]+LL[M,J]*A[B,M];
HT[B,M,L]:=HT[B,M-1,Q]*H[M,J];
LABEL: "IF" R=TEST "THEN" "GOTO" INC;
R:=R+1; QQ[B,M,R]:=LL[M,J]; "GOTO" LABEL;
LEAP: M:=M+1; MAX:=LIMIT[B]*MAX; L:=J:=0; Q:=1;
"IF" M>N[B] "THEN" "GOTO" FURTHER; "GOTO" CYCLE;
"COMMENT" NOW WE SORT THE LINES BY POSITION;
FURTHER: "FOR" X:=ML[B] "STEP" -1 "UNTIL" 2 "DO"
"FOR" J:=2 "STEP" 1 "UNTIL" X "DO"
"IF" PL[B,N[B], J-1]>PL[B,N[B], J] "THEN" "BEGIN"
CHANGE:=PL[B,N[B], J-1]; PL[B, N[B], J-1]:=PL[B, N[B], J];
PL[B, N[B], J]:=CHANGE;
CH:=HT[B, N[B], J-1]; HT[B, N[B], J-1]:=HT[B, N[B], J];
HT[B, N[B], J]:=CH;
"FOR" M:=1 "STEP" 1 "UNTIL" N[B] "DO" "BEGIN"
CH:=QQ[B, M, J-1]; QQ[B, M, J-1]:=QQ[B, M, J];
QQ[B,M,J]:=CH;   "END";  "END";  "END";
MM:=1;
"FOR" B:=1 "STEP" 1 "UNTIL" MOLNO "DO" "BEGIN"
"PRINT" ``L2S20`ESR DATA FOR `;
```

```
OUTSTRING(HEAD,MM);
"PRINT" SAMELINE, B, ''L2'';
"PRINT" ''S7'ATOM'S4'NO IN GROUP'S7'SPIN',
SAMELINE, ''S7'SPLITTING CONSTANT'S8'LINE WIDTH';
"PRINT" ''L1S45'CMS'S8'GAUSS'S7'CMS'S7'GAUSS';
"PRINT" ''L2S67'', SAMELINE, ALIGNED(1,3), CWID[B],
''S4'', ALIGNED(1,3), GWID[B], ''L2'';
"FOR" M:=1 "STEP" 1 "UNTIL" N[B] "DO"
"PRINT" ''L1'', M, SAMELINE, ''S4'', NO[B,M],
''S11'', ALIGNED(1,1), SP[B,M]/2, ''S5'', ALIGNED(3,3), CA[B,M],
''S4'', ALIGNED(3,3), GA[B,M];
"PRINT" ''L4S6'LINE NO'S9'LINE POSITION'S10'DEGENERACY',
SAMELINE, ''S6'GROUP SPIN QUANTUM NOS'; "PRINT" ''L1S21'CMS'S9'GAUSS';
"PRINT" ''L2S55'';
SAMELINE; "FOR" M:=1 "STEP" 1 "UNTIL" N[B] "DO"
"PRINT" SAMELINE, ''S1'', M; "PRINT" ''L2'';
"FOR" J:=1 "STEP" 1 "UNTIL" ML[B] "DO" "BEGIN"
"PRINT" ''L1S1'', J, SAMELINE, ''S7'',
ALIGNED(4,3), PL[B, N[B], J]*1.27, ''S4'', ALIGNED(4,3),
PL[B,N[B],J]*CONFAC*1.27, ''S3'', HT[B,N[B],J], ''S5'';
"FOR" M:=1 "STEP" 1 "UNTIL" N[B] "DO"
"PRINT" ''S4'', ALIGNED(3,1), QQ[B,M,J]/2; "END"; "END";
"COMMENT" NOW SORT OUT BOTH GROUPS OF LINES BY POSITION;
"PRINT" ''L4S20'COMBINED DATA FOR BOTH MOLECULES'L2'';
"FOR" B:=1 "DO" "BEGIN"
J:=O:=0;
IND1: J:=J+1; O:=O+1; SS[O]:=1;
DL[O]:=PL[B,N[B],J];
DT[O]:=HT[B,N[B],J];
"FOR" M:=1 "STEP" 1 "UNTIL" N[B] "DO" DQ[M,O]:=QQ[B,M,J];
"IF" J=ML[B] "THEN" "GOTO" OUTD1;
"GOTO" IND1; OUTD1:
"END";
"FOR" B:=2 "DO" "BEGIN"
J:=0; O:=C;
IND2: J:=J+1; O:=O+1; SS[O]:=2;
DL[O]:=PL[B,N[B],J]+(CENSEP/1.27);
DT[O]:=HT[B,N[B],J];
"FOR" M:=1 "STEP" 1 "UNTIL" N[B] "DO" DQ[M,O]:=QQ[B,M,J];
"IF" J=ML[B] "THEN" "GOTO" OUTD2;
"GOTO" IND2; OUTD2:
"END";
"FOR" TN:=NML "STEP" -1 "UNTIL" 2 "DO"
"FOR" O:=2 "STEP" 1 "UNTIL" TN "DO"
"IF" DL[O-1]>DL[O] "THEN" "BEGIN"
CHAN:=DL[O-1]; DL[O-1]:=DL[O]; DL[O]:=CHAN;
CHA:=DT[O-1]; DT[O-1]:=DT[O]; DT[O]:=CHA;
CHA:=SS[O-1]; SS[O-1]:=SS[O]; SS[O]:=CHA;
"FOR" M:=1 "STEP" 1 "UNTIL" N[SS[O-1]] "DO" TQ[M,O]:=DQ[M,O];
"FOR" M:=1 "STEP" 1 "UNTIL" N[SS[O]] "DO" DQ[M,O]:=DQ[M,O-1];
"FOR" M:=1 "STEP" 1 "UNTIL" N[SS[O-1]] "DO" DQ[M,O-1]:=TQ[M,O];
"END";
"PRINT" ''L2S6'LINE NO'S9'LINE POSITION'S10'DEGENERACY',
SAMELINE, ''S6'GROUP SPIN QUANTUM NOS'; "PRINT" ''L1S21'CMS'S9'GAUSS';
"PRINT" ''L2S55''; NMAX:=0;
"FOR" B:=1 "STEP" 1 "UNTIL" MOLNO "DO"
"IF" N[B]>NMAX "THEN" NMAX:=N[B];
SAMELINE; "FOR" M :=1 "STEP" 1 "UNTIL" NMAX "DO"
"PRINT" SAMELINE, ''S1'', M; "PRINT" ''L2'';
O:=0;  SORT: O:=O+1;
```

```
"PRINT" ``L1S1``, SAMELINE, O, ``S7``;
"PRINT" SAMELINE, ALIGNED(4,3), DL[O]*1.27, ``S4``, ALIGNED(4,3),
DL[O]*CONFAC*1.27, ``S3``, DT[O], ``S5``;
"FOR" M:=1 "STEP" 1 "UNTIL" N[SS[O]] "DO" "PRINT" SAMELINE, ``S4``,
ALIGNED(3,1), DQ[M,O]/2;
"PRINT" SAMELINE, ``S5``, SS[O];
"IF" O=NML "THEN" "GOTO" OUTSORT;
"GOTO" SORT;  OUTSORT:
"IF" CHOICE=0 "THEN" "GOTO" FINIS;  PUNCH(5);
"FOR" BS:=1 "STEP" 1 "UNTIL" MOLNO "DO" HMAX[BS]:=0;
"FOR" O:=1 "STEP" 1 "UNTIL" NML "DO" "BEGIN"
BS:=SS[O];
"IF" DT[O]>HMAX[BS] "THEN" HMAX[BS]:=DT[O]; "END";
"FOR" BS:=1 "STEP" 1 "UNTIL" MOLNO "DO"
HHMAX[BS]:=(HMAX[BS]*14.72)/HITE[BS];
SETORIGIN(1300,1); MOVEPEN(-4,0);
"FOR" BS:=1 "STEP" 1 "UNTIL" MOLNO "DO"
IGNORE[BS]:=WIDTH[BS]*1500.0;
FINAL:=ENTIER(DL[NML]*100.0+200.0);
"FOR" XX:=0 "STEP" 2 "UNTIL" 2*FINAL "DO" "BEGIN"
RX:=XX-FINAL; Y:=0.0;
"FOR" O:=1 "STEP" 1 "UNTIL" NML "DO" "BEGIN"
BS:=SS[O];
NEWPL:=DL[O]*100.0;
"IF" ABS(RX-NEWPL)>IGNORE[BS] "THEN" "GOTO" CUT;
T:=(0.011547*(RX-NEWPL))/WIDTH[BS]; DEN:=1+T*T;
Y:=Y+(T*DT[O])/(DEN*DEN*HHMAX[BS]);  CUT: "END";
YY:=-(1800.0*Y);  DRAWLINE(XX,YY);
"END"; FINIS: "END";  "END";  "END";  ERROR: "END";
```

APPENDIX IV

The program ACTPAR is described in section 4.7 and is given below in Algol.

```
ACTPAR ACTIVATION PARAMETERS;
"BEGIN""INTEGER"N;"READ"N;
"PRINT"´CALCULATION OF ACTIVATION PARAMETERS FOR SYSTEM :´L9``;
"BEGIN""REAL"A,B,C,D,F,G,H,M,P,DM,DC,DDY;
"INTEGER"I;"ARRAY"X,Y,DY,W[1:N];
A:=B:=D:=F:=G:=H:=0;
"PRINT"´ TEMPERATURE        RATE          WEIGHT´L``;
"PRINT"´(CENTIGRADE)      CONSTANT´L2``;
"FOR"I:=1"STEP"1"UNTIL"N"DO"
"BEGIN""READ"X[I],Y[I],DY[I];
"IF"DY[I]-1=0"THEN""GOTO"L1;
DY[I]:=DY[I]/Y[I];
L1:W[I]:=1/(DY[I]*DY[I]);
"PRINT"´´S3``,SAMELINE,ALIGNED(3,1),X[I],´´S7``,
SCALED(4),Y[I],´´S6``,W[I],´´L``;
X[I]:=1000/(273.1+X[I]);Y[I]:=LN(Y[I]);
H:=H+W[I];A:=A+W[I]*X[I];
B:=B+W[I]*X[I]*Y[I];D:=D+W[I]*Y[I];
F:=F+W[I]*X[I]*X[I];"END";
P:=H*F-A*A;M:=(H*B-A*D)/P;C:=(F*D-A*B)/P;
"FOR"I:=1"STEP"1"UNTIL"N"DO"G:=G+((M*X[I]+C-Y[I])↑2)*W[I];
DDY:=SQRT(G/(N-2));DM:=DDY*SQRT(H/P);DC:=DDY*SQRT(F/P);
"PRINT"´´L4`ARRHENIUS PARAMETERS :´L2``;
"PRINT"´´S2`ENERGY OF ACTIVATION = `,SAMELINE,
ALIGNED(2,2),-1.9872*M,´´S4`E.S.D. = `,1.9872*DM,´ KCALS. PER MOLE`;
"PRINT"´´L``,SAMELINE,´´S8`LOG10(A-FACTOR) = `,
ALIGNED(2,2),C/2.303,´´S4`E.S.D. = `,DC/2.303,´´L3``;
"PRINT"´ENTHALPY OF ACTIVATION = `,SAMELINE,
ALIGNED(2,2),-1.9872*(M+0.2981),
´´S4`E.S.D. = `,1.9872*DM,´ KCALS. PER MOLE AT 25 DEGREES CENTIGRADE`;
"PRINT"´´L``,SAMELINE,´ ENTROPY OF ACTIVATION = `,
ALIGNED(2,2),1.9872*(C-30.4575),´´S4`E.S.D. = `,
1.9872*DC,´ E.U.`,´´S12`AT 25 DEGREES CENTIGRADE´F``;"END";
"COMMENT"INPUTS AS FOLLOWS: N(NO. OF POINTS), T[1](CENTIGRADE),
K[1](RATE CONSTANT AT T[1], UNITS OF MOLES AND SECS.), E.S.D. K[1].....
T[N], K[N], E.S.D. K[N];
"COMMENT" IF EQUAL WEIGHTING OF POINTS REQUIRED SET ALL ESD K VALUES
TO UNITY;
"END" OF PROGRAM;
```

APPENDIX V

The program ALWETEST enables the computer simulation of an esr spectrum of a species which is undergoing slow limit interchange between conformations of equal lifetimes. The program operates in the same way as ESRTEST with the exception that a contribution, $\Delta\Gamma$, to the principal linewidth, Γ_0, is given by

$$\Delta\Gamma = \left[\frac{1}{2\tau\gamma_e}\right] [m_I(A) - m_I(B)]^2$$

where 2τ is the mean lifetime in one conformation and $m_I(A)$ and $m_I(B)$ are the quantum numbers of an exchanging proton in axial and equatorial positions. The value of the second bracket is zero for lines which do not broaden and one for those which do.

The input data are as follows:

CHOICE — 0 if only tabular output is required and 1 for graphical presentation

CONFAC — Conversion factor in oersted per centimetre, which allows all measured data to be input in centimetres while output in oersteds is obtained

CWID — Peak-to-peak line width

HITE — Peak-to-peak height of the largest line. This factor allows scaling of the simulated spectrum to the experimental one

ALWENO — The number of exchanging protons

N — The number of magnetically non-equivalent groups in the molecule in question

For each group of equivalent nuclei the following data are input:

NO[M] — The number of equivalent nuclei

SP[M] Twice the spin for the nucleus

CA[M] The coupling constant for the group

The data for exchanging protons are input first, in pairs.

TAU Lifetime of one conformation

The program, in Algol, is presented below.

```
ALWETEST;
"COMMENT" THIS PROGRAM SIMULATES ALTERNATING LINEWIDTH EFFECTS ROR
ESR SPECTRA OF RADICALS UNDERGOING SLOW LIMIT CONFORMATIONAL
INTERCONVERSIONS;
"BEGIN" "INTEGER" N, XX, MOVE, CHOICE, FINAL,ALWNO,CYC,NN,FF;
"REAL" Y,YP,YY, RX, WIDMAX, CONFAC, HMAX,CWID,FWID,TAU,
TT,
T, DEN, NEWPL, IGNORE, HITE;
WIDMAX:=0;
"READ" CHOICE, CONFAC,CWID,  HITE,ALWNO;
CYC:=ALWNO/2;
FWID:=CWID    *CONFAC;
"IF" CHOICE=0 "THEN" "GOTO" OK;  "IF" CHOICE=1 "THEN" "GOTO" OK;
"PRINT" `YOU FORGOT THE VARIABLE THAT SELECTS WHETHER OR NOT YOU USE
THE GRAPH PLOTTER`; "GOTO" ERROR; OK:
"PRINT" ``S7`ATOM`S4`NO IN GROUP`S7`SPIN`,
SAMELINE, ``S7`SPLITTING CONSTANT`S6`PRINCIPAL LINE WIDTH`;
"PRINT" ``L1S45`CMS`S8`GAUSS`S7`CMS`S7`GAUSS`;
"PRINT"``L2S67``,SAMELINE,ALIGNED(1,3),CWID,``S4``,ALIGNED(1,3),
CWID*CONFAC;
"READ" N;
"BEGIN" "INTEGER" "ARRAY" BLIM, NO, SP, LIMIT[1:N];
"REAL" "ARRAY" A[1:N], CA[1:N];
"INTEGER" M, L, BLIMAX, LIMAX, J, I, Z, P, K, X, CH, ML;
"REAL" CHANGE;
LIMAX:=BLIMAX:=0; ML:=1;
"PRINT" ``L2``;   "FOR" M:=1 "STEP" 1 "UNTIL" N "DO"
"BEGIN" "READ" NO[M], SP[M], CA[M];
A[M]:=CA[M]/2.54;
"PRINT" ``L1``, M, SAMELINE, ``S4``, NO[M],
``S11``, ALIGNED(1,1), SP[M]/2, ``S5``, ALIGNED(3,3), CA[M],
``S4``, ALIGNED(3,3), CA[M]*CONFAC;
BLIM[M]:=(SP[M]+1)↑NO[M];
"IF" BLIM[M]> BLIMAX "THEN" BLIMAX:= BLIM[M];
LIMIT[M]:= SP[M]* NO[M] +1;
"IF" LIMIT[M] > LIMAX "THEN" LIMAX:= LIMIT[M];
ML:=ML* LIMIT[M]; "END";
"BEGIN" "INTEGER" "ARRAY"AA[1:N,1:BLIMAX] , LL, H[1:N,1:LIMAX],
HT,QQ[0:N,1:ML];
"REAL""ARRAY"ACTHT[1:ML];"REAL"ALT;
"REAL""ARRAY"WIDTH[1:ML,0:CYC],QDIF[1:ML,1:CYC];
"REAL""ARRAY"CAD[1:CYC];
"REAL" "ARRAY" PL[0:N,1:ML];
"INTEGER" Q, MAX, LIMIT, TEST, SCOPE, R, F, D, E, MAXI, SPIN;
"FOR"E:=1"STEP"1"UNTIL"ML"DO"
```

```
WIDTH[E,0]:=FWID ;
"READ"TAU;
TT:=1/(TAU*2.8*10↑6);
"FOR" M:=1 "STEP" 1 "UNTIL" N "DO" "BEGIN" "COMMENT" WE FIND ALL POSS-
-IBLE NUCLEAR SPIN CONFIGURATIONS FOR EACH GROUP;

"INTEGER" "ARRAY"  B[0:NO[M],1:BLIM[M]];
B[0,1]:= 0;  F:= D:= E:= MAXI:=1;
NEWROW: SPIN:= -SP[M];
ADD: "IF" SPIN=SP[M]+ 2 "THEN" "BEGIN" F:=F+1;
SPIN:= -SP[M]; "END";
"IF" F> MAXI "THEN" "GOTO" NEWDEE;

B[D,E]:= B[D-1,F] + SPIN;

E:= E+1; SPIN:= SPIN + 2; "GOTO" ADD;
NEWDEE: "IF" D= NO[M] "THEN" "GOTO" CONDENSE;

MAXI:= MAXI * (SP[M] + 1); D:= D+1;  E:= F:= 1; "GOTO" NEWROW;
CONDENSE: "FOR" E:=1 "STEP"1 "UNTIL" BLIM[M] "DO"AA[M,E]:=B[NO[M],E];
J:= I:= Z:=0; NEXT: J:= J+1; NEW: Z:= Z+1;
"IF" Z> BLIM[M] "THEN" "GOTO" MORE;
I:= Z;  P:=AA[M,I];
"IF" I =1 "THEN" "GOTO" START;
"FOR" K:=1 "STEP" 1 "UNTIL" Z-1 "DO" "IF"AA[M,K]=AA[M,I] "THEN"
"GOTO" NEW;  START: LL[M,J]:= P;  H[M,J]:= 1;
"IF"  Z= BLIM[M] "THEN" "GOTO" MORE;
"FOR" I:=1+Z "STEP" 1 "UNTIL" BLIM[M] "DO"
"IF"AA[M,I] = P "THEN" H[M,J]:= H[M,J] + 1;
"GOTO" NEXT; MORE: "END";
"COMMENT"  NOW WE PUT THE GROUP QUANTUM NUMBERS TOGETHER TO GET
LINE POSITIONS AND DEGENERACIES; L:= J:= 0;  M:= Q:= MAX:= 1;
PL[0,1] := 0;  HT[0,1] := 1;
CYCLE: LIMIT:= SP[M] * NO[M] + 1; R:=0;  TEST:=0 ;
      SCOPE:=ML/ (MAX * LIMIT );
INC: "IF" J = LIMIT "THEN" "BEGIN" J:=0; Q:= Q+1;
"END";  "IF" Q > MAX "THEN" "GOTO" LEAP ;
TEST:= TEST + SCOPE;
L:=L+1; J:=J+1;
PL[M,L]:=PL[M-1,Q]+LL[M,J]*A[M];
HT[M,L]:= HT[M-1,Q] * H[M,J];
LABEL: "IF" R= TEST "THEN" "GOTO" INC;
R:= R+1; QQ[M,R]:= LL[M,J];  "GOTO" LABEL ;
LEAP: M:= M+1;  MAX:= LIMIT * MAX;  L:= J:= 0;  Q:=1;
"IF" M>N "THEN" "GOTO" FURTHER; "GOTO" CYCLE;
        "COMMENT" NOW WE SORT THE LINES BY POSITION;
FURTHER:
"FOR"X:=ML "STEP" -1 "UNTIL" 2 "DO" "FOR" J:=2 "STEP" 1 "UNTIL" X "DO"
"IF"PL[N,J-1] >PL[N,J] "THEN" "BEGIN"
CHANGE:=PL[N,J-1]; PL[N,J-1]:=PL[N,J]; PL[N,J]:= CHANGE;
CH    := HT[N,J-1];  HT[N,J-1]:= HT[N,J];  HT[N,J]:= CH    ;
"FOR"M:=1 "STEP" 1 "UNTIL" N "DO" "BEGIN"
CH    :=QQ[M,J-1]; QQ[M,J-1]:=QQ[M,J]; QQ[M,J]:= CH    ; "END"; "END";
"PRINT"  ´´L4S6´LINE NO´S9´LINE POSITION´S10´DEGENERACY´,
SAMELINE, ´´S6´GROUP SPIN QUANTUM NOS´; "PRINT"  ´´L1S21´CMS´S9´GAUSS´;
"PRINT"  ´´L2S55´´;
SAMELINE; "FOR" M:=1 "STEP" 1 "UNTIL" N "DO"
"PRINT" SAMELINE,  ´´S1´´, M;   "PRINT"  ´´L2´´;
"FOR" J:=1 "STEP" 1 "UNTIL" ML "DO" "BEGIN"
"PRINT"  ´´L1S1´´, J, SAMELINE,  ´´S7´´, ALIGNED(4,3), PL[N,J]*1.27,
 ´´S4´´, ALIGNED(4,3), PL[N,J]*CONFAC*1.27,  ´´S3´´, HT[N,J],  ´´S5´´;
"FOR" M:=1 "STEP" 1 "UNTIL" N "DO"
"PRINT"  ´´S4´´, ALIGNED(3,1), QQ[M,J]/2;   "END";
```

```
"PRINT"´´L5``;
"COMMENT" FIND THE LINES THAT BROADEN DURING EXCHANGE BY FINDING CHAN-
GES IN QUANTUM NUMBERS FOR THE DIFFERENT CONFORMATIONS;
M:=1;
"FOR"E:=1"STEP"1"UNTIL"CYC"DO""BEGIN"
NN:=M+1;
"FOR"J:=1"STEP"1"UNTIL"ML"DO"
QDIF[J,E]:=((QQ[M,J]/2)-(QQ[NN,J]/2))↑2;
M:=E+2;
"END";
"PRINT"´´L2``;
"COMMENT" CALCULATE NEW LINEWIDTHS;
"FOR"E:=1"STEP"1"UNTIL"CYC"DO""BEGIN"
FF:=E-1;
"FOR"J:=1"STEP"1"UNTIL"ML"DO""BEGIN"
WIDTH[J,E]:=WIDTH[J,FF]+(TT*QDIF[J,E]);
"IF"WIDTH[J,E]>WIDMAX"THEN"WIDMAX:=WIDTH[J,E];
"END";
"END";
WIDMAX:=WIDMAX/CONFAC;
"PRINT"´´L4S7`CONFORMATIONAL LIFETIME =`,SAMELINE,ALIGNED(1,8),
TAU,´´S1`SEC`;
"PRINT"´´L4S25`LINE NO´S20`CORRECTED LINEWIDTH GAUSS`;
"PRINT"´´L2S42``;SAMELINE;
"FOR"M:=1"STEP"1"UNTIL"CYC"DO"
"PRINT"SAMELINE,´´S5``,M;
"FOR"J:=1"STEP"1"UNTIL"ML"DO""BEGIN"
"PRINT"´´L1S21``,J;SAMELINE;
"PRINT"´´S13``;
"FOR"E:=1"STEP"1"UNTIL"CYC"DO"
"PRINT"´´S9``,ALIGNED(1,4),WIDTH[J,E];
"END";
ALT:=0;
"FOR"J:=1"STEP"1"UNTIL"ML"DO""BEGIN"
ACTHT[J]:=HT[N,J]/WIDTH[J,CYC];
"IF"J=1"THEN"ALT:=ACTHT[J];
ACTHT[J]:=ACTHT[J]/ALT;
"END";
"IF" CHOICE=0 "THEN" "GOTO" FINIS;   PUNCH(5);
HMAX:=0;  "FOR" J:=1 "STEP" 1 "UNTIL" ML "DO" "IF" ACTHT[J] > HMAX
"THEN"HMAX:=ACTHT[J];
                        HMAX:=(HMAX*14.72)/HITE; SETORIGIN(1300,1);
MOVEPEN(-4,1300);
"PRINT"WAY(0,6),´CONFORMATIONAL LIFETIME=`,ALIGNED(1,8), TAU,´´S1`SEC`;
MOVEPEN(-4,0);
IGNORE:=WIDMAX*1500.0; FINAL:=PL[N,ML]*100.0+50.0;
"FOR" XX:=0 "STEP" 2 "UNTIL" 2*FINAL "DO" "BEGIN" RX:=XX-FINAL;
Y:=0.0;  "FOR" J:=1 "STEP" 1 "UNTIL" ML "DO" "BEGIN"
NEWPL:= PL[N,J] * 100.0;
"IF" ABS(RX-NEWPL) > IGNORE "THEN" "GOTO" CUT;
T:=(0.011547*(RX-NEWPL))/(WIDTH[J,CYC]/CONFAC);
DEN:=1+T*T;
Y:=Y+(T*ACTHT[J])/(DEN*DEN); CUT: "END";
YP:=(1800.0*Y)/HMAX; YY:=-YP; DRAWLINE(XX,YY);
"END"; FINIS: "END"; "END"; ERROR: "END" ;
```

REFERENCES

REFERENCES

1. W. L. Jolly and C. J. Hallada, "Non-Aqueous Solvent Systems", T. C. Waddington, Ed.,Academic Press, 1965, Chap. 1., and references therein.

2. "Metal-Ammonia Solutions", G. Lapoutre and M. J. Sienko, Ed., Colloque Weyl I, W. A. Benjamin, Inc., New York, N.Y., 1964.

3. a) "Metal-Ammonia Solutions", J. T. Lagowski and M. J. Sienko, Ed., Colloque Weyl II, Butterworths & Co., London, 1970.

   b) See ref. 3(a), p. 247.

   c) See ref. 3(a), p. 1.

4. W. Weyl., Ann. Physik, 1864, 121, 601.

5. C. A. Kraus, J. Amer. Chem. Soc., 1908, 30, 1323.

6. E. Huster, Ann. Physik, 1938, 33, 477.

7. W. Bingel, ibid., 1953, 12, 57.

8. M. F. Deigen, Tr. Inst. Fiz. Akad. Nauk Ukr. S.S.R., 1954, 5, 119 ; Zh. Eksperim. i Teor. Fiz., 1954, 26, 300.

9. S. Golden, C. Guttman and T. R. Tuttle, Jr., J. Amer. Chem. Soc., 1965, 87, 135 ; J. Chem. Phys., 1966, 44, 3791.

10. E. Arnold and A. Patterson, Jr., J. Chem. Phys., 1964, 41, 3089 and 3098.

11. E. Becker, R. H. Lindquist and B. J. Alder, ibid., 1956, 25, 971.

12. R. A. Ogg, Jr., ibid., 1946, 14, 295 and 1141.

13. J. Kaplan and C. Kittell, ibid., 1953, 21, 1429.

14. R. Catterall and M. C. R. Symons, J. Chem. Soc. (A), 1966, 13.

15. M. Gold, W. L. Jolly and K. S. Pitzer, J. Amer. Chem. Soc., 1962, 84, 2264, and ref. 2, p. 144.

16. I. Hurley, T. R. Tuttle, Jr., and S. Golden, ref., 3, p. 449.

17. R. Catterall, ref., 3, p. 105.

18. J. L. Dye, M. G. DeBacker, J. A. Eyre and L. M. Dorfman, J. Phys. Chem., 1972, 76, 839.

19. L. M. Dorfman and M. S. Matheson, "Progress in Reaction Kinetics 3", G. Porter, Ed., Pergamon Press, London, 1965, Chap. 6, p. 273.

20. A. von Baeyer, Ann., 1892, 269, 145.

21. R. Willstätter, F. Seitz and E. Bumm, Ber., 1928, 61, 871.

22. H. Burton and C. K. Ingold, J. Chem. Soc., 1929, 2022.

23. W. Hückel and H. Bretschneider, Ann., 1939, 540, 157.

24. a) J. B. Conant, Chem. Rev., 1926-27, 3, 1.

b) R. Kuhn and M. Hoffer, Ber., 1932, 65, 170.

c) H. J. Prins, Rev. Trav. Chim., 1923, 42, 473.

d) H. J. Prins, ibid., 1925, 44, 1093.

25. L. Michaelis and M. P. Schubert, Chem. Rev., 1938, 22, 437.

26. A. J. Birch, Quart. Rev. (London), 1950, 4, 69.

27. A. R. Buick, Ph.D. Thesis, University of Warwick, 1970.

28. G. T. Neal, Ph.D. Thesis, University of Warwick, 1969.

29. W. L. Jolly, ref. 3, p. 167.

30. J. L. Dye, Accounts Chem. Res., 1968, 1, 306, and references therein.

31. M. Anbar and P. Neta, Intern. J. Appl. Radiat. Isotopes, 1967, 18, 493.

32. D. Y. P. Chou, M. J. Pribble, D. C. Jackman and C. W. Keenan, J. Amer. Chem. Soc., 1963, 85, 3530.

33. W. L. Jolly and C. J. Hallada, ref., 1, p. 38.

34. L. M. Dorfman and I. A. Taub, J. Amer. Chem. Soc., 1963, 85, 2370.

35. W. L. Jolly and L. Prizant, Chem. Comm., 1968, 1345.

36. M. Bertholet, Ann. Chim., 1867, 12, 1955.

37. W. Schlenk, J. Appenrodt, A. Michael and A. Thal, Chem. Ber., 1914, 47, 473.

38. a) D. Lipkin, D. E. Paul, J. Townsend and S. I. Weissman, Science, 1953, 117, 534.

b) S. I. Weissman, J. Townsend, D. E. Paul and G. E. Pake, J. Chem. Phys., 1953, 21, 2227.

39. M. Szwarc, Prog. Phys. Org. Chem., 1968, 6, 323.

40. E. T. Kaiser and L. Kevan, Ed., "Radical-Ions", Interscience, New York, 1968, p. 783.

41. E. J. Lande, ref. 19, p. 369.

42. a) D. H. Eargle, Anal. Chem., 1966, 38, 371R.

b) D. H. Eargle, ibid., 1968, 40, 303R.

c) A. Carrington and G. R. Luckhurst, Ann. Rev. Phys. Chem., 1968, 19, 31.

d) B. Mile, Angew. Chem. Internat. Ed., 1968, 7, 507.

e) A. Carrington, Ann. Rept., 1964, 13, 1089.

f) N. M. Atherton, A. J. Parker and H. Steiner, ibid., 1966, 63, 62.

g) N. M. Atherton, Lab. Pract., 1964, 13, 1089.

h) R. O. C. Norman, ibid, 1964, 13, 1084.

i) M. C. R. Symons, Adv. in Phys. Org. Chem., 1963, 1, 283.

j) R. O. C. Norman and B. C. Gilbert, ibid., 1967, 5, 53.

k) P. B. Ayscough, "Electron Spin Resonance in Chemistry", Methuen & Co. Ltd., 1967.

43. J. E. Bennett and A. Thomas, Proc. Roy. Soc., 1964, A280, 123.

44. F. Rachig, Z. Angew. Chem., 1905, 18, 281.

45. H. Hartridge and F. J. W. Roughton, Proc. Roy. Soc., 1923, A104, 376 and 395.

46. T. J. Stone and W. A. Waters, J. Chem. Soc., 1964, 213.

47. a) W. T. Dixon and R. O. C. Norman, Nature, 1962, 196, 891.

b) W. T. Dixon and R. O. C. Norman, ibid., 1963, 3119.

48. A. R. Buick, T. J. Kemp, G. T. Neal and T. J. Stone, J. Chem. Soc. (A), 1969, 666.

49. E. G. Janzen, Accounts Chem. Res., 1971, 4, 31.

50. a) H. R. Ward, ibid., 1972, 5, 18.

b) R. G. Lawler, ibid., 1972, 5, 25.

51. S. Forshult, C. Lagercrantz and K. Torsell, Acta. Chem. Scand., 1969, 23, 522.

52. See references in J. E. Wertz, Ann. Rev. Phys. Chem., 1959, 10, 435.

53. See references in G. K. Fraenkel and B. Segal, ibid., 1958, 1, 406.

54. B. Smaller and M. S. Matherson, ibid., 1958, 28, 1169.

55. T. Cole, H. O. Pritchard, N. R. Davidson and H. M. McConnell, Mol. Phys., 1958, 1, 406.

56. R. W. Fessenden and R. H. S. Schuler, J. Chem. Phys., 1963, 39, 2147.

57. R. W. Fessenden, ibid., 1962, 37, 747.

58. P. Neta, M. Z. Hoffman and M. Simic, J. Phys. Chem., 1972, 76, 847.

59. K. Eiben and R. W. Fessenden, ibid., 1971, 75, 1186.

60. P. Neta, R. W. Fessenden and R. H. S. Schuler, ibid., 1971, 75, 1654.

61. P. Neta and R. W. Fessenden, ibid., 1970, 74, 2263.

62. A. Horsfield, J. R. Morton and D. H. Whiffen, Mol. Phys., 1961, 4, 169.

63. a) N. Tamura, M. A. Collins and D. H. Whiffen, Trans. Faraday Soc., 1966, 62, 2434.

b) K. Leibler, J. Wozniac, S. Krauze and K. Checinski, J. Chim. Phys., 1970, 67, 743.

64. Y. Nakajima, S. Sato and S. Shida, Bull. Chem. Soc., Japan, 1969, 42, 2132.

65. a) R. J. Cook, J. R. Rowlands and D. H. Whiffen, Mol. Phys., 1963-4, 7, 31.

b) M. T. Rogers, S. J. Bolte and P. S. Rao, J. Amer. Chem. Soc., 1965, 87, 1875.

66. a) J. R. Morton, ibid., 1964, 86, 2325.

b) M. A. Collins and D. H. Whiffen, Mol. Phys., 1965-66, 10, 317.

67. a) A. H. Maki and D. H. Geske, J. Amer. Chem. Soc., 1960, 82, 2671.

b) A. H. Maki and D. H. Geske, J. Chem. Phys., 1960, 33, 825.

68. P. H. Rieger and G. K. Fraenkel, ibid., 1962, 37, 2795.

69. A. H. Maki, ibid., 1961, 35, 761.

70. P. H. Rieger and G. K. Fraenkel, ibid., 1962, 37, 2811.

71. C. Elschenbroich and M. Cais, J. Organometal. Chem., 1969, 18, 135.

72. J. Voss and W. Walter, Tetrahedron Letters, 1968, 1751.

73. J. Voss and W. Walter, Ann., 1970, 734, 1.

74. J. Voss and W. Walter, ibid., 1971, 743, 177.

75. D. H. Levy and R. J. Myers, J. Chem. Phys., 1964, 41, 1062.

76. W. M. Tolles and D. W. Moore, ibid., 1966, 46, 2102.

77. C. L. Talcott and R. J. Myers, Mol. Phys., 1967, 12, 549.

78. S. Konishi, S. Niizuma and M. Koizuma, Bull. Chem. Soc., Japan, 1970, 43, 3358.

79. T. J. Stone and W. A. Waters, J. Chem. Soc., 1964, 4302.

80. T. J. Stone and W. A. Waters, Proc. Chem. Soc., 1962, 253.

81. C. J. W. Gutch and W. A. Waters, ibid., 1964, 230.

82. P. Smith, J. T. Pearson, P. B. Wood and T. C. Smith, J. Chem. Phys., 1965, 43, 1535.

83. R. O. C. Norman and P. R. West, J. Chem. Soc. (B), 1969, 389.

84. a) H. Fisher, C. Corvaja and G. Giacometti, Z. Phys. Chem., Frankfurt, 1965, 45, 1.

b) D. J. Edge and R. O. C. Norman, J. Chem. Soc. (B), 1969, 182.

85. A. L. J. Beckwith and R. O. C. Norman, ibid., 1969, 400.

86. R. O. C. Norman, P. M. Story and P. R. West, ibid., 1970, 1087.

87. A. R. Buick, T. J. Kemp, G. T. Neal and T. J. Stone, ibid., J. Chem. Soc. (A), 1970, 2227.

88. A. R. Buick, T. J. Kemp G. T. Neal and T. J. Stone, J. Chem. Soc. (A), 1969, 1609.

89. A. R. Buick, T. J. Kemp and T. J. Stone, J. Phys. Chem., 1970, 74, 3439.

90. J. K. Kochi and P. J. Krusic, J. Amer. Chem. Soc., 1968, 90, 7155.

91. J. K. Kochi and P. J. Krusic, ibid., 1968, 90, 7157.

92. J. K. Kochi, P. J. Krusic and D. R. Eaton, ibid., 1969, 91, 1877 and 1879.

93. P. Bakuais, J. K. Kochi and P. J. Krusic, ibid., 1970, 92, 1434.

94. P. J. Krusic and J. K. Kochi, ibid., 1969, 91, 3938 and 6161.

95. J. K. Kochi and P. J. Krusic, Chem. Soc. Sp. Publications, 1970, 24, 185.

96. H. D. Burrows, D. Greatorex and T. J. Kemp, J. Amer. Chem. Soc., 1970, 93, 2539.

97. a) G. A. Russell, R. D. Stephens and E. R. Talaty, Tetrahedron Letters, 1965, 1139.

b) See also ref. 40 p. 87.

98. a) G. A. Russell, E. T. Strom, E. R. Talaty and S. A. Weiner, J. Amer. Chem. Soc., 1966, 88, 1998.

b) G. A. Russell and R. D. Stephens, J. Phys. Chem., 1966, 70, 1320.

c) G. A. Russell and E. T. Strom, J. Amer. Chem. Soc., 1964, 86, 744.

99. G. J. Hoijtink, J. van Schooten, E. de Boer and W. I. J. Aalfbersberg, Rec. Trav. Chim., 1954, 73, 355.

100. R. J. Hagemann and H. A. Schwarz, J. Phys. Chem., 1967, 71, 2694.

101. a) R. C. Kerber, G. W. Urry and N. Kornblum, J. Amer. Chem. Soc., 1965, 87, 4520.

b) G. A. Russell and W. C. Danen, ibid., 1968, 90, 347.

c) N. Kornblum, R. E. Michel and R. C. Kerber, ibid., 1966, 88, 5606 and 5662.

102. See references in N. L. Holy and J. D. Marcum, Angew. Chem. Internat. Ed., 1971, 10, 115.

103. J. Chaudhuri, S. Kune, J. Jagur-Grodzinski and M. Szwarc, J. Amer. Chem. Soc., 1968, 90, 6421.

104. T. L. Staples, J. Jagur-Grodzinski and M. Szwarc, ibid., 1969, 91, 3721.

105. M. Matsuda, J. Jagur-Grodzinski and M. Szwarc, Proc. Roy. Soc., 1965, A288, 212.

106. a) M. Szwarc, M. Levy and R. Milkovitch, J. Amer. Chem. Soc., 1956, 78, 2656.

b) M. Szwarc, Nature, 1956, 178, 1168.

107. S. Arai and L. M. Dorfman, J. Chem. Phys., 1964, 41, 2190.

108. a) R. S. Davidson and R. Wilson, J. Chem. Soc. (B), 1970, 71.

b) G. Porter and F. Wilkinson, Trans. Faraday Soc., 1961, 57, 1686.

109. M. T. Jones, ref. 40, p. 245.

110. D. A. Dadley and A. G. Evans, J. Chem. Soc. (B), 1968, 107.

111. J. F. Garst, Accounts Chem. Res., 1971, 4, 400.

112. E. Fermi, Z. Physik, 1930, 60, 320.

113. S. I. Weissman, J. Chem. Phys., 1954, 22, 1378.

114. H. S. Jarrett and G. J. Sloan, ibid., 1954, 22, 1783.

115. a) H. M. McConnell, J. Chem. Phys., 1956, 24, 764.

b) R. Bersohn, ibid., 1956, 24, 1066.

c) S. I. Weissman, ibid., 1956, 25, 890.

d) H. S. Jarret, ibid., 1956, 25, 1289.

116. A. D. McLachlan, Mol. Phys., 1958, 1, 233.

117. M. Karplus and G. K. Fraenkel, J. Chem. Phys., 1961, 35, 1312.

118. F. Bloch, Phys. Rev., 1946, 70, 460.

119. For references see P. D. Sullivan and J. R. Bolton, Advan. Magnetic Resonance, 1970, 4, 39.

120. J. A. Pople, W. G. Schneider and H. J. Berstein, "High Resolution Nuclear Magnetic Resonance", McGraw-Hill Book Company, New York, 1959, Chap. 10.

121. H. S. Gutowsky and C. H. Holm, J. Chem. Phys., 1956, 25, 1228.

122. G. K. Fraenkel, J. Phys. Chem., 1967, 71, 139.

123. J. H. Freed and G. K. Fraenkel, J. Chem. Phys., 1964, 41, 699.

124. a) N. M. Atherton and A. E. Goggins, Mol. Phys., 1964, 8, 99.

b) N. M. Atherton and A. E. Goggins, Trans. Faraday Soc., 1965, 61, 1399.

125. F. Gerson, E. Heilbronner, H. A. Reddoch, H. A. Paskovitch and N. C. Das, Helv. Chim. Acta, 1967, 50, 813.

126. A. Streitweisser, "Molecular Orbital Theory for Organic Chemists", Wiley, New York, 1961.

127. A. D. McLachlan, Mol. Phys., 1960, 3, 233.

128. a) S. I. Weissman, T. R. Tuttle and E. de Boer, J. Phys. Chem., 1959, 947.

b) E. de Boer and S. I. Weissman, J. Amer. Chem. Soc., 1958, 80, 4549.

c) A. Carrington, F. Dravnieks and M. R. C. Symons, J. Chem. Soc., 1959, 947.

d) S. I. Weissman, E. de Boer and J. J. Conradi, J. Chem. Phys., 1957, 26, 963.

129. a) T. Cole, C. Heller and H. M. McConnell, Proc. Natl. Acad. Sci. U.S., 1959, 45, 525.

b) G. W. Canters and E. de Boer, Mol. Phys., 1967, 13, 395.

130. M. Anbar and E. J. Hart, J. Amer. Chem. Soc., 1964, 86, 5633.

131. A. H. Maki and D. H. Geske, ibid., 1961, 83, 1852.

132. M. D. Sevilla, J. Phys. Chem., 1970, 74, 669.

133. W. C. Fernelius and Wesp, unpublished work, quoted in G. W. Watt, Chem. Rev., 1950, 646, 317.

134. R. A. Abramovitch and D. L. Struble, Tetrahedron, 1968, 24, 714.

135. F. S. Okumura and T. Moritani, Bull. Chem. Soc., Japan, 1967, 40, 2209.

136. H. Smith, "Organic Reactions in Liquid Ammonia", Interscience, New York, 1963, p. 46.

137. M. J. Aroney, R. J. W. Le Fevre and A. N. Singh, J. Chem. Soc., 1965, 3179.

138. L. A. Laplanche and M. T. Rogers, J. Amer. Chem. Soc., 1963, 85, 3728.

139. G. Schwenker and H. Rosswag, Tetrahedron Letters, 1967, 43, 4237.

140. G. R. Bedford, D. Greatbanks and B. D. Rogers, Chem. Comm., 1966, 330.

141. T. H. Siddall, Tert. and W. E. Stewart, ibid., 1967, 393.

142. E. W. Stone and A. H. Maki, J. Chem. Phys., 1963, 38, 1999.

143. C. S. Johnson, Jnr., and R. Chang, J. Chem. Phys., 1965, 43, 3183.

144. N. M. Atherton, F. Gerson and J. N. Ockwell, J. Chem. Soc. (A), 1966, 109.

145. R. E. Sioda and W. S. Koski, J. Amer. Chem. Soc., 1967, 89, 475.

146. M. Hirayama, Bull. Chem. Soc., Japan, 1967, 40, 1557.

147. S. F. Nelsen, J. Amer. Chem. Soc., 1967, 89, 5256.

148. L. Lunnazzi, G. Maccagani, G. Mazzanti and G. Placucci, J. Chem. Soc. (B), 1971, 162.

149. P. H. Rieger and G. K. Fraenkel, J. Chem. Phys., 1963, 39, 609.

150. R. W. G. Wyckoff, "Crystal Structures", Interscience, New York, 1969, 6, p. 51.

151. M. Anbar and P. Neta, Internat. J. Appl. Radiat. Isotopes, 1965, 16, 965.

152. J. E. Bennett, B. Mile and A. Thomas, Proc. Roy. Soc., 1966, A293, 246.

153. P. B. Ayscough, R. G. Collins and F. S. Dainton, Nature, 1965, 205, 965.

154. C-C Liu, Microfilm Abstracts, 1941, 3, 5; Chem. Abs., 1941, 35, 3876; ref. 136, p. 32.

155. See ref. 136, p. 231.

156. a) A. J. Birch and H. Smith, J. Chem. Soc., 1956, 4909.

b) W. S. Johnson, E. R. Rogier, J. Szmuszkovicz, H. I. Hadler, J. Ackermann, B. K. Bhattacharyya, B. M. Bloom, L. Stalmann, R. A. Clement, B. Barrister and H. Wynberg, J. Amer. Chem. Soc., 1956, 78, 6289.

c) F. Sondheimer, R. Yashin, G. Rosenkranz and C. Djerassi, J. Amer. Chem. Soc., 1952, 74, 2696.

157. K. N. Campbell and B. K. Campbell, Chem. Rev., 1942, 31, 124.

158. M. M. Baizer, Tetrahedron Letters, 1963, 15, 973.

159. E. Touboul, F. Weisbuch and J. Wieman, Bull. Soc. Chim., France, 1967, 11, 4291.

160. J. Weiman, S. Risse and P.-F. Casals, ibid., 1966, 1, 381.

161. P. Angibeaud, M. Larcheveque, H. Normant and B. Tchoubar, ibid., 1968, 2, 595.

162. P. Martinet and J. Simonet, ibid., 1967, 3533.

163. K. Noack and R. N. Jones, Canad. J. Chem., 1961, 39, 2225.

164. A. J. Bowles, W. O. George and W. F. Maddams, J. Chem. Soc. (B), 1969, 810.

165. F. H. Cottee, B. P. Straughan and C. J. Timmons, ibid., 1967, 146.

166. F. H. Cottee and C. J. Timmons, ibid., 1968, 326.

167. G. A. Russell and G. R. Stevenson, J. Amer. Chem. Soc., 1971, 93, 2432.

168. H. -L. J. Chen and M. Bersohn, Mol. Phys., 1967, 13, 573.

169. K. N. Bowers, R. W. Giese, J. Grinshaw, H. O. House, N. H. Kolodny, K. Kronberger and D. K. Roe, J. Amer. Chem. Soc., 1970, 92, 2783.

170. a) J. Harbour and A. V. Guzzo, Mol. Phys., 1971, 20, 565.

b) J. Harbour and A. V. Guzzo, ibid., 1972, 23, 151.

171. N. K. Ray, R. K. Gupta and P. T. Narashimhan, Mol. Phys., 1966, 10, 601.

172. W. G. Dauben, G. W. Shaffer and N. D. Vietmeyer, J. Org. Chem., 1968, 33, 4060.

173. F. G. Bordwell and K. M. Wellman, ibid., 1963, 28, 1347.

174. M. S. de Groot and J. Lamb, Proc. Roy. Soc., 1967, A242, 36.

175. J. B. Bentley, K. B. Everard, R. J. B. Marsden and L. E. Sutton, J. Chem. Soc., 1949, 2957.

176. I. H. Elson and T. J. Kemp, J. Amer. Chem. Soc., 1971, 93, 7091.

177. A. I. Prokofev, S. P. Solodomikov, A. A. Volodkin and V. V. Ershov, Izv. Acad. Nauk S.S.S.R., Ser. Khim., 1960, 1712.

178. P. B. Ayscough, "Electron Spin Resonance in Chemistry", Methuen and Co. Ltd., London, 1967, p. 290.

179. C. Y. Chen and R. J. W. Le Fevre, J. Chem. Soc. (B), 1966, 180; see also ref. 170 (b).

180. F. Gerson, E. Heilbronner, W. A. Boll and E. Vogel, Helv. Chim. Acta, 1965, 48, 1494.

181. S. A. Manley and J. K. Tyler, Chem. Comm., 1970, 382.

182. D. Greatorex, Private Communication.

183. See ref. 40, p. 90.

184. G. A. Russell, G. R. Underwood and D. C. Lini, J. Amer. Chem. Soc., 1967, 89, 6636.

185. R. Livingston and H. Zeldes, J. Chem. Phys., 1966, 44, 1245.

186. G. E. Arth, G. I. Poos, P. M. Lukes, F. M. Robinson, W. F. Johns, M. Feurer and L. H. Sarett, J. Amer. Chem. Soc., 1954, 76, 1715.

187. A. C. Cope and E. M. Mancock, ibid., 1938, 60, 2644.

188. S. F. Nelsen, Tetrahedron Letters, 1967, 39, 3795.

189. a) P. Neta and R. W. Fessenden, J. Phys. Chem., 1972, 76, 1957.

see also

b) P. Neta, M. Z. Hoffman and M. Simic, ibid., 1972, 76, 847.

190. A. J. Bowles, W. O. George and D. B. Cunliffe-Jones, J. Chem. Soc. (B), 1970, 401.

191. W. O. George, D. V. Hassid and W. F. Maddams, J.C.S. Perkin II, 1972, 401.

192. J. B. Pedersen and J. H. Freed, J. Chem. Phys., 1972, 57, 1004, and references therein.

193. K. W. Chambers, E. Collinson and F. S. Dainton, Trans. Faraday Soc., 1970, 66, 142.

194. D. R. Howton and R. H. Davies, J. Org. Chem., 1951, 16, 1405.

195. P. Neta, J. Phys. Chem., 1971, 75, 2570.

196. G. C. Jones and T. H. Ledford, Tetrahedron Letters, 1967, 7, 615.

197. W. F. Forbes and P. D. Sullivan, Canad. J. Chem., 1966, 44, 1501.

198. G. P. Rabold, R. T. Ogata, M. Okamura, L. H. Piette, R. E. Moore and P. J. Scheuer, J. Chem. Phys., 1967, 46, 1161.

199. W. F. Forbes and P. D. Sullivan, ibid., 1968, 48, 1411.